

MOUNTAIN-PLAINS CONSORTIUM

MPC 18-364 | N. Wehbe, R. Reid, H. Mahgoub, J. Stripling, B. Postma Edgar,
and M. Underberg

Jointed Plain Concrete Pavement Design and Construction Review



A University Transportation Center sponsored by the U.S. Department of Transportation serving the Mountain-Plains Region. Consortium members:

Colorado State University
North Dakota State University
South Dakota State University

University of Colorado Denver
University of Denver
University of Utah

Utah State University
University of Wyoming

JOINTED PLAIN CONCRETE PAVEMENT DESIGN AND CONSTRUCTION REVIEW

Nadim Wehbe, Ph.D., PE
Richard Reid, Ph.D., PE
Jason Stripling, PE
Brooke Edgar
Hesham Mahgoub, Ph.D.
Mason Underberg, PE

Department of Civil and Environmental Engineering
South Dakota State University
Brooking, SD 57007

September 2018

Acknowledgments

The authors would like to acknowledge the financial support of the Mountain-Plains Consortium (MPC) for funding this study through project MPC-305.

Disclaimer

The contents of this report reflect the views of the authors, who are responsible for the facts and the accuracy of the information presented. This document is disseminated under the sponsorship of the Department of Transportation, University Transportation Centers Program, in the interest of information exchange. The U.S. Government assumes no liability for the contents or use thereof.

NDSU does not discriminate in its programs and activities on the basis of age, color, gender expression/identity, genetic information, marital status, national origin, participation in lawful off-campus activity, physical or mental disability, pregnancy, public assistance status, race, religion, sex, sexual orientation, spousal relationship to current employee, or veteran status, as applicable. Direct inquiries to Vice Provost, Title IX/ADA Coordinator, Old Main 201, 701-231-7708, ndsu.eoaa@ndsu.edu.

ABSTRACT

An experimental research study was conducted to develop optimized concrete mixtures for jointed plain concrete (JPC) pavements and field evaluation of newly constructed JPC pavement sections along South Dakota highways.

Using South Dakota aggregates, different concrete mixtures were assessed for optimum workability, durability, and cost. The optimized mixtures incorporated 1.5" aggregate top size and reduced cement content. Mixtures containing pea rock exhibited poor freeze-thaw durability. Mixtures with 1.0" aggregate top size and 65/35 coarse-to-fine aggregate ratio exhibited low workability. A new laboratory technique that involves measuring the "specific work" of fresh concrete was developed to compare workability of different mixtures.

Field data obtained from newly constructed JPC pavements demonstrated the following: thicker concrete pavement results in greater change in joint gap width, while the presence of asphalt underlayment results in lesser change in joint gap width; unsealed transverse joints allow for significantly higher moisture ingress than silicone sealed or hot-pour sealed joints; silicone sealed joints exhibited the least moisture ingress; treating the freshly placed JPC pavement with 1.5 times the normal amount of curing compound had a significant effect on maintaining pavement smoothness with time; high initial load transfer efficiency was achieved at joints with reduced dowel bar arrangements; and joint faulting was negligible across joints with either standard dowel bar configuration or reduced dowel bar configuration.

TABLE OF CONTENTS

1. INTRODUCTION	1
1.1 Problem Statement	1
1.2 Objectives	3
1.3 Scope.....	4
2. LITERATURE REVIEW	5
2.1 Introduction.....	5
2.2 Performance of Concrete Mixtures	5
2.2.1 Effect of Aggregates on Mix Performance	5
2.2.1.1 Aggregate Size, Shape, Texture, Gradation, and Weatherability.....	5
2.2.1.2 Aggregate Mixture Grading	6
2.2.1.3 General Guidelines for Coarse Aggregate Gradation.....	7
2.2.1.4 Previous Research on the Effects of Aggregate Gradation on Concrete Properties	7
2.2.2 Effect of Freeze-Thaw Damage on Concrete Durability.....	8
2.2.2.1 Factors Affecting Freeze-Thaw Durability	8
2.2.2.2 Previous Research on Freeze-Thaw Durability.....	8
2.2.3 Workability	9
2.3 Development of Deficiencies in JPC Pavements	10
2.3.1 Pumping and Faulting	10
2.3.2 Joint Sealant Failures	11
2.3.2.1 Adhesive Sealant Failures	11
2.3.2.2 Cohesive Sealant Failures	11
2.3.2.3 Loss of Sealant	11
2.3.3 Spalling	12
2.4 Factors Affecting Performance of JPC Pavements	12
2.4.1 Joint Sealing.....	12
2.4.2 Reduced Number of Dowel Bars in Transverse Joints	14
2.4.3 Curing Compound Material and Amount.....	14
3. EVALUATION OF PAVEMENT CONCRETE MIXTURES	16
3.1 Concrete Mixtures and Constituent Materials	16
3.1.1 Mix Design Matrix.....	16
3.1.2 Measured Aggregate Properties	18

3.1.2.1	Density, Specific Gravity, and Absorption	19
3.1.2.2	Aggregate Gradation and Fineness Modulus	19
3.1.2.3	Flat and Elongated Particles	21
3.1.2.4	Resistance to degradation.....	21
3.1.2.5	Soundness of Aggregates	22
3.1.3	Mix Design.....	22
3.2	Measured Fresh Concrete Properties	29
3.2.1	Slump, Air Content, and Mix Temperature.....	29
3.2.2	Concrete Workability	32
3.2.2.1	The Specific Work Method for Measuring Workability	32
3.2.2.2	Workability Test Results.....	34
3.3	Measured Hardened Concrete Properties.....	36
3.3.1	Compressive Strength	36
3.3.2	Flexural Strength (Modulus of Rupture).....	40
3.3.3	Freeze-Thaw Durability	41
3.4	Analysis of Experimental Results.....	45
3.4.1	Concrete workability.....	45
3.4.1.1	Workability versus Slump.....	45
3.4.1.2	Workability versus Air Content	46
3.4.1.3	Effect of Aggregates on Workability	46
3.4.2	Concrete Compressive Strength.....	48
3.4.2.1	28-Day Compressive Strength versus W/C Ratio	48
3.4.2.2	Compressive Strength Gain Rate	49
3.4.3	Concrete Flexural Strength (Modulus of rupture).....	51
3.4.4	Concrete Durability-Resistance to Rapid Freezing and Thawing.....	52
4.	EVALUATION OF NEW JPC PAVEMENT IN SOUTH DAKOTA.....	55
4.1	Testing Parameters.....	55
4.1.1	Transverse Contraction Joint Type	55
4.1.2	Curing Compound Application Rate.....	56
4.1.3	Dowel Bar Configuration and Corresponding Transverse Contracting	56
Joint Spacing.....	56
4.2	Test Sites and Test Sections.....	58
4.2.1	Test Sites	58

4.2.2	Test sections.....	60
4.3	Test Methods and Protocols.....	66
4.3.1	Pavement Surface Strain and Transverse Joint Movement.....	66
4.3.2	Moisture Ingress.....	70
4.3.3	Load Transfer Efficiency.....	72
4.3.3	International Roughness Index (IRI).....	73
4.3.4	Joint Faulting.....	74
4.3.5	Data Collection History.....	75
4.4	Data Analysis.....	76
4.4.1	Statistical Methods.....	76
4.4.2	Pavement Surface Strain and Transverse Joint Movement.....	77
4.4.2.1	Surface Strain.....	77
4.4.2.2	Joint Width.....	80
4.4.3	Moisture Ingress.....	84
4.4.4	Load Transfer Efficiency.....	86
4.4.5	International Roughness Index.....	91
4.4.4.5	Comparison of IRI Values at the Different Test Sites.....	93
4.4.4.6	Influence of Curing Compound Application Rate on Change of IRI Values with Time.....	94
4.4.5	Joint Faulting.....	95
5.	SUMMARY, CONCLUSIONS, RECOMMENDATIONS, AND IMPLEMENTATION.....	97
5.1	Summary.....	97
5.2	Conclusions.....	98
5.2.1	Concrete Mixtures Optimization.....	98
5.2.1.1	Plastic Concrete Behavior.....	98
5.2.1.2	Hardened Concrete Behavior.....	98
5.2.2	Performance of Newly Constructed JPC Pavements.....	99
5.3	Recommendations.....	100
5.4	Implementation.....	102
	REFERENCES.....	103
	APPENDIX A: MIX DESIGN RECOMMENDATIONS.....	106
	APPENDIX B: CEMENT, FLY ASH, AND AIR ENTRAINER DATA.....	111
	APPENDIX C: EPOXY ADHESIVE DATA SHEET.....	115

LIST OF TABLES

Table 2.1	ASTM Grading Limits for Concrete Aggregates	7
Table 3.1	Concrete Mix Combinations and Labels	17
Table 3.2	Measured Density, Specific Gravity, and Absorbtion.....	19
Table 3.3	Flat and Elongated Particles Test Results	21
Table 3.4	Loss by Abrasion and Impact in the Los Angeles Machine.....	21
Table 3.5	Sodium Sulfate Soundness Test of Pea Rock.....	22
Table 3.6	Mix Design – Quartzite Aggregate Mixtures	23
Table 3.7	Mix Design – Limestone Aggregate Mixtures	23
Table 3.8	Measured Slump, Air Content, and Mix Temperature	31
Table 3.9	Workability Test Results.....	35
Table 3.10	Average Compressive Strength for the Limestone Aggregate Mixes	36
Table 3.11	Average Compressive Strength for the Quartzite Aggregate Mixes	37
Table 3.12	Average Flexural Strength for the Limestone Aggregate Mixes.....	40
Table 3.13	Average Flexural Strength for the Quartzite Aggregate Mixes.....	41
Table 3.14	Average Relative Dynamic Modulus and Durability Factor for the Limestone Aggregate Mixes	43
Table 3.15	Average Relative Dynamic Modulus and Durability Factor for the Quartzite Aggregate Mixes.....	44
Table 3.16	Ratio of Average Specific Work of Identical Mixes with Different Coarse Aggregate Top Size	48
Table 3.17	Measured and Theoretical 7-Day Compressive Strength.....	50
Table 4.1	Summary of the Test Sites.....	60
Table 4.2	Levels of Faulting Severity	74
Table 4.3	Data Collection History for the I-29 Brookings County Test Site	75
Table 4.4	Data Collection History for the US 212 Butte County Test Site.....	75
Table 4.5	Data Collection History for the SD 50 Yankton County Test Site.....	75
Table 4.6	Measured Pavement Surface Temperature at Initial Gauge Length Measurements.....	77
Table 4.7	Summary of Change in Surface Strain Data.....	78
Table 4.8	Characteristics of $\Delta\varepsilon - \Delta T$ Best Fit Lines Stratified for Test Site and Joint Type	79
Table 4.9	Tukey HSD Test Results for Change in Surface Strain by Joint Type.....	80
Table 4.10	Tukey HSD Test Results for Change in Surface Strain by Test Site.....	80
Table 4.11	Summary of Joint Gap Width Data	81
Table 4.12	Characteristics of $\Delta w - \Delta T$ Best Fit Lines Stratified for Test Site and Joint Type.....	82
Table 4.13	Tukey HSD Test Results for Change in Joint Gap Width by Joint Type.....	83

Table 4.14	Tukey HSD Test Results for Change in Joint Gap Width by Test Site.....	83
Table 4.15	Summary of Moisture Ingress Data.....	85
Table 4.16	Tukey HSD Test Results for Moisture Ingress by Joint Type.....	85
Table 4.17	Summary of LTE Values for the Unlocked Condition.....	87
Table 4.18	Summary of LTE Values for the Locked Condition	88
Table 4.19	Tukey HSD Test Results for LTE by Location, All Joint Types.....	89
Table 4.20	Tukey HSD Test Results for LTE by Location for each Joint Type	90
Table 4.21	Summary of IRI Values for Various Data Group Combinations	92
Table 4.22	Tukey HSD Test Results for IRI by Location and Curing Compound Application Rate	94
Table 4.23	Tukey HSD Test Results for IRI by Year – All Test Site Locations.....	94
Table 4.24	Summary of Faulting Values for Various Data Group Combinations	96

LIST OF FIGURES

Figure 1.1	JPC Pavement North of Brookings, SD	1
Figure 1.2	Saw-Cut Joint (with Joint Sealant).....	2
Figure 2.1	Faulting at Transverse Joints and Cracks (Miller and Bellinger 2003).....	10
Figure 2.2	Spalling of Transverse Joints in JPC Pavements (Miller and Bellinger 2003)	12
Figure 2.3	Typical Dowel Bar Configuration Used in South Dakota (SDDOT 2007).....	14
Figure 3.1	Concrete Mix Labeling	16
Figure 3.2	Quartzite Coarse Aggregates.....	18
Figure 3.3	Limestone Coarse Aggregates.....	18
Figure 3.4	3/8" Pea Rock Coarse Aggregates.....	18
Figure 3.5	Coarse Aggregate Measured Grain Size Distribution	20
Figure 3.6	Fine Aggregate Measured Grain Size Distribution	20
Figure 3.7	Combined Total Aggregate Gradation for the Quartzite Aggregate Mixes	24
Figure 3.8	Combined Total Aggregate Gradation for the Limestone Aggregate Mixes	24
Figure 3.9	0.45 Power Gradation for the Coarse Aggregates of the Quartzite Mixes.....	25
Figure 3.10	0.45 Power Gradation for the Coarse Aggregates of the Limestone Mixes.....	26
Figure 3.11	Coarseness Factor Charts for the Quartzite Aggregate Mixes	27
Figure 3.12	Coarseness Factor Charts for the Limestone Aggregate Mixes	28
Figure 3.13	Steel Box Configuration.....	32
Figure 3.14	Concrete Workability Test Apparatus.....	33
Figure 3.15	Schematic Plot of a Workability Test Load-Displacement Data	33
Figure 3.16	Measured Load-Displacement of Four Workability Tests	34
Figure 3.17	Measured Strength Gain of the Limestone Aggregate Concrete Mixes.....	38
Figure 3.18	Measured Strength Gain of the Quartzite Aggregate Concrete Mixes.....	39
Figure 3.19	Beam Specimens in the Freeze-Thaw Cabinet.....	41
Figure 3.20	Measurement of Concrete Fundamental Frequency Using a Sonometer	42
Figure 3.21	Slump vs. W/C Ratio.....	45
Figure 3.22	Specific Work vs. Slump.....	46
Figure 3.23	Specific Work vs. Air Content	46
Figure 3.24	Specific Work for the Limestone Aggregate Mixes.....	47
Figure 3.25	Specific Work for the Quartzite Aggregate Mixes.....	47
Figure 3.26	28-Day Compressive Strength versus W/C Ratio	48
Figure 3.27	7-Day Theoretical and Measured Compressive Strength.....	51
Figure 3.28	Measured f_r versus $\sqrt{f'_c}$ for the Limestone Aggregate Mixes.....	51

Figure 3.29	Measured f_r versus $\sqrt{f'_c}$ for the Quartzite Aggregate Mixes.....	52
Figure 3.30	Durability Factor Change with Number of Freeze-Thaw Cycles-Mixes with Pea Rock.....	52
Figure 3.31	Durability Factor Change with Number of Freeze-Thaw Cycles-Mixes without Pea Rock	53
Figure 3.32	Durability Factor for Limestone Aggregate Mixes	54
Figure 3.33	Durability Factor for the Quartzite Aggregate Mixes	54
Figure 4.1	Types of Transverse Contraction Joints Considered in the Study.....	56
Figure 4.2	Typical Standard SDDOT Dowel Bar Configuration for 12' Lanes	57
Figure 4.3	Typical Reduced Dowel Bar Configuration for 12' Lanes.....	58
Figure 4.4	Map of Test Site Locations in South Dakota (Google Maps).....	59
Figure 4.5	Schematic View of a Typical Joint Test Section (Brookings, Butte, and Test Sites)	61
Figure 4.6	Schematic View of a Modified Joint Test Section (Union County Test Site).....	61
Figure 4.7	Location of Test Sections at the Brookings County Test Site.....	62
Figure 4.8	Location of Test Sections at the Butte County Test Site.....	63
Figure 4.9	Location of Test Sections at the Yankton County Test Site	64
Figure 4.10	Location of Test Sections at the Union County Test Site	65
Figure 4.11	Plan View of the Pavement Reference Points Pattern.....	66
Figure 4.12	¼" x 1¼" Stainless Steel Hex Bolt and Bit	67
Figure 4.13	Reference Points Pattern Template	67
Figure 4.14	Installation of Reference Points on Pavement.....	68
Figure 4.15	Placement of Reference Points along a Transverse Joint.....	69
Figure 4.16	Instrumented Joints in a Joint Test Section.....	69
Figure 4.17	Distance Measurements between Reference Points	70
Figure 4.18	Moisture Sensor and Datalogger (after Campbell Scientific).....	70
Figure 4.19	Moisture Content Instrumentation Plan	71
Figure 4.20	Installation of the Moisture Instrumentation.....	71
Figure 4.21	FWD Apparatus	72
Figure 4.22	FWD Sensors Arrangement	72
Figure 4.23	FWD Test at a Transverse Joint.....	73
Figure 4.24	Ranges for IRI Values (Sayers and Karamihas 1998).....	74
Figure 4.25	Measured Change in Surface Strain.....	78
Figure 4.26	Change in Surface Strain vs. Change in Surface Temperature	79
Figure 4.27	Measured Change in Joint Gap Width	81
Figure 4.28	Change in Joint Gap Width vs. Change in Surface Temperature.....	82

Figure 4.29	Theoretical relationships between ΔT , Δw and $\Delta \epsilon$	84
Figure 4.30	Moisture Ingress versus Time	85
Figure 4.31	LTE for the Unlocked Condition	86
Figure 4.32	LTE for the Locked Condition.....	88
Figure 4.33	IRI Values – Standard Curing Compound Application Rate	91
Figure 4.34	IRI Values – Increased Curing Compound Application Rate	92
Figure 4.35	Average Absolute Faulting Values versus Time.....	95

EXECUTIVE SUMMARY

This report is part of SDDOT Research Project SD2008-06, “Jointed Plain Concrete Pavement Design and Construction Review.” The objectives of this research were to: 1) review available literature and field performance of various concrete pavement designs—especially in regard to joint and sealant systems—to determine possible beneficial changes to current practice, 2) develop optimized concrete mix designs incorporating larger top-size aggregate and pea gravel to provide good workability at lower cement contents and resist thermal effects, and 3) construct and evaluate appropriate JPC test sections to resolve any performance issues in regard to potential changes in design or construction.

The research covered in this report included experimental studies of optimized concrete mixtures for JPC pavements and field evaluation of newly constructed JPC pavement sections along South Dakota highways.

Concrete mixtures with reduced cement content and 36 combinations of coarse aggregate types (quartzite and limestone), aggregate top sizes (1.5" and 1.0"), blending aggregate types (3/8" aggregate in quartzite chip, limestone chip, and pea rock), coarse-to-fine aggregate ratios (60/40 and 65/35), and water/cementitious materials (w/cm) ratios (0.41, 0.39, and 0.37) were tested to develop an optimized mix for use in JPC pavement applications. Freeze-thaw durability, workability (consolidation ability), and mechanical properties of the mixes were measured and evaluated. A new energy-based experimental method for assessing the workability of concrete was devised. The method introduces a performance parameter called “Specific Work” to compare the workability of different concrete mixes.

Four newly constructed JPC pavement sites on South Dakota highways were selected for instrumentation, monitoring, and data collection. The four sites were located on I-29 north of Brookings in Brookings County, US 212 west of Belle Fourche in Butte County, South Dakota, 50 west of Vermillion in Yankton County, and I-29 south of Vermillion in Union County. The parameters considered in the study included the transverse joint sealant type, dowel bar configuration at the transverse joints, and amount of curing compound. Three different transverse joint sealing types were incorporated in the pavement at each test site: hot-pour sealant, silicone sealant, and green cut with no sealant (unsealed). Two dowel bar configurations at the transverse joints were included in the study. The I-29 sites were provided with normal dowel bar configuration (12 dowels per lane), whereas the US 212 and the SD 50 sites were provided with reduced dowel bar configuration (nine dowels per lane). Test sections at the test sites in Brookings, Butte, and Yankton counties were treated with increased amount of curing compound (1.5 times the normal amount).

The test site in Union County was used to only measure moisture content of the subbase under the transverse joints through the use of moisture sensors. Data collected from the Brookings County, Butte County, and Yankton County test sites were:

- Pavement surface gauge length measurements to determine change in pavement surface strain and transverse joint width
- Falling weight deflectometer (FWD) to assess the load transfer efficiency (LTE) at the transverse joint
- Profilometer measurements to evaluate the pavement ride quality through the International Roughness Index (IRI)
- Rod-and-level measurements to determine faulting at the transverse joints

A byproduct of this study was development of a new laboratory apparatus and testing method for comparative evaluation of concrete workability. The method measures the “specific work” of a fresh concrete sample. The specific work is the work per unit weight needed to displace and consolidate a concrete sample. Lower specific work values correspond to higher concrete workability. No attempt was made to correlate laboratory results and workability in the field since such work was not part of the scope of this study.

The following conclusions were made in this study:

Concrete Mixtures Optimization

- This specific work method provides a rigorous approach in a laboratory setting for comparative evaluation of concrete workability.
- A weak negative correlation exists between specific work and slump. Workability is highly influenced by factors that could not be captured in the slump test.
- No correlation exists between specific work and air content.
- The use of 1.5" instead of 1.0" aggregate top size increases the workability of concrete mixtures for concrete mixtures with 3/8" limestone or quartzite chip aggregates. Except for the quartzite mixes with pea rock aggregates, mixes with 1.0" aggregate top size consistently exhibited higher specific work (lower workability) than their counterpart mixes with 1.5" aggregate top size.
- Mixes with 65/35 coarse-to-fine aggregate ratio and 1.0" top aggregate size exhibited high specific work. Therefore, mixes with 65/35 coarse-to-fine aggregate ratio would be unsuitable for concrete pavement applications.
- The 1.5" maximum aggregate size mixes exhibited specific work higher than their 1.0" maximum aggregate size counterpart mixes when pea rock was used as the blending aggregate with the quartzite mixes.
- The compressive strength gain of the concrete mixes in this study could be predicted with reasonable accuracy using the Branson equation. The limestone mixes compressive strengths were on average 3.1 percent higher than the predicted seven day values. The quartzite mixes averaged a compressive strength 6.9 percent higher than the predicted values at seven days
- The measured modulus of rupture was higher than the value obtained from the ACI code empirical equation. The mean f_r for the limestone mixes is $11.84\sqrt{f'_c}$ with a standard deviation of $1.5\sqrt{f'_c}$. The mean f_r for the quartzite mixes is $9.90\sqrt{f'_c}$ with a standard deviation of $0.75\sqrt{f'_c}$. Both means are above the value obtained from the code empirical equation of $7.5\sqrt{f'_c}$.
- Mixes with pea rock exhibited rapid durability degradation with increased number of freeze-thaw cycles, whereas those without pea rock showed mild durability degradation. At the end of 150 freeze-thaw cycles, all mixes with pea rock had a durability factor (DF) less than the acceptable limit of 85, with most of them significantly below 85. On the other hand, all of the mixes that did not contain pea rock had a DF higher than 85.

Performance of Newly Constructed JPC Pavements

- The joint type did not show significant influence on the concrete surface strain close to the joint. However, one test site (SD 50) exhibited significantly higher surface strains than the other two test sites (I-29 and US 212). It is unclear why the surface strain at one test site was significantly different than those at the other two sites because no association between surface strain on one hand and the subbase material and the pavement thickness on the other could be established.
- The joint type did not have a significant influence on the joint gap width. However, the test site location, which reflects the variation in slab thickness and subbase material and thickness, had a significant influence on the measured change in joint gap width. For identical subbase material

and thickness, increasing the slab thickness resulted in increase in the change of the joint gap width. For practically similar slab thicknesses, asphalt subbase results in lower change in joint gap width than gravel subbase.

- The joint type had a significant influence on moisture ingress. On average, the moisture ingress at the unsealed joint and the hot-pour sealed joint was 34.5% and 14.2% higher than that at the silicone sealed joint.
- The pavement test sections in this study did not allow for comparison of the performance of different dowel bar arrangements under otherwise identical pavement conditions. In general, test sections with reduced dowel bar arrangement exhibited higher LTE than test sections with standard dowel bar arrangement. However, the effect of the dowel bar arrangement on LTE may not necessarily be result of the dowel bar arrangement, but rather is reflective of the age of the pavement and the stiffness of the subbase.
- The LTE at US 212 and SD 50 where the reduced dowel bar arrangement was used were relatively high. Therefore, the initial load transfer provided by the reduced dowel bar arrangement seems to be adequate.
- The IRI values of the test sections were all well within the range for new pavement. However, pavement surfaces that were treated with 1.5 times the curing compound normal application rate maintained their original smoothness over time, while the surfaces treated with the standard application rate exhibited statistically significant reduction in smoothness (increase in IRI).
- The joint faulting for all of the joints included in this study was either close to the lower limit or below the low severity faulting level as specified by the US Army Corps of Engineers paver distress manual.

Based on the results of this study, the following recommendations were made:

- Pea rock exhibits poor freeze-thaw durability and must not be used in concrete mixtures.
- The use of 1.5" top aggregate size enhances the workability of the concrete mix and should be specified by SDDOT for future JPC pavements.
- The 65/35 coarse-to-fine aggregate ratio exhibited poor workability and should not be specified for future JPC pavements.
- The two concrete mix designs presented in Appendix A exhibited optimum performance and cost (least amount of cement content). It is recommended that future mix designs for JPC pavement be based on these two mix designs.
- The use of 1.5 times the normal curing compound application rate resulted in better pavement surface smoothness over time. Therefore, SDDOT should specify the increased curing compound application rate for future JPC pavements.
- The moisture ingress at the unsealed transverse joints was significantly higher than that at the silicone sealed joints. Although the long-term effect of higher moisture ingress was not evaluated in this study, it is believed that higher moisture ingress will lead to increased pumping at the joint. It is recommended that SDDOT continue to use of silicone sealant for transverse joints.

1. INTRODUCTION

1.1 Problem Statement

Well-designed and constructed highway concrete pavements can be expected to provide excellent long term performance under a range of traffic loads and site conditions. With the rapid increase in traffic and loads, the State of South Dakota cannot afford the effects of poorly performing pavements on the state’s economy and risk road closures or reduced capacity due to frequent maintenance and repairs. It is recognized that even if a pavement is designed to the highest standards, it will not perform well if it is not constructed well. In short, quality must be built into the pavement.

Jointed plain concrete (JPC) pavements for interstate highways are common in the upper Midwest. In JPC pavements, the concrete’s dimensional changes due to thermal effects are accommodated at pre-determined saw-cut contraction joints. In the absence of properly designed joints, new concrete pavement will experience random cracking within 72 hours after placement due to plastic shrinkage caused by moisture loss. Random cracking negatively affects the long-term durability of a concrete pavement and is aesthetically displeasing. The preplanned transverse joints are saw-cut across the entire pavement width and are placed at constant intervals. The joint spacing is normally between 12 and 20 feet. Wheel load transfer at the joint between two adjacent slabs is accomplished by means of steel dowel bars embedded in the concrete at the joint location. Figure 1.1 shows a two-lane JPC pavement under construction on I-29 north of Brookings, South Dakota. Figure 1.2 shows a saw cut joint with a shrinkage crack extending along the depth of the concrete pavement.



Figure 1.1 JPC Pavement North of Brookings, SD

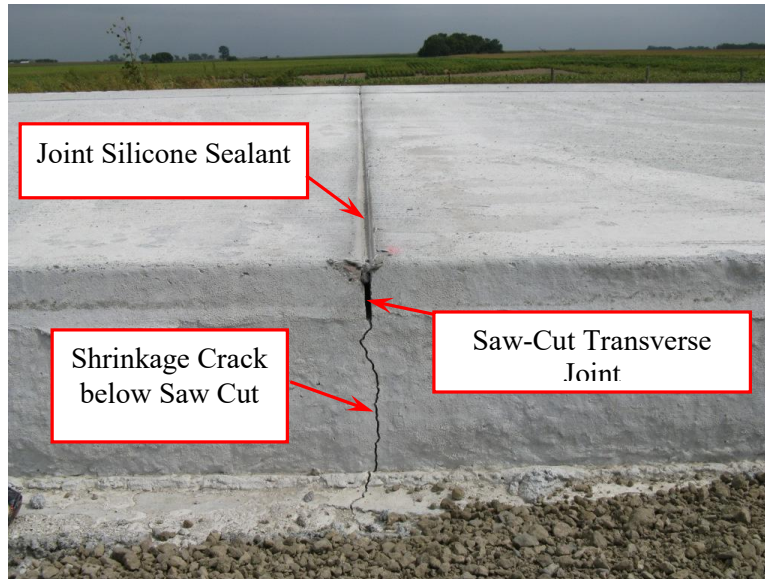


Figure 1.2 Saw-Cut Joint (with Joint Sealant)

Recent inspections of highway pavements in South Dakota revealed that once the pavements go through one to two freeze-thaw cycles, curling and warping start to occur, which could lead to uneven pavement surface and pavement cracking. The problem is compounded by repetitious joint spacing and both vehicle tires crossing the joint plane at the same time.

The South Dakota Department of Transportation (SDDOT) has not reviewed design and construction methods of JPC pavements for many years. Research is needed to review the current design and construction procedures, and examine joint performance as related to ride quality and overall pavement performance. The overall goal is to optimize current joint design and sealing practices and enhance pavement smoothness, minimizing costs and improving quality.

Currently, many state highway agencies require sealing of joints immediately after construction for JPC pavements. For many years, joint sealing has been thought to be beneficial to concrete pavement performance. Sealed joints are believed to reduce water infiltration into the pavement structure and reduce or prevent the infiltration of incompressible materials into the joints. A few highway agencies have designed and constructed JPC pavements with unsealed joints for many years. The decisions by some states to eliminate joint sealant requirements were based on in-state research indicating that sealing and resealing transverse joints was not cost-effective (Crovetti and Bischoff 2001). That is, the performance enhancement and/or life extension attributable to joint sealants did not offset additional costs associated with sealant installation and maintenance. The State of Wisconsin reported having achieved excellent overall performance for up to 25 years in JPC pavements with narrow unsealed joints (Rasmussen et al. 2007).

The effectiveness of load transfer between adjacent slabs is an important component of concrete pavements performance. Dowel bars are placed at contraction joints in rigid pavement as a mechanism for distributing traffic loads over multiple slabs through vertical shear and/or bending moments, thereby reducing stresses in the slab and the base. In Wisconsin, a reduced the number of dowels per lane was used without sacrificing the pavement performance (Rasmussen et al. 2007). In South Dakota, there is a need to study the effect of reducing the standard procedure of 12 dowels per lane to nine dowels per lane on the performance of JPC pavement.

Adequate curing helps ensure that concrete achieves and maintains its designed properties. Curing can help control moisture and temperature conditions—promote cement hydration and concrete microstructure development. There is a need to study the use of newer, more effective concrete curing compounds and/or the rate of curing compound application to minimize curling and warping while enhancing ride quality and extending service life.

Concrete mix design can have a significant effect on the durability, smoothness and cost of concrete pavements. Of the major components of Portland cement concrete, Portland cement is the most expensive. Moreover, cement is a main cause for dimensional instabilities, such as shrinkage and creep, in the concrete. Therefore, by limiting the cement content in concrete it may be possible to produce a more cost-efficient mix, while simultaneously improving some of its engineering characteristics. One way to reduce the cement content is to fill as much of the volume of concrete as possible with aggregate. Large size coarse aggregates can enhance the workability of concrete. However, research is needed to quantify the effect of large size aggregate on workability and ensure that the use of large size aggregate does not compromise the concrete engineering properties.

1.2 Objectives

Three main objectives were addressed in this study. Following is a description of those objectives.

- Review available literature and field performance of various concrete pavement designs, especially with regard to joint and sealant systems, to determine any possible beneficial changes to current practice. The work was initiated with a thorough search of available literature on concrete pavement design and performance. Parameters of particular interest during the literature search included: 1) mix design (w/c ratio, coarse aggregate size and type, coarse aggregate and pea gravel content, workability, and durability), 2) joint design (joint spacing, type and sealant), 3) dowel bars at the joints (size, number, distribution), and 4) amount of curing compound. Results of the literature search were used to provide guidance in this study. A summary of the literature search is compiled in this report.
- Develop optimized concrete mix designs incorporating larger top size aggregate and pea gravel to provide good workability at lower cement contents and resist thermal effects. Extensive laboratory work was conducted to address this objective. A wide array of concrete mixtures was batched and tested in the material laboratory at South Dakota State University. Optimum mix designs were identified and reported for future use by SDDOT.
- Construct and evaluate appropriate JPC test sections to resolve any performance issues with regard to potential changes in design or construction. Highway test sections were selected from newly constructed highway pavement sections. The test sections were monitored and tested over time to assess the pavement performance under different design conditions such as joint type and spacing, dowel bar number and configuration, and curing conditions. The test sections were identified in coordination with SDDOT research and design personnel.

1.3 Scope

The research covered in this report included experimental studies of optimized concrete mixtures for JPC pavements and field evaluation of newly constructed JPC pavement sections along South Dakota highways.

Concrete mixtures with reduced cement content and 36 combinations of coarse aggregate types, aggregate top sizes, blending aggregate types, coarse-to-fine aggregate ratios, and water/cementitious materials (w/cm) ratios were tested to develop an optimized mix for use in JPC pavement applications. Freeze-thaw durability, workability (consolidation ability), and mechanical properties of the mixes were measured and evaluated. A new energy-based experimental method for assessing the workability of concrete was devised. The method introduces a performance parameter, called “Specific Work,” to compare the workability of different concrete mixes.

Four newly constructed JPC pavement sites on South Dakota highways were selected for instrumentation, monitoring, and data collection. The four sites were located on I-29 north of Brookings in Brookings County, US 212 west of Belle Fourche in Butte County, South Dakota, 50 west of Vermillion in Yankton County, and I-29 south of Vermillion in Union County.

The parameters considered in the study included the transverse joint sealant type, the dowel bar configuration at the transverse joints, and the amount of curing compound. Three different transverse joint sealing types were incorporated in the pavement at each test site: hot-pour sealant, epoxy sealant, and green cut with no sealant (unsealed). Two dowel bar configurations at the transverse joints were included in the study. The I-29 sites were provided with normal dowel bar configuration (12 dowels per lane), whereas the US 212 and the SD 50 sites were provided with reduced dowel bar configuration (9 dowels per lane). Test sections at the test sites in Brookings, Butte, and Yankton counties were treated with increased amount of curing compound (1.5 times the normal amount).

The test site in Union County was used to only measure moisture content of the subbase under the transverse joints through the use of moisture sensors. The data collected from the Brookings County, Butte County, and Yankton County test sites were:

- Pavement surface gauge length measurements to determine change in pavement surface strain and transverse joint width
- Falling weight deflectometer (FWD) to assess the load transfer efficiency (LTE) at the transverse joint
- Profilometer measurements to evaluate the pavement ride quality through the International Roughness Index (IRI)
- Rod-and-level measurements to determine faulting at the transverse joints

2. LITERATURE REVIEW

2.1 Introduction

This section presents relevant literature regarding JPC pavement mixtures and performance. The literature review covers two main topics: (1) performance of concrete mixtures and (2) performance of JPC pavements.

2.2 Performance of Concrete Mixtures

Concrete mix designs can be optimized for cost and performance by adjusting the aggregate gradation at the top and the bottom ends of the gradation. For a given workability, increasing the maximum aggregate size often results in lower cement paste requirements (McNally 1998). This leads to more economical concrete mixes since cement is the most expensive constituent in concrete. The addition of small-size gravel produces denser gradation and improves workability. Concrete pavements in areas that experience freezing temperatures during the winter season commonly face freeze-thaw durability issues. This following presents a survey of the current understanding of the influence of aggregate properties on concrete mix performance and the factors that affect workability and freeze-thaw durability.

2.2.1 Effect of Aggregates on Mix Performance

Coarse and fine aggregate make up approximately 70–80% by volume of concrete. For this reason, aggregate characteristics, such as shape, maximum size, texture, gradation, and angularity greatly influence the properties of a concrete mix (Mindness et al. 2003).

2.2.1.1 Aggregate Size, Shape, Texture, Gradation, and Weatherability

Particle size has a significant effect on concrete properties. Larger coarse aggregates have a lower surface-to-volume ratio than smaller aggregates resulting in a decrease in the required volume of cement paste for a given w/cm. For a given mix volume, increasing the amount of coarse aggregate reduces the amount of paste. However, mixes with high quantities of coarse aggregate have low workability and finishability (McNally 1998).

Aggregate particle shape can be broadly classified as either rounded or angular. Rounded aggregate is typically comprised of natural aggregates such as river rock. Angular aggregate is typically mechanically crushed rock. Aggregate with a high surface-to-volume ratio requires more paste to achieve a given workability. Flat or elongated aggregates should be avoided due to increased surface-to-volume ratio. Additionally, flat or elongated aggregates are prone to segregation, which can reduce fatigue life of concrete pavement (Mindness et al. 2003).

Surface texture is a function of many variables including surface roughness, mineralogy, and the moisture content. Surface texture influences cement adhesion to the aggregate. Surface textures are classified as either rough or smooth. Aggregates with a rough surface create a stronger bond with the cement paste than smooth aggregate (Mindness et al. 2003).

Grading determines the paste requirements for a workable concrete. The most economical mix is one that uses the least amount of cement paste to achieve the desired mix properties. The optimum grading of the coarse aggregate depends on the maximum aggregate size. For a given cement content, the strength of

concrete increases proportionally to aggregate size due to a lower water-to-cement (w/c) ratio necessary to produce a target workability (Neville 1996).

Weatherability can be defined as aggregate resistance to the effects of weathering. Soundness, abrasability, and durability are the parameters typically related to weatherability. Soundness originally was related to the sound an aggregate emanates when struck with a dull hammer. Currently, soundness is more often related to the extent that aggregates will break up in the sulfate soundness test. The standard test to measure soundness is American Society for Testing Materials (ASTM) C 88, “Standard Test Method for Soundness of Aggregates by Use of Sodium Sulfate or Magnesium Sulfate” (ASTM 2009). Abradability refers to failure that may occur due to the wear and breakdown resulting from impact. In the case of JPC pavement, the impact typically refers to the impact of tires on the pavement over time. Durability is a measure of the concrete strength degradation over time. Two types of durability of particular interest are the freeze-thaw durability and the chemical durability. Freeze-thaw durability of concrete reflects concrete strength degradation when concrete is subjected to repeated cycles of freezing and thawing. Chemical durability, on the other hand, reflects concrete strength degradation stemming from the reaction between reactive silica in the aggregates and alkalis in the cement (Mindness et al. 2003).

2.2.1.2 Aggregate Mixture Grading

Particle size and gradation of an aggregate mixture affects the concrete’s economy, workability, and strength. The main factors governing the desired gradation are: the surface area of the aggregate, which determines the amount of water necessary to wet all the solids; the relative volume occupied by the aggregate; the workability of the mix; and the tendency for segregation.

Aggregate mixtures can be broadly classified in terms of their particle size distribution into three types:

- **Dense-Graded Mixes**

Dense-graded aggregate mixes are also known as well-graded or continuous-graded mixes. They are characterized by an even distribution of particle sizes such that finer grains can fill the voids between larger ones. The reduced void space of dense-graded mixes leads to increased concrete strength (Neville 1996).

- **Gap-Graded Mixes**

Gap-graded mixes are missing one or more intermediate size fractions, generally either coarse sand or fine gravel. Gap grading can provide a more economical mix. Less sand can be used for a given workability, lowering the w/c ratio needed for a given slump. Gap-graded concrete can result in segregation and honeycomb if there is not enough fine aggregate in the mixture. Gap-graded mixes are commonly used in architectural concrete to achieve uniform texture (Kosmatka et al. 2002).

- **Open-Graded Mixes**

Open-graded mixes, also known as no-fines mixes, are a special case of gap-grading in which the fine aggregate is omitted. Consequently, no-fines concrete lacks cohesiveness and cannot reach a void-free condition. This results in a low-strength, high-permeability material. The advantages of open-graded concrete include a low density, low drying shrinkage, and high thermal insulation. These advantages are only valid when low-strength concrete is acceptable (Mindness et al. 2003).

2.2.1.3 General Guidelines for Coarse Aggregate Gradation

Unsatisfactory gradation of the aggregates may lead to segregation, bleeding, settling of aggregates, increased use of cement, excessive use of water, higher material costs, and reduced service life. ASTM C33, “Standard Specification for Concrete Aggregates” (ASTM 2009) sets grading limits on coarse and fine aggregates. These limits for fine and coarse aggregates are summarized in Table 2.1 according to the nominal maximum aggregate size.

Table 2.1 ASTM Grading Limits for Concrete Aggregates

Fine Aggregate		Coarse Aggregate				
Sieve Size	% Passing ^a	Sieve Size	% Passing (Nominal Maximum Size)			
			1 1/2 in.	1 in.	3/4 in.	1/2 in.
3/8 in.	100	1 1/2 in.	95-100	100	—	—
No. 4	95-100	1 in.	—	95-100	100	—
No. 8	80-100	3/4 in.	35-70	—	90-100	100
No. 16	50-85	1/2 in.	—	25-60	—	90-100
No. 30	25-60	3/8 in.	10-30	—	20-55	40-70
No. 50	10-30	No. 4	0-5	0-10	0-10	0-15
No. 100	2-10	No. 8	—	0-5	0-5	0-5

^a Not more than 45% should be retained between two consecutive sieves

2.2.1.4 Previous Research on the Effects of Aggregate Gradation on Concrete Properties

Ioannides and Mills (2006)

Ioannides and Mills explored the use of larger coarse aggregates in Portland cement concrete for use in pavements. Three different aggregate gradations and two different aggregate types were used. It was observed that the gradation with the largest aggregate size had the highest 28-day compressive strength when using crushed aggregates. Ioannides and Mills concluded that coarse aggregate gradation had little effect on the mechanical properties of concrete. Therefore, larger maximum sized coarse aggregates can be used for pavements without considerably compromising the mechanical properties of the concrete.

Cramer et al. (1995)

Cramer et al. performed tests using optimized coarse aggregate gradation. The optimized gradation attempted to obtain a gradation to improve workability, durability, and strength while considering practical and economic restraints. The researchers found that the performance of the optimized gradation mixture was relatively similar to the control dense-graded aggregate mixture. The optimized mixture outperformed the gap-graded mixes by 10-20% in compressive strength. There was also a decrease as high as 15% in water demand for a given slump. The optimized mixture also resulted in higher spacing factors in the air-void system of the hardened concrete.

Baker and Scholer (1973)

Baker and Scholer performed a study to determine the effect of aggregate gradation in concrete mixes on the compressive strength. The study examined several different aggregate gradations including both gap-graded and dense graded mixtures. Results showed that variation in the gradation of smaller sized aggregates rather than larger sized aggregate had greater influence on compressive strength. Additionally, it was found that gap-graded mixes resulted in higher compressive strengths than dense-graded concrete mixes.

2.2.2 Effect of Freeze-Thaw Damage on Concrete Durability

Freeze-thaw durability is an important characteristic of concrete performance in northern climates where temperatures fall below freezing during the winter. Freeze-thaw durability is measured according to the standard method from ASTM C 666 (ASTM 2009). The test result obtained from ASTM C 666 is expressed as a durability factor (DF) for the concrete specimens tested. A DF value less than 40 suggests poor concrete durability, whereas a DF above 60 indicates satisfactory performance (Mindness et al. 2003). A common indication of freezing and thawing deterioration is the appearance of deterioration line (D-line) cracking. D-line cracks usually form near the joint between adjacent concrete slabs. The D-line cracks initiate parallel to the joints and propagate outward away from the joint as deterioration progresses. D-line cracks are caused by expansion in the voids of concrete due to the freezing of the water present in the voids. The cracks initially form along lines of equal saturation which run parallel to joints (Cordon 1966).

2.2.2.1 Factors Affecting Freeze-Thaw Durability

Factors that affect freeze-thaw durability include air content, rate of freezing, w/c ratio, concrete strength, void spacing, aggregate size, and degree of saturation. Freeze-thaw durability of concrete depends largely on the amount of air in the concrete. An air content of 5-8% is optimal for freeze-thaw resistance (ACI 2006). The correct air content will eliminate freeze-thaw deterioration in most concretes. However, other factors can decrease freeze-thaw durability. To resist freezing and thawing, the concrete w/c ratio should not exceed 0.50 and the concrete should not be subjected to cycles of freezing and thawing until obtaining a compressive strength of 3500 psi (ACI 2006).

Due to multiple sources causing freeze-thaw deterioration, complete control of the deterioration is complex. However, improved concrete construction can be achieved by following a few general rules (Cordon 1966):

- Entrain 4 to 6 percent air in all concrete exposed to surface conditions.
- Avoid aggregates having high absorption values.
- Use the minimum amount of mixing water possible.
- Allow the hydration of Portland cement to be well advanced before subjecting concrete to freezing and thawing conditions.
- Allow exposed concrete to dry before sealing the surface after the curing process.

2.2.2.2 Previous Research on Freeze-Thaw Durability

Several research studies have been performed on freeze-thaw performance of concrete pavement. Following is a summary of some relevant studies.

Cramer and Walls (2001)

Cramer and Walls performed a study for the Wisconsin Department of Transportation on strategies to enhance freeze-thaw durability. The study focused on tradeoffs between air content and w/cm ratio in freeze-thaw durability. They hypothesized that decreased w/cm would lead to increased strength and durability.

Fly ash and ground granulated blast furnace slag (GGBFS) were used as partial replacements for Type I Portland cement. Twenty-three mixes were evaluated using a modified ASTM protocol that significantly extended the evaluation period.

Cramer and Walls found that freeze-thaw durability overwhelmingly depends on the adequacy of the air void system. A minimum air content of 4% and a spacing factor of not more than 0.4 mm were necessary to avoid rapid freeze-thaw failure. Research showed, as expected, that the concrete compressive strength increased with a decrease in the w/cm; however, the concrete compressive strength showed no correlation with freeze-thaw durability. Cramer and Walls also found that reduction in w/c does not compensate for degradation in durability resulting from reductions in air content.

From their research, Cramer and Walls determined that a mix design with 6% air content and w/c of 0.4 represent an optimal mix design. They also recommended that further research be conducted on the interrelationships between shrinkage, strength and freeze/thaw deterioration.

Janssen and Snyder (1994)

Janssen and Snyder performed research to determine the effects of w/c ratios, water-reducing and air-entraining admixtures, pozzolanic admixtures, and GGBFS on the frost resistance of concrete. The study included procedures for rapid freezing and thawing, nondestructive evaluation of the damage from rapid freezing and thawing, and methods of evaluating the water pore system in hardened concrete. During their research, Janssen and Snyder developed new procedures to decrease variability of rapid freezing and thawing test results.

Janssen and Snyder created a database based on the results of the research. The database provides a relevant model for freeze-thaw behavior due to changes in pozzolan and admixture quantities.

2.2.3 Workability

The American Concrete Institute (ACI) defines workability as “that property of freshly mixed concrete which determines the ease and homogeneity with which it can be mixed, placed, consolidated, and finished” (ACI 2006). It has been customary to use the slump test as a measure of workability. The concrete slump test correlates well with the shear stress of plastic concrete. However, slump is not a good measure of workability since it is a static test and does not represent the full range of workability requirements, especially for low-slump concrete such as that used for highway pavements. Workability is affected by almost every constituent of concrete. Factors affecting workability include w/c ratio; cement type and quantity; size, shape, angularity, surface texture and gradation of aggregates; coarse-to-fine aggregate ratio; amount of entrained air and other admixtures; and the amount of time since the cement gets in contact with water. If the w/c ratio is fixed, the workability is primarily governed by the aggregate properties of size, angularity, texture and grading (Wong et al. 2000).

Several testing methods for measuring concrete workability have been developed over the years. In a Federal Highway Administration report (FHWA 2001), 21 workability testing methods, some of which have been patented, were described and evaluated to identify the most appropriate testing method(s). The evaluation was based on the following five criteria: practicality; costs; applicability to wide range of concretes; user-friendliness and simplicity; and ruggedness. Of the 21 methods, four were deemed to be candidate methods and warranted further analysis and assessment. The four methods are: (1) Free-Orifice Rheometer; (2) Moving-Object Rheometer, also known as Moving Ball Rheometer; (3) Vibrating Slope Viscometer; and (4) Colebrand Tester. The four candidate methods were further assessed in a laboratory setting. Based on the laboratory assessment, a new apparatus for measuring concrete workability, called the Vibrating-Slope Apparatus (VSA), was proposed in the FHWA report. The VSA is a modified version of the Vibrating Slope Viscometer. The VSA and the test procedure to be followed are described in the FHWA report.

2.3 Development of Deficiencies in JPC Pavements

Joints in JPC pavements are placed to control premature cracking. The four common types of joints in concrete pavements are contraction, expansion, construction, and longitudinal. Contraction joints are transverse joints used to relieve the tensile stresses that occur during curing and those resulting from contraction due to temperature change. Expansion joints are less common transverse joints and are necessary for the relief of compressive stresses from concrete expansion. Construction joints occur if the placement of fresh concrete must stop due to an emergency, machine malfunction, or any construction stoppage. Longitudinal joints are used for the relief of curling and warping stresses which may be caused by differential temperature or moisture gradients in the slab (Huang 2004). The SDDOT's Concrete Paving Manual (2010) requires joints in concrete pavements be sealed and specifies the use of types of sealants for the sealing of longitudinal and transverse joints. In general, a hot-pour elastic joint sealer is used on the longitudinal joints and a low modulus silicone sealant is used on transverse joints.

2.3.1 Pumping and Faulting

Pumping is the loss of fines under the pavement. For pumping to occur, three conditions must be present: (1) frequent heavy wheel loads, (2) an erodible soil below the joint, crack or pavement edge, and (3) saturated soil. Pumping is a load-actuated erosion incident by which fine materials and water are ejected from any opening, such as a joint or crack, in the pavement (Huang 2004). When heavy wheel loads cross the susceptible areas, pumping occurs. This process may lead to pavement cracking and faulting. Faulting is the difference in elevation across a joint or crack. It may be caused by the loss of support beneath the slab due to pumping. When load transfer at a joint is inadequate, the potential for joint faulting increases. Faulting reduces the ride quality of the roadway. The repair costs of a roadway due faulting increases the maintenance cost for that roadway dramatically. Figure 2.1 shows schematic plan and section views of positive and negative faults. Positive and negative faults are defined as decrease and increase in the pavement surface elevation, respectively, while moving in the direction of traffic (see Figure 2.1).

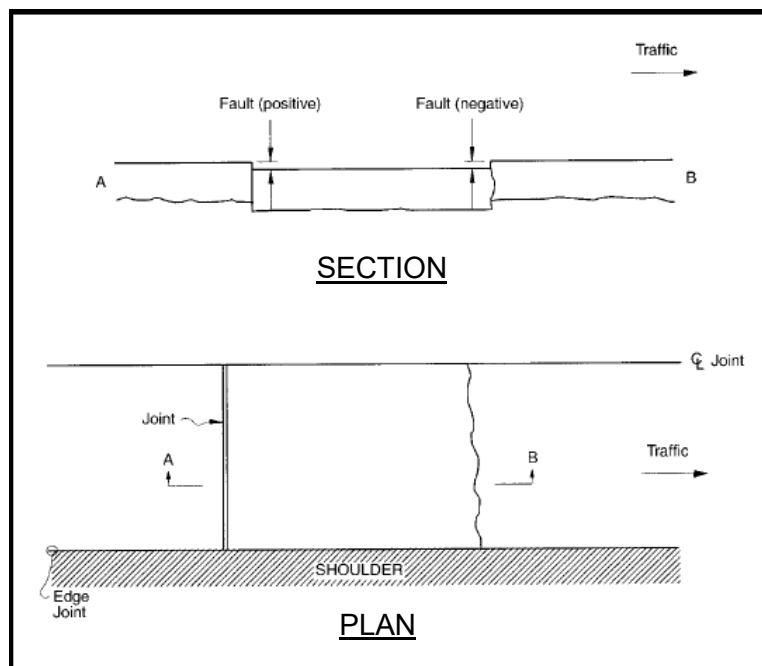


Figure 2.3 Faulting at Transverse Joints and Cracks (Miller and Bellinger 2003)

Repair methods for faulting are costly. Typical corrective measures range from grinding and subsealing with a grout at the early stages of faulting, and retrofitting with load transfer devices or full depth replacement at the late stages of faulting (Morian and Stoffels 1998).

Pumping can be detected by the presence of fine materials at joints or cracks. It can be visually detected by water or other discolorations at the pavement surface near the openings. Faulting at a joint or crack may be an indication that pumping is occurring.

2.3.2 Joint Sealant Failures

Transverse contraction joints (joints perpendicular to traffic direction) are saw-cut to allow for shrinkage and contraction resulting from moisture loss (curing) and temperature change. The saw-cut joint is normally sealed with adhesive or cohesive joint sealant. In South Dakota, it is customary to use silicone sealant (cohesive) for transverse joints and hot-pour sealant (adhesive) for longitudinal joints. Before joints can be sealed, they must be cleaned. Removal of incompressible materials (sand and small stones) is a must before sealants can be applied. According to Hall and Crovetti (2000), different methods for removing incompressible materials, include air, water, or sand blasting, can be used depending on state or local specifications. A good sealant should be able to withstand repeated expansion and contraction due to frequent heating and cooling cycles while adhering to both sides of the joint. The proper sealing of joints prevents incompressible materials from being lodged into the joint space and water from infiltration beneath the pavement. Preventing incompressible materials from entering the joint opening reduces pressure-related joint distresses, spalling, and blowups. Restricting water from infiltrating into the pavement structure reduces the occurrence of moisture-related joint distresses. Some of those distresses are pumping, faulting, corner breaking, freeze-thaw damage, and durability cracking (Hall and Crovetti 2000).

2.3.2.1 Adhesive Sealant Failures

Adhesive (bonding) sealant failures are separation of the sealant from the joint side. These failures can be identified by using a small straightedge to penetrate between the sealant and the joint sides. Adhesive sealant failure may propagate progressively along the joint leading to adhesive failure across the entire joint (Hall et al 2007). This failure primarily allows moisture to infiltrate into the joint. If severe adhesive failures occur, incompressible materials may enter the joint and the sealant may eventually pull out of the joint altogether.

2.3.2.2 Cohesive Sealant Failures

Cohesive (splitting) sealant failures are the internal splitting of the sealant material. This generally occurs at the center of the sealant in the joint. Cohesive failures are caused by an inadequate amount of sealant that is well bonded to the sides; this type of failure can be identified visually and tends to allow water and incompressible materials being forced into the joint (Hall et al 2007).

2.3.2.3 Loss of Sealant

Complete loss of sealant in a joint can occur when too much sealant had been applied to the joint. When the sealant protrudes higher than the pavement surface, the traffic will cause the sealant to be damaged by tire impact, or even pulled up by the tire treads (Hall et al 2007). Poor construction procedures are generally the cause this type of failure. Loss of sealant allows for moisture and incompressible materials to enter the joint.

2.3.3 Spalling

Longitudinal or transverse joint or crack spalling is the breaking, chipping, cracking, or fraying of edges within two feet in any direction from the face of the joint or crack. Joint spalls intersect the joint at an angle and are usually the result of the infiltration of incompressible materials into the joint (Huang 2004). Another cause of spalling is from late sawing of the joint. Spalling can also occur if joint sawing is done too early or too late. According to the South Dakota Department of Transportation (SDDOT) Paving Manual (SDDOT, 2010), contractors have a window of 4 to 24 hours to saw cut the joint. After that window has passed, there is a greater risk of spalling. Disadvantages of spalling are that spalls increase the pavement roughness, and increase the pavement rehabilitation and repair costs (Hall and Crovetto 2000). The final issue to consider with spalling is that these distresses direct water to the joints which can cause the spalls to increase in severity and cause additional moisture related joint distresses to appear. Figure 2.2 shows schematic plan and cross sectional views of joint spalling. Spalling can be classified as high (H), low (L), and moderate (M) severity spalling as shown in Figure 2.2.

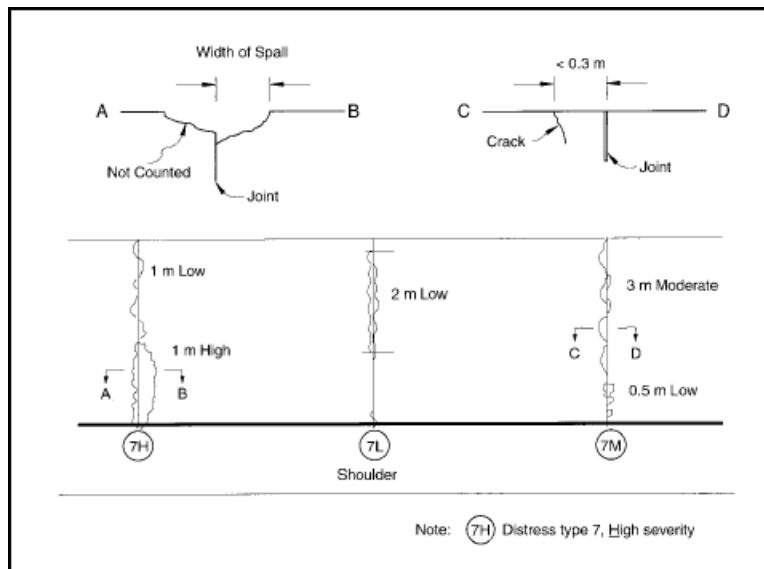


Figure 2.4 Spalling of Transverse Joints in JPC Pavements (Miller and Bellinger 2003)

2.4 Factors Affecting Performance of JPC Pavements

In the first half of the 20th century, there were concerns about controlling pumping in concrete pavements. Infiltration of moisture into joints and cracks was determined to be the primary cause of pumping. Many methods were developed to control pumping, including incorporation of new drainage features in JPC pavements, overlays and underseals of bituminous materials, and full-depth concrete replacement. By 1948, the Highway Research Board Committee on Maintenance of Concrete Pavements as Related to the Pumping Action of Slabs declared that “it has been the observation of this committee that proper filling and sealing of joints and cracks has been beneficial in minimizing pumping or delaying its recurrence.” (Allen 1948).

2.4.1 Joint Sealing

In a FHWA funded study on cost effectiveness of joint sealing, Hall et al. (2007) reported that proper installation and maintenance of joint sealants has been proven to reduce the occurrence of pumping, faulting, and corrosion of steel dowel and tie bars. Hall et al also concluded that proper joint sealing

prevents the infiltration of moisture and incompressible materials into the joint, pavement and subgrade. Incompressible materials in joints lead to distresses at joints such as blowups and spalling, which decreases load transfer across the joint. To determine cost effectiveness of transverse joint sealing, Hall et al (2007) collected data from a number of sites across the United States. At each site, a number of test sections were laid out and background information was recorded. The background information included, but was not limited to, location, year of construction, relevant design information, traffic counts, and types of sealants used. Then, each section was surveyed and evaluated. Special attention was given to joint faulting, spalling, sealant damage, and the results of the Falling Weight Deflectometer (FWD) testing. Four joint sealing types were covered in the study. The sealing types were: silicone (S), preformed (P), hot pour (H) and unsealed (U). Following is a summary of the findings.

- The FWD testing results showed that the majority of the slabs tested had poor edge support. There was no trend between the sealing method and the degree of inadequacy of the edge support and failure. However, many of the test sections in wet-freeze climate locations had areas of significant support problems.
- Unsealed joints showed the highest average joint faulting among the four joint types. However, the average faulting at all four joint types was relatively small. The average measured 1-ft faulting was approximately 1.0 mm, 0.79 mm, 0.66 mm and 0.48 mm, and for the unsealed, hot pour, preformed, and silicone joints, respectively. According to Hall et al., the results suggest that the presence of dowel bars is a more important factor in the development of joint faulting than the joint sealant type
- Unsealed joints had the highest infiltration of incompressible materials. The infiltration of fine incompressibles (as a percent of joint gap) in unsealed joints was approximately five times that in preformed joints and more than 16 times those in hot pour and silicone joints. The infiltration of coarse incompressibles in unsealed joints was more than twice that in preformed joints and more than six times those in hot-pour and silicone joints. The relatively high infiltration of incompressible material in unsealed joints suggests that unsealed joints may fail earlier than other types of joints.
- Spalling at the joints was determined as a percentage of the joint length. The measured Low-Severity spalling was found to be approximately 30%, 13%, 18%, and 11% for the unsealed, hot-pour, preformed, and silicone joints, respectively. The measured Medium-Severity spalling was found to be approximately 11%, 23%, 8%, and 5% for the unsealed, hot-pour, preformed, and silicone joints, respectively. The measured High-Severity spalling was found to be approximately 3%, 3%, 6%, and 6% for the unsealed, hot-pour, preformed, and silicone joints, respectively. The relatively high percentage of Low-Severity spalling in unsealed joints could be the result of the high infiltration of incompressible materials. The amount of High-Severity cracking was relatively small in all joint types. However, sealed joints are cut in a two-stage process and the second sawing may cause removal of some concrete edges that were damaged by the first sawing. This may explain the existence of High-Severity spalling in sealed joints.

Hall and Croveti (2000) determined that neither the presence nor the type of joint sealant were significant factors in causing joint faulting.

Shober (1996) concluded that for joint spacing between 14 and 20-feet, unsealed narrow transverse joints will have no disadvantages in three different situations: light traffic areas, heavy traffic areas with dry climates, and heavy traffic areas with doweled joints under any climate conditions.

2.4.2 Reduced Number of Dowel Bars in Transverse Joints

Dowel bars are used in concrete pavements at transverse joints to transfer traffic loads across the joint and allow the load applied to one slab to be partially carried by adjacent slabs. Adequate placement of dowel bars reduces pumping, faulting, and corner breaks in heavy traffic loads.

According to SDDOT specifications (SDDOT, 2004), the free ends of epoxy-coated dowel bars (minimum of one-half of the dowel bar length plus two inches) is given a thin uniform coating of form oil or multipurpose grease. This coating is applied within two hours of being covered by concrete. After being clearly marked, concrete paving is placed and transverse joints are cut along the centerline of the dowels. The dowels are typically placed at one-foot intervals across each lane. Common practice is to use 12 dowel bars across a 12-foot lane (SDDOT 2007). Figure 2.3 shows the typical dowel bar configuration used in South Dakota.

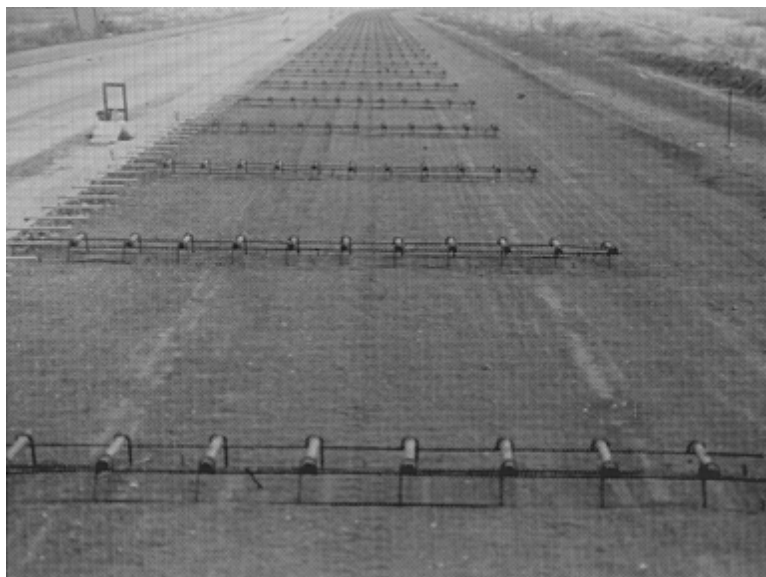


Figure 2.5 Typical Dowel Bar Configuration Used in South Dakota (SDDOT 2007)

The WisDOT funded a project to evaluate alternative concrete pavement designs beginning in 1997 (Crovetti and Bischoff 2001). The researchers not only had four alternative dowel patterns, but they also compared alternative dowel materials. One of the alternative dowel arrangements consisted of placing three dowel bars in each wheel path. As of 2000, there was no evidence to suggest that the alternative dowel bar arrangement has an effect on ride quality (Crovetti and Bischoff 2001).

2.4.3 Curing Compound Material and Amount

Concrete requires adequate moisture during curing to achieve appropriate durability. If the curing process is not allowed to occur properly, damages such as shrinkage cracking and spalling may occur. Curing compounds are applied to the surface of the freshly finished pavement to protect the pavement from environmental conditions that may increase the drying rate and the rate at which moisture is evaporated. The curing compound controls the loss of moisture needed for proper hydration of the cement and helps prevent premature cracking due to plastic shrinkage and thermal stresses (Huang 2004).

Research performed by Iowa State University (Cable et al 2003) for the Iowa Department of Transportation (IDOT) and the Iowa Highway Research Board investigated three different curing compounds at two application rates (single and double).

Based on the Iowa State University study (Cable et al 2003), weather conditions affect the time when the curing compound should be applied. In hot weather, the compound must be applied earlier after pavement is placed than in conditions with milder temperatures. Temperature control of the pavement can be accomplished by placing burlap or insulating blankets on the pavement. This proved ideal in the past; however, because that method is labor intensive, liquid membrane-forming curing compounds have been proven to provide a similar insulation with proper application. Adequate coverage of the entire surface area of the pavement is the major contributor to temperature control of curing concrete (Cable et al 2003). Cable et al (2003) reported that the most effective temperature control of the fresh pavement surface was wet curing. When curing compounds are used, the curing rate varied depending mostly on the curing compound type and not the application rate. However, the double application rates were more effective at controlling surface temperatures than the single application rates of the same compound.

The durability of concrete is an important property for pavements. Permeability of concrete can be related to the durability because it is a direct measure of the rate of entry of moisture into the pavement. Moisture infiltrating the pavement may contain chemicals that are harmful, especially in climates like South Dakotas where de-icing chemicals are necessary. It was found in the Iowa State University study that there were no statistically distinct differences in the permeability of concretes subjected to different curing methods (Cable et al 2003).

3. EVALUATION OF PAVEMENT CONCRETE MIXTURES

This section covers the experimental and analytical work done in this study to evaluate the performance of different concrete mixtures for JPC pavement applications. The experimental evaluation entailed aggregate testing, fresh concrete properties including a newly developed method for assessing workability, and hardened concrete properties including freeze-thaw durability. The experimental work was conducted at the Materials Laboratory of the Civil and Environmental Engineering Department at South Dakota State University. The analytical work was primarily limited to either assessing correlations among the different mix parameters or comparing the measured properties to expected properties as determined from empirical equations found in the literature and design codes.

3.1 Concrete Mixtures and Constituent Materials

3.1.1 Mix Design Matrix

Thirty-six different concrete mix designs were prepared and tested. The mix designs were determined in coordination with SDDOT Office of Research to study the effects of coarse aggregate type, coarse aggregate top size, 3/8 inch blending aggregate type, coarse-to-fine aggregate ratio and w/cm ratio on fresh and hardened concrete properties, including durability and workability. Following are the parameters selected in this study for design of the concrete mixes:

- Two coarse aggregate types: Del Rapids quartzite and Rapid City limestone
- Two coarse aggregate top sizes: 1.5" and 1.0"
- Three 3/8" blending aggregate types: quartzite chip, limestone chip and pea gravel
- Two coarse-to-fine aggregate ratios: 60/40 and 65/35
- Three w/cm ratios: 0.41, 0.39 and 0.37

Each mix design was labeled with a string of alpha-numeric characters representing the different parameters. Figure 3.1 shows the mix labeling scheme.

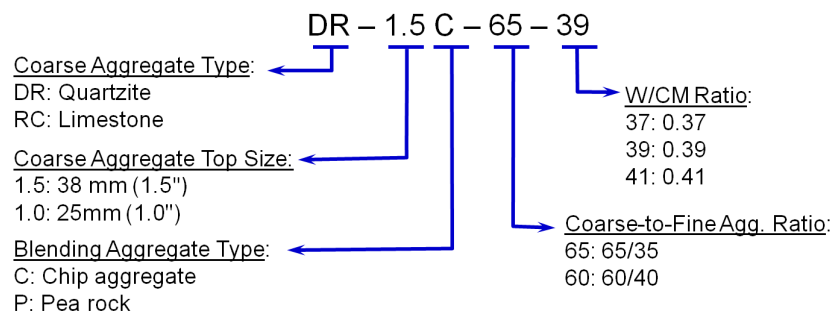


Figure 3.6 Concrete Mix Labeling

Concrete mixtures with pea rock blending aggregates were produced in only 60/40 coarse-to-fine aggregate ratio. A complete list of all 36 mixes is presented in Table 3.1.

Table 3.2 Concrete Mix Combinations and Labels

	Coarse Aggregate Max Size	3/8" Aggregate Type	Coarse-to-Fine Agg. Ratio	w/c Ratio	Mix Label
1.5" Quartzite Mixes	1.5"	Chip	60/40	0.41	DR-1.5C-60-41
	1.5"	Chip	60/40	0.39	DR-1.5C-60-39
	1.5"	Chip	60/40	0.37	DR-1.5C-60-37
	1.5"	Chip	65/35	0.41	DR-1.5C-65-41
	1.5"	Chip	65/35	0.39	DR-1.5C-65-39
	1.5"	Chip	65/35	0.37	DR-1.5C-65-37
	1.5"	Pea Rock	60/40	0.41	DR-1.5P-60-41
	1.5"	Pea Rock	60/40	0.39	DR-1.5P-60-39
	1.5"	Pea Rock	60/40	0.37	DR-1.5P-60-37
1.0" Quartzite Mixes	1.0"	Chip	60/40	0.41	DR-1.0C-60-41
	1.0"	Chip	60/40	0.39	DR-1.0C-60-39
	1.0"	Chip	60/40	0.37	DR-1.0C-60-37
	1.0"	Chip	65/35	0.41	DR-1.0C-65-41
	1.0"	Chip	65/35	0.39	DR-1.0C-65-39
	1.0"	Chip	65/35	0.37	DR-1.0C-65-37
	1.0"	Pea Rock	60/40	0.41	DR-1.0P-60-41
	1.0"	Pea Rock	60/40	0.39	DR-1.0P-60-39
	1.0"	Pea Rock	60/40	0.37	DR-1.0P-60-37
1.5" Limestone Mixes	1.5"	Chip	60/40	0.41	RC-1.5C-60-41
	1.5"	Chip	60/40	0.39	RC-1.5C-60-39
	1.5"	Chip	60/40	0.37	RC-1.5C-60-37
	1.5"	Chip	65/35	0.41	RC-1.5C-65-41
	1.5"	Chip	65/35	0.39	RC-1.5C-65-39
	1.5"	Chip	65/35	0.37	RC-1.5C-65-37
	1.5"	Pea Rock	60/40	0.41	RC-1.5P-60-41
	1.5"	Pea Rock	60/40	0.39	RC-1.5P-60-39
	1.5"	Pea Rock	60/40	0.37	RC-1.5P-60-37
1.0" Limestone Mixes	1.0"	Chip	60/40	0.41	RC-1.0C-60-41
	1.0"	Chip	60/40	0.39	RC-1.0C-60-39
	1.0"	Chip	60/40	0.37	RC-1.0C-60-37
	1.0"	Chip	65/35	0.41	RC-1.0C-65-41
	1.0"	Chip	65/35	0.39	RC-1.0C-65-39
	1.0"	Chip	65/35	0.37	RC-1.0C-65-37
	1.0"	Pea Rock	60/40	0.41	RC-1.0P-60-41
	1.0"	Pea Rock	60/40	0.39	RC-1.0P-60-39
	1.0"	Pea Rock	60/40	0.37	RC-1.0P-60-37

3.1.2 Measured Aggregate Properties

Aggregates used for preparing concrete mixtures in this study were provided by SDDOT and obtained from different locations in South Dakota. Aggregates were delivered to the materials lab at SDSU inside bins labeled for the aggregate top size. The quartzite coarse aggregates (1.5", 1.0", and 3/8" chip) were obtained from Dell Rapids, the limestone aggregates (1.5", 1.0", and 3/8" chip) were obtained from Rapid City, and the 3/8" pea rock and sand were obtained from Brookings. The quartzite, limestone, and pea rock aggregates are shown in Figure 3.2, Figure 3.3 and Figure 3.4, respectively.



Figure 3.7 Quartzite Coarse Aggregates



Figure 3.8 Limestone Coarse Aggregates

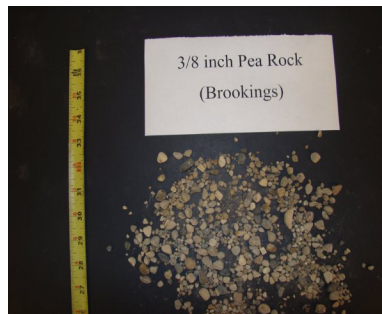


Figure 3.9 3/8" Pea Rock Coarse Aggregates

All aggregate testing was performed in accordance with ASTM standards (ASTM 2009). Sampling of the aggregates was performed according to ASTM C702: “Standard Practice for Reducing Samples of Aggregate to Testing Size.” The following tests were performed to measure the material properties of the aggregates:

- ASTM C127-07: “Standard Test Method for Density, Relative Density (Specific Gravity), and Absorption of Coarse Aggregate”
- ASTM C128-07a: “Standard Test Method for Density, Relative Density (Specific Gravity), and Absorption of Fine Aggregate”
- ASTM C136-06: “Standard Test Method for Sieve Analysis of Fine and Coarse Aggregates”
- ASTM C131-06: “Standard Test Method for Resistance to Degradation of Small-Size Coarse Aggregate by Abrasion and Impact in the Los Angeles Machine”
- ASTM C88-05: “Standard Test Method for Soundness of Aggregates by Use of Sodium Sulfate”
- ASTM C4791-05: “Standard Test Method for Flat Particles, Elongated Particles, or Flat and Elongated Particles in Coarse Aggregate”

3.1.2.1 Density, Specific Gravity, and Absorption

Three samples of each aggregate type were tested for saturated-surface dry (SSD) density, SSD specific gravity, and absorption. The average measured values are presented in Table 3.2. The values fell within expected ranges for the aggregate properties. The measured SSD specific gravity values varied between 2.59 and 2.67. A typical specific gravity of aggregate is between 2.4 and 2.9 (Kosmatka et al. 2002). The measured absorption of the fine aggregate was 1.63% while that of the course aggregates varied between 0.22 and 2.38. Typical absorption of aggregate varies between 0.2% and 2% for fine aggregate and 0.2% and 4% for course aggregate (Kosmatka et al. 2002).

Table 3.3 Measured Density, Specific Gravity, and Absorbtion

Aggregate	SSD Density (lb/ft ³)	SSD Specific Gravity	Absorption %
Dell Rapids 1.5" Quartzite	164.2	2.64	0.32
Dell Rapids 1.0" Quartzite	163.1	2.62	0.55
Dell Rapids 3/8" Quartzite	161.6	2.59	1.42
Rapid City 1.5" Limestone	166.2	2.67	0.22
Rapid City 1.0" Limestone	165.6	2.66	0.34
Rapid City 3/8" Limestone	165.5	2.66	0.43
Brookings 3/8" Pea Rock	165.8	2.66	2.38
Brookings Sand	163.7	2.63	1.63

3.1.2.2 Aggregate Gradation and Fineness Modulus

Figure 3.5 shows the measured gradation for the quartzite and limestone course aggregates labeled 1.0" and 1.5". Results indicate that the difference between the grain size distributions of the 1.0"- and 1.5"-labeled quartzite aggregates was small. The 1.5" quartzite had only 1.2% retained aggregates on the 1.5" sieve. On the other hand, the difference between 1.5"- and 1.0"-labeled limestone aggregates was noticeable; however, the 1.5" limestone had no retained aggregates on the 1.5" sieve and 78% retained on the 1.0" sieve. It should be emphasized that the reported final results in this study are limited to the material used in the study. Since different size coarse aggregates were blended to achieve the desired gradation for the concrete mixes in this study, no attempt was made in Figure 3.5 to compare the

gradation of each size coarse aggregate to SDDOT specifications. It was desired that at least 12 percent of the 1.5" aggregate was retained on the 1.0" sieve; however, the 1.5" quartzite did not meet this requirement. Therefore, additional 1.0" sized quartzite aggregate was added during mixing. The 3/8" quartzite and limestone aggregates were each separated out at the source for 100% passing the 1/2" sieve and retention on the 3/8" sieve. The tabulated sieve analysis results are given in Appendix A.

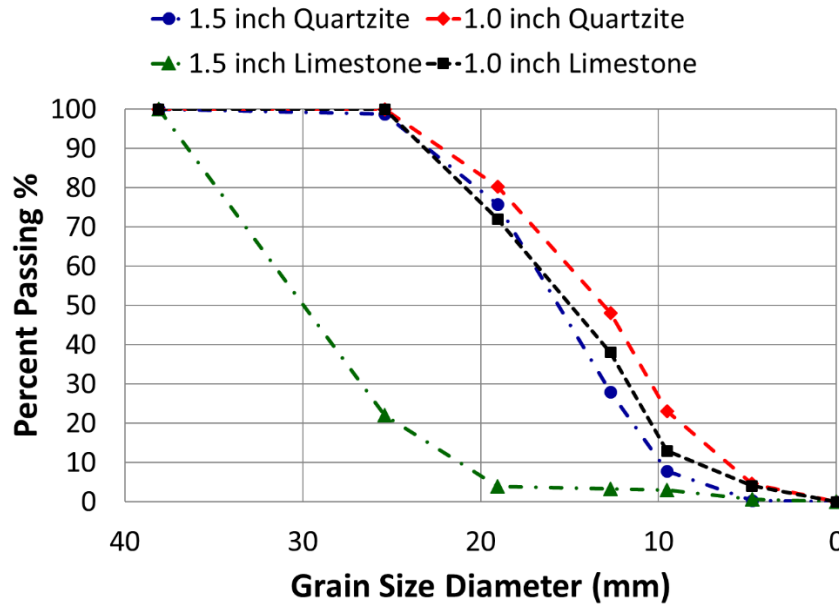


Figure 3.10 Coarse Aggregate Measured Grain Size Distribution

Figure 3.6 shows the grain size distribution for the fine aggregate. The fine aggregate gradation was compared to the SDDOT acceptable limits given in the SDDOT Standard Specification for Roads and Bridges (SDDOT 2004). The upper and lower gradation envelopes are plotted in Figure 3.6. The plots in Figure 3.6 clearly show that the fine aggregate gradation was within the SDDOT specifications acceptable gradation range. The fineness modulus of the fine aggregate was found to be 2.96.

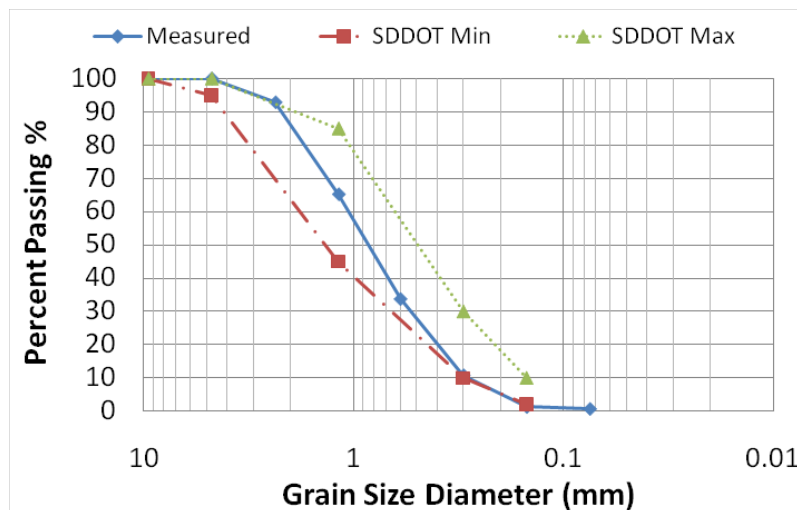


Figure 3.11 Fine Aggregate Measured Grain Size Distribution

3.1.2.3 Flat and Elongated Particles

An aspect ratio of 5:1 was considered as the lower limit for a particle to be classified as flat and elongated (SDDOT 2004). Table 3.3 lists the measured percentage of flat and elongated particles for the 1.5 inch and 1 inch maximum size aggregates. The flat, elongated, or flat and elongated particles measure percentage varied between 0 and 7 percent. The SDDOT limit on flat and elongated particles is 10 percent of the total number of particles for a 5:1 and higher aspect ratio (SDDOT 2004). The coarse aggregates used in this study were considered as non-flat and elongated.

Table 3.4 Flat and Elongated Particles Test Results

	Sieve Size	Total Particles	Flat	Elongated	Both
Quartzite-1.5"	1"	100	6	1	0
	3/4"	100	5	1	1
	1/2"	100	6	2	0
Quartzite-1.0"	1"	100	5	0	0
	3/4"	100	5	1	0
	1/2"	100	6	2	0
Limestone-1.5"	1.5"	100	4	2	0
	1"	100	6	1	0
Limestone-1.0"	1"	100	7	1	0
	3/4"	100	5	2	0
	1/2"	100	4	2	0

*** Note: Aspect ratio of 5:1 was used for all tests ***

3.1.2.4 Resistance to degradation

The resistance to degradation test was performed on the 1.5" maximum size limestone aggregate. Quartzite is less susceptible to abrasion than limestone. No degradation tests were performed on the quartzite aggregate. The measured average percentage weight loss of the limestone aggregate was 34 percent. Table 3.4 shows information relevant to the material and test results. The maximum degradation loss allowed by SDDOT is 40 percent (SDDOT 2004). Therefore, the limestone aggregate used in this study met the degradation resistance required by SDDOT.

Table 3.5 Loss by Abrasion and Impact in the Los Angeles Machine

Aggregate Source	Rapid City
Aggregate Type	Limestone
Nominal Max Size (inches)	1.5
Grading ¹	A
Average Percent Loss	34

¹ Grading designation from Table 1 in ASTM C131-06

3.1.2.5 Soundness of Aggregates

The sodium sulfate soundness of aggregates test was performed on the pea rock aggregate. The SDDOT maximum acceptable loss after five cycles of the sodium sulfate soundness test is 10 percent (SDDOT 2004). The experimental results, summarized in Table 3.5, show a sodium sulfate soundness of 6.3 percent. Therefore, the pea rock met the SDDOT requirements for soundness of aggregates.

Table 3.6 Sodium Sulfate Soundness Test of Pea Rock

Sieve Size	Grading of Original Sample, %	Weight of Test Fractions Before Test, g	Percentage Passing Designated Sieve After Test	Weighted Percentage Loss
Minus No. 100	0.3
No. 50 to No. 100	0.1
No. 30 to No. 50	0.1
No. 16 to No. 30	0.5	...	12.0	0.1
No. 8 to No. 16	6	100	12.0	0.7
No. 4 to No. 8	37	100	8.3	3.1
3/8 inch to No. 4	56	100	4.2	2.4
Totals	100			6.3

3.1.3 Mix Design

The cement used to prepare the concrete mixes was GCC Dacotah Type I/II cement. The fly ash was Headwaters class F fly ash. The air entrainer was Daravair M[®]. Literature on the cement, fly ash, and air entrainer can be found in Appendix B. The amount of air entrainer was adjusted for each mix to maintain the same amount of entrained air in the different mixes. Mix designs are shown in Table 3.6 and Table 3.7 for the quartzite and limestone aggregate mixes, respectively.

Table 3.7 Mix Design – Quartzite Aggregate Mixtures

	DR-1.5C-60	DR-1.5C-65	DR-1.5P-60	DR-1.0C-60	DR-1.0C-65	DR-1.0P-60
1.5" Coarse, lb/cu yd	876	922	876	0	0	0
1.0" Coarse, lb/cu yd	664	687	664	1625	1699	1625
3/8" Chip, lb/cu yd	331	353	0	280	300	0
Pea Rock, lb/cu yd	0	0	331	0	0	280
Fine, lb/cu yd	1148	1056	1148	1170	1076	1170
Cement, lb/cu yd	460					
Fly Ash, lb/cu yd	115					
w/cm ratio	0.41 0.39 0.37					
Water, lb/cu yd	236 with w/c = 0.41 224 with w/c = 0.39 213 with w/c = 0.37					
Daravair M, oz/cmwt	1.10	1.10	1.10	1.00	1.00	1.00

Table 3.8 Mix Design – Limestone Aggregate Mixtures

	RC-1.5C-60	RC-1.5C-65	RC-1.5P-60	RC-1.0C-60	RC-1.0C-65	RC-1.0P-60
1.5" Coarse, lb/cu yd	720	774	720	0	0	0
1.0" Coarse, lb/cu yd	535	575	535	1625	1699	1625
3/8" Chip, lb/cu yd	591	635	0	280	300	0
Pea Rock, lb/cu yd	0	0	591	0	0	280
Fine, lb/cu yd	1230	1092	1230	1170	1076	1170
Cement, lb/cu yd	460					
Fly Ash, lb/cu yd	115					
w/cm ratio	41 39 37					
Water, lb/cu yd	236 with w/c = 0.41 224 with w/c = 0.39 213 with w/c = 0.37					
Daravair M, oz/cmwt	1.00	1.00	1.00	0.85	0.85	0.85

The combined aggregate total gradation for the quartzite and limestone mixes are shown in Figure 3.7 and Figure 3.8, respectively.

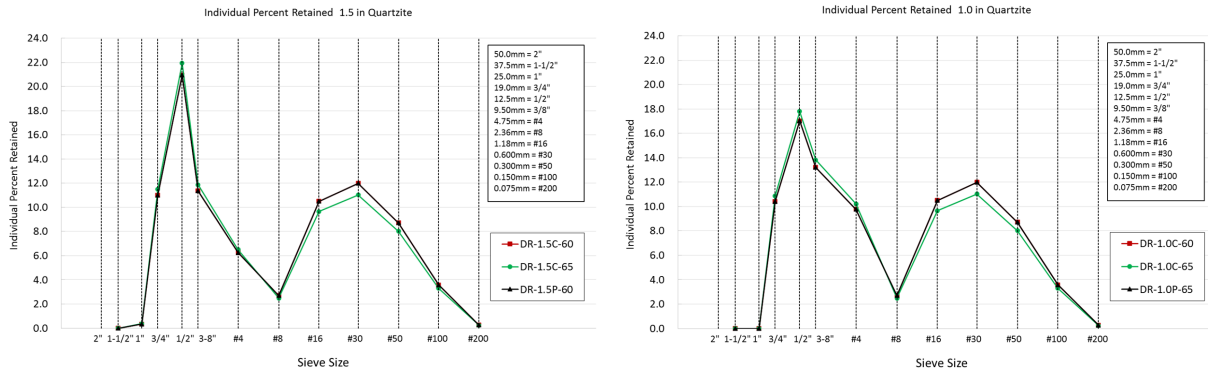


Figure 3.12 Combined Total Aggregate Gradation for the Quartzite Aggregate Mixes

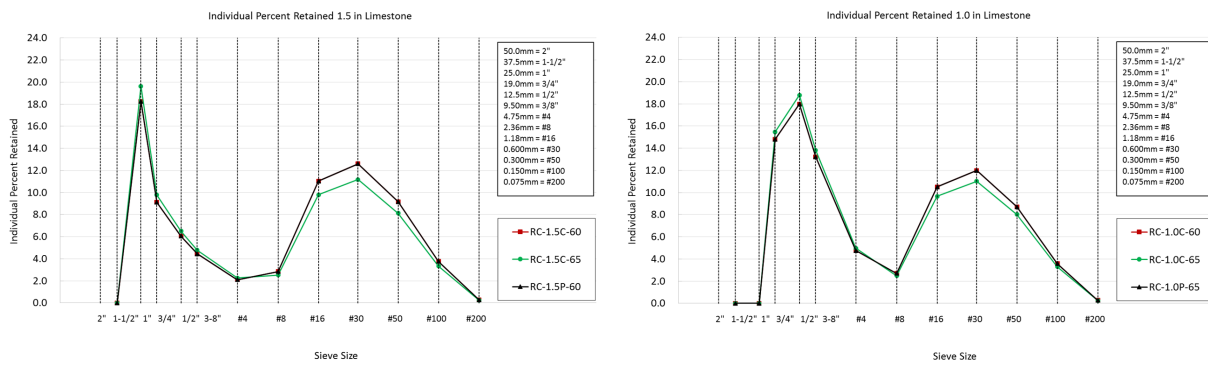


Figure 3.13 Combined Total Aggregate Gradation for the Limestone Aggregate Mixes

The plots in Figure 3.7 and Figure 3.8 clearly indicate a gap in the gradation with two humps and a valley at the #8 sieve. The first peak occurred at 1" for the 1.5" maximum size limestone aggregate gradation and at 1/2" for the other three gradations. The second peak occurred at the #30 sieve for all mixes. The 1.5" maximum size quartzite aggregate mix gradation clearly shows that large-size aggregate (1.5" and 1") content was negligible.

The 0.45 Power gradation for the coarse quartzite and limestone aggregate mixes are shown in Figure 3.9 and Figure 3.10, respectively.

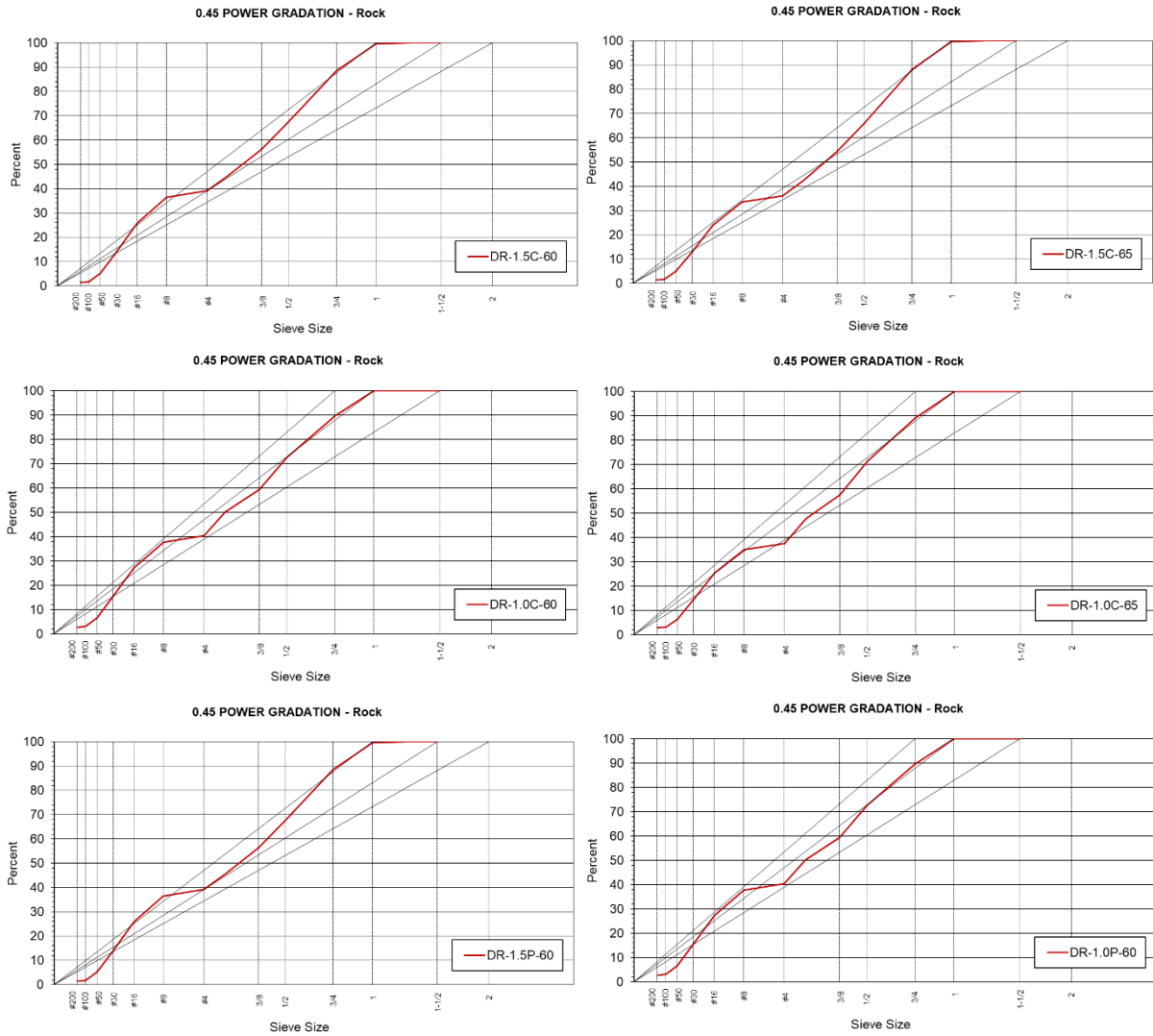


Figure 3.14 0.45 Power Gradation for the Coarse Aggregates of the Quartzite Mixes

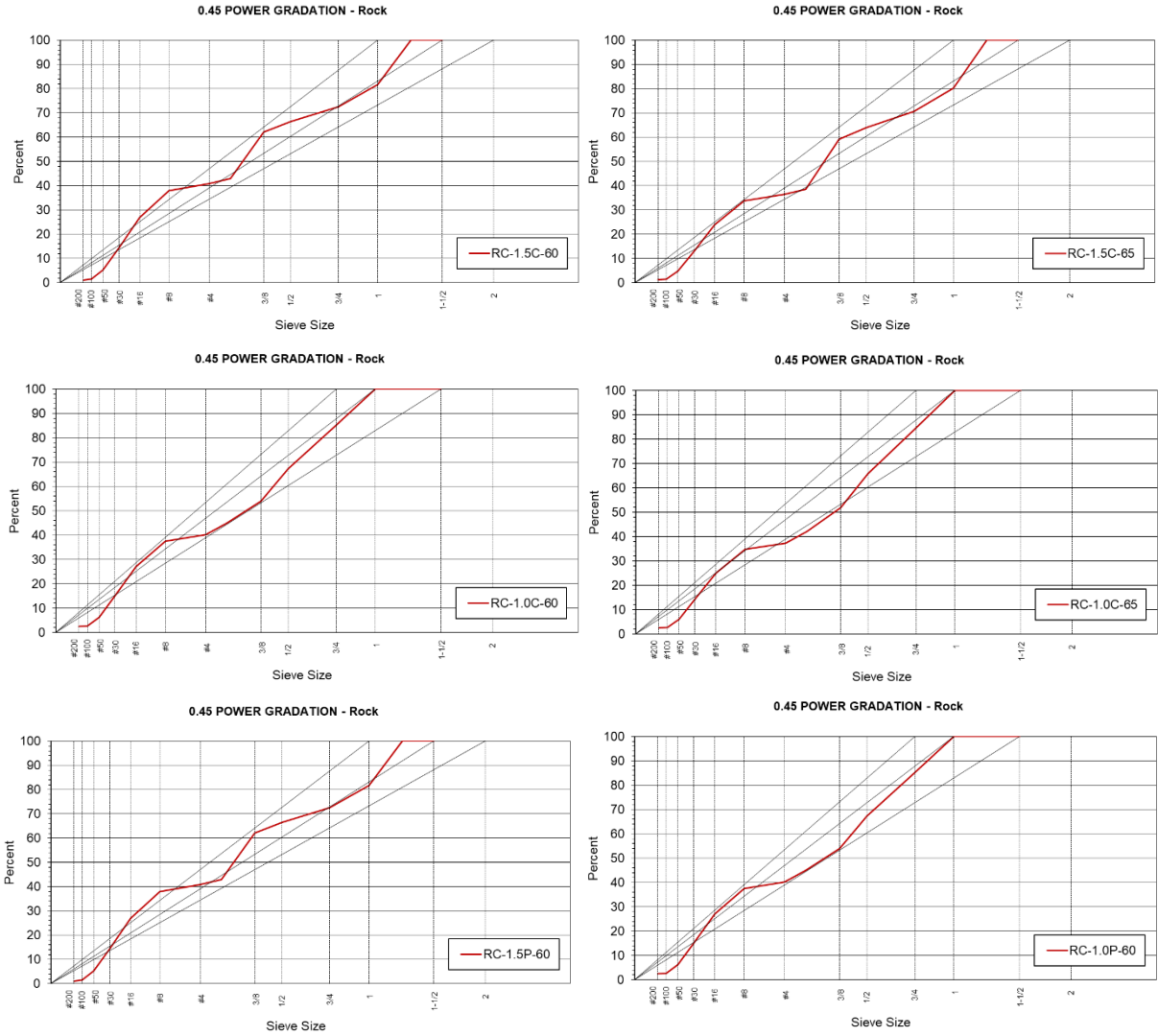


Figure 3.15 0.45 Power Gradation for the Coarse Aggregates of the Limestone Mixes

The coarseness factor (workability) charts for the quartzite aggregate and limestone aggregate mixes are shown in Figure 3.11 and Figure 3.12, respectively. The charts indicate that all mixes plotted in Zone II which is ideal for slabs on ground (Harrison, 2004).

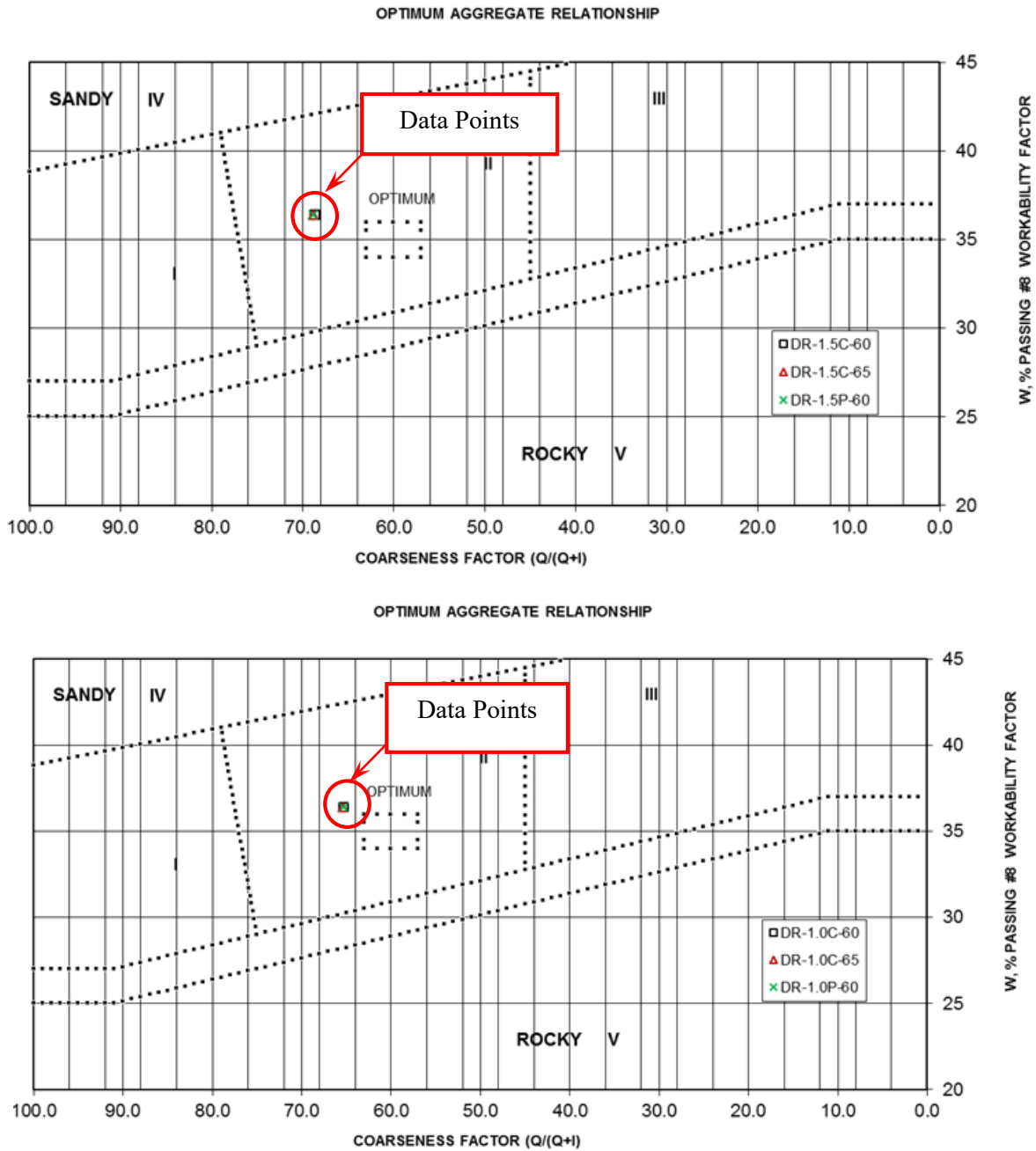


Figure 3.16 Coarseness Factor Charts for the Quartzite Aggregate Mixes

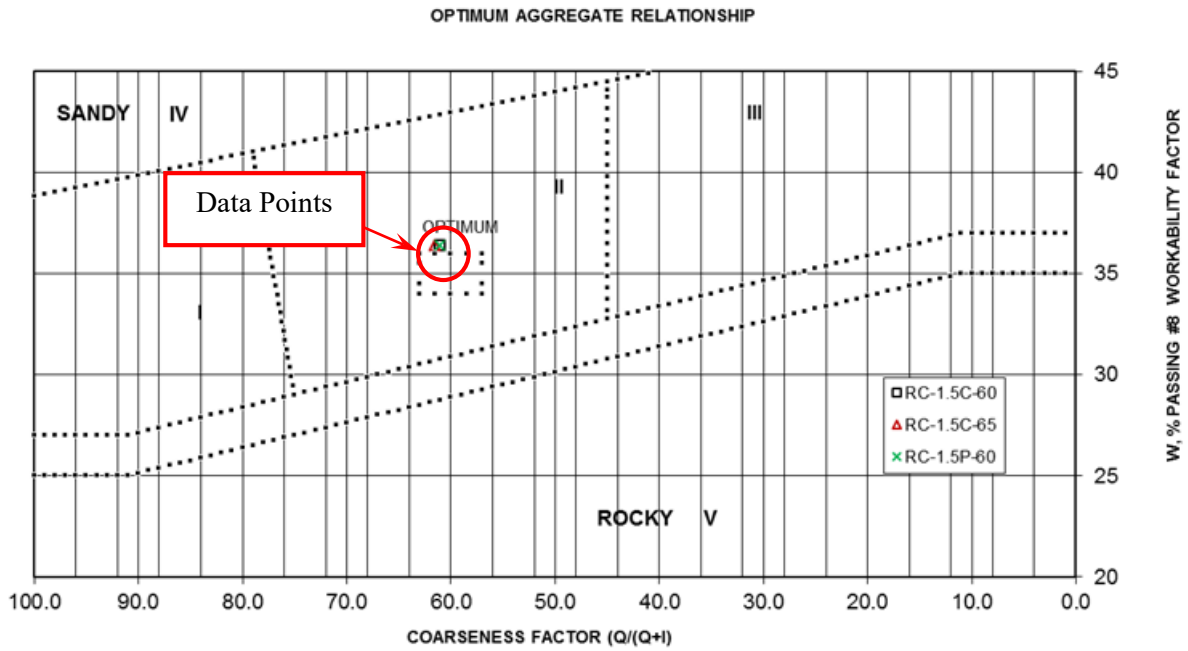


Figure 3.17 Coarseness Factor Charts for the Limestone Aggregate Mixes

3.2 Measured Fresh Concrete Properties

A tilt-drum concrete mixer was used to prepare the fresh concrete mixes. The mixer drum was fitted with three paddles and had a capacity of 0.4 cubic yards; however, the maximum batch size was limited to only 0.15 cubic yards to allow the concrete to mix well without spilling.

The fresh concrete was tested to evaluate slump, air content, mix temperature and workability. The concrete was sampled according to ASTM C172-08, "Standard Practice for Sampling Freshly Mixed Concrete" (ASTM 2009), with some modifications to accommodate laboratory conditions. According to ASTM C172, two or more samples should be taken from the middle of a batch for testing. This could not be followed due to the small size of the concrete mixer. The mixer yielded batch sizes of approximately 0.15 yd³. Therefore, the entire batch was used for testing. The slump, air content and temperature tests were performed within the first 15 minutes of sampling in accordance with ASTM C172.

Testing for slump, air content, and temperature was performed in accordance with the following ASTM standards (ASTM 2009):

- ASTM C143-08: "Standard Test Method for Slump of Hydraulic-Cement Concrete"
- ASTM C231-08: "Standard Test Method for Air Content of Freshly Mixed Concrete by the Pressure Method"
- ASTM C 1064-08: "Standard Test Method for Temperature of Freshly Mixed Hydraulic-Cement Concrete"

A new test method was developed and used in this study to measure the workability of freshly mixed concrete. The method and apparatus used for the workability test are presented in Section 3.2.2.1. The same mixing procedure was followed for the preparation of all the mixes developed in this research. The mixer drum was first moistened to prevent the absorption of mixing water to the drum. The dry ingredients (coarse aggregate, fine aggregate, fly ash, and cement) were added to the mixer. The air entrainer was added to the mixing water. Once the dry ingredients were well mixed the water and air entrainer were added to the mixer. The concrete was mixed for five minutes and then discharged from the mixer for sampling and testing of fresh properties and consolidation. A modified mixing protocol that captures realistic conditions in the field was used for the preparation of additional consolidation tests. In the modified protocol, the concrete is initially mixed for three minutes before the mixer is stopped and covered with wet burlap for two minutes. The burlap is then removed and the mixer is run for an additional three minutes. The slump, unit weight, air content and temperature are recorded immediately after mixing. The concrete in the mixer is covered again with wet burlap and allowed to sit for a time period of 20 minutes before performing an additional slump test. After the second slump test is completed, the workability test is performed.

3.2.1 Slump, Air Content, and Mix Temperature

After testing and analyzing the freeze-thaw performance of the pea rock mixes with quartzite, it was found that the pea rock concrete mixes underwent significant deterioration. The researchers and the SDDOT Office of Research determined there was no value in testing the remaining pea rock mixes. The measured fresh concrete properties are summarized in Table 3.8. Blank spaces in the table represent the pea rock mixes eliminated from the original mix design matrix.

The measured slump varied between 1.0" and 4.5". SDDOT Standard Specifications for Roads and Bridges (SDDOT, 2004) specifies concrete slump for the slip form paving method to be not more than 2" and for the stationary side form method to be between 1 and 3-inches. Many of the measured slump values were above the specified upper limits for concrete paving. However, the concrete samples for the

slump tests— mostly collected from small concrete batches discharged immediately after mixing the concrete for five minutes—may not be representative of actual site conditions. The modified mixing protocol described above (Section 3.2) and used for preparing four additional mixes (see footnotes of Table 3.8) resulted in reduced slump measurements. Thus, the modified mixing protocol would probably result in more slump measurements being in the specified limits. The measured unit weight varied between 137.4 lb/ft³ and 145.8 lb/ft³. The measured air content varied between 5.50% and 7.50%. The measured air content values were in the SDDOT acceptable limits of +1% and -1.5% of the target air content of 6.50% (SDDOT 2004). The mix temperature varied between 65°F and 81°F. This wide range of concrete temperatures was due to the long mixing schedule which spanned over nine months. The measured mix temperatures were all in the acceptable limits of 50°F – 90°F for pavement applications (SDDOT 2004).

Table 3.9 Measured Slump, Air Content, and Mix Temperature

Mix ID†	Slump (in)	Unit Weight (pcf)	Air Content (%)	Temperature (°F)
DR-1.5C-60-41	3.50	140.3	6.00	80
DR-1.5C-60-39	2.50	144.5	5.50	79
DR-1.5C-60-37	1.00	143.2	5.75	80
DR-1.5C-65-41	3.25	139.9	6.50	77
DR-1.5C-65-39	2.00	138.4	5.75	78
DR-1.5C-65-37	1.75	142.0	5.50	73
DR-1.5P-60-41	3.50	144.8	6.00	81
DR-1.5P-60-39	2.50	142.0	5.50	79
DR-1.5P-60-37	1.00	143.9	5.75	80
DR-1.0C-60-41	3.50	147.3	6.50	74
DR-1.0C-60-39	4.50	145.8	7.00	71
DR-1.0C-60-37	1.00	143.0	6.25	70
DR-1.0C-65-41	3.50	141.2	5.75	68
DR-1.0C-65-39	2.25	143.2	6.50	72
DR-1.0C-65-37	2.00	144.4	5.50	72
DR-1.0P-60-41	2.75	145.2	5.75	79
DR-1.0P-60-39	2.50	141.3	5.50	79
DR-1.0P-60-37	1.50	145.4	6.00	73
RC-1.5C-60-41	4.00	141.8	7.50	72
RC-1.5C-60-39	3.00	142.5	7.50	73
RC-1.5C-60-37	2.50	140.1	6.00	70
RC-1.5C-65-41	3.50	142.7	5.75	67
RC-1.5C-65-39	3.50	141.3	7.25	66
RC-1.5C-65-37	2.75	140.5	7.50	65
RC-1.0C-60-41	4.50	143.1	7.50	70
RC-1.0C-60-39	3.50	140.6	7.50	69
RC-1.0C-60-37	3.00	140.7	7.50	65
RC-1.0C-65-41	4.00	137.7	7.50	69
RC-1.0C-65-39	3.50	137.4	6.75	70
RC-1.0C-65-37	2.50	146.2	5.75	69
RC-1.0P-60-41	3.50	143.0	6.00	71
RC-1.0P-60-39	2.50	142.6	6.25	70
DR-1.0C-60-39‡	2.75 (initial) 2.25 (after 20 min.)	147.2	5.75	Not Measured
DR-1.0C-60-37‡	2.50 (initial) 1.25 (after 20 min.)	144.5	7.00	Not Measured
DR-1.5C-60-39‡	2.75 (initial) 2.50 (after 20 min.)	135.0	7.50	Not Measured
DR-1.5C-60-37‡	2.25 (initial) 1.25 (after 20 min.)	145.0	7.00	Not Measured

†RC-1.5P-60-41, RC-1.5P-60-39, RC-1.5P-60-37, and RC-1.0P-60-37 were not tested

‡Tested using the modified test procedure

3.2.2 Concrete Workability

3.2.2.1 The Specific Work Method for Measuring Workability

Concrete mixtures used for highway pavement are normally stiff with slump values ranging between one and three inches. Due to this narrow slump range, the slump test would not constitute a reliable measure to compare concrete workability. The literature review conducted in this study (Section 2.2.3) did not reveal any commonly accepted rigorous test method that can be used in lieu of the slump test. The FHWA report on concrete workability (FHWA 2001) proposes the development of a vibrating slope apparatus (VBA) for measuring concrete workability; however, to the best knowledge of the researchers, no such apparatus has been standardized. Therefore, a new test method was devised in this study to measure the work required to displace and consolidate a given amount of fresh concrete. The “Specific Work” is obtained by normalizing the measured work with respect to the weight of the specimen. Since the unit of work is “(Force) x (Length)” and the unit of weight is “Force,” then specific work can be expressed in units of “Length”. Measured specific work provides comparative evaluation of the workability of different concrete mixtures. Higher specific work values indicate lower concrete workability. This test method can be used in a laboratory setting.

An apparatus was designed and used in this study for measuring the work required to displace fresh concrete. The apparatus consists of a 36" long by 12" wide by 12" high hollow steel box and a hydraulic actuator. A schematic diagram of the steel box is shown in Figure 3.13. The box's bottom, sides and top are made of 6-gauge steel plates. On one end, the top side of the box is fitted with a 12" by 12" overflow opening. One of the narrow sides (12" by 12") is left open to allow for insertion of a push plate. The push plate consists of a 1-inch thick steel plate sized slightly narrower than a 12-inch square opening. The push plate is attached to a hydraulic actuator head on one side and to a 3/4-inch thick rubber squeegee pad on the other. The hydraulic actuator is used to drive the push plate and the squeegee pad inside the box. The squeegee pad is sized to provide a tight clearance between the plate edges and the interior surfaces of the box. Thus, the squeegee plate can be pushed to slide inside the box with negligible force.

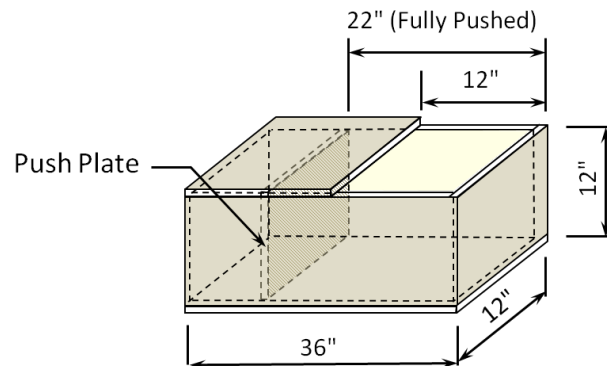
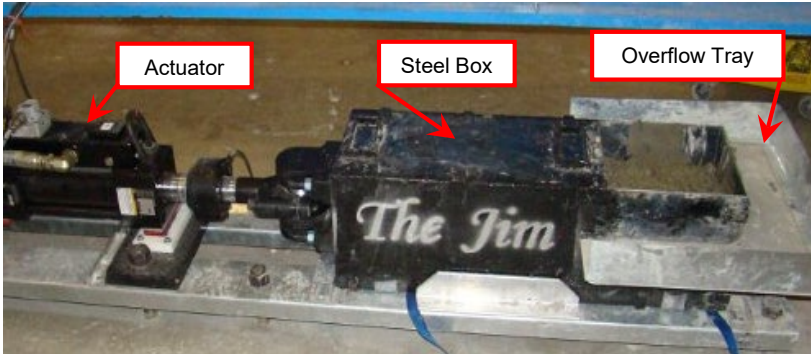


Figure 3.18 Steel Box Configuration

Figure 3.14 shows the workability apparatus during a test. The workability test starts by retracting the push plate and the squeegee to 4 inches from the end of the box. A fresh concrete specimen of approximately 1.5 cubic feet is weighed and placed in one lift inside the box. The concrete specimen in the box is vibrated slightly until a roughly level surface is achieved. The actuator head is then advanced forward, pushing and displacing the concrete in front of the squeegee pad. The actuator head is moved at a uniform speed of one-half-inch per second for a total distance of 10 inches. As the concrete gets

displaced and consolidated inside the box, the excess concrete overflows through the top opening. The actuator load and displacement are recorded at approximately one-half-inch displacement intervals.



Workability Test Apparatus at the Beginning of the Test



Concrete Sample During the Test



Concrete Overflow at the End of the Test

Figure 3.19 Concrete Workability Test Apparatus

Figure 3.15 shows a schematic plot of the measured load-displacement data. The area under the load-displacement curve is the work done on the fresh concrete specimen. The measured specific work can be determined for different concrete mixes to compare their workability and consolidation ability.

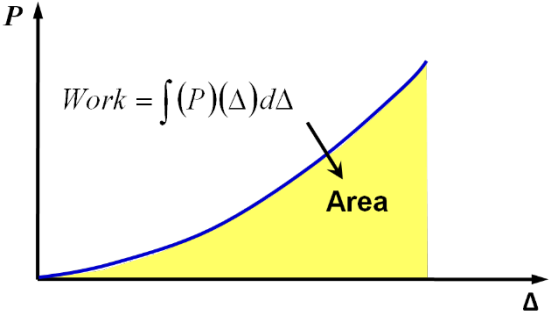


Figure 3.20 Schematic Plot of a Workability Test Load-Displacement Data

3.2.2.2 Workability Test Results

Freshly mixed concrete specimens were tested for workability using the test apparatus and procedure described in Section 3.2.2.1. Figure 3.16 shows a plot of the test data for four different concrete mixtures. The area under each curve represents the work done on the respective concrete specimen. Using the measured work, the specific work was determined for each mix combination of the mix design matrix described in Section 3.1.1. Table 3.9 presents a summary of the specific work values obtained from the workability test.

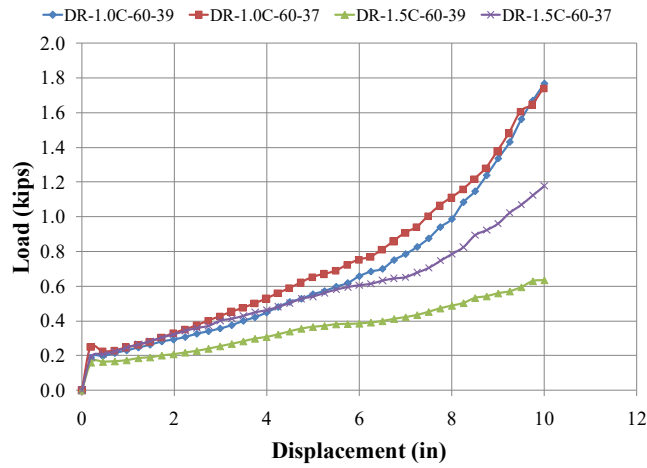


Figure 3.21 Measured Load-Displacement of Four Workability Tests

Table 3.10 Workability Test Results

Mix ID	Specific Work (in)
DR-1.5C-60-41	25.23
DR-1.5C-60-39	18.90
DR-1.5C-60-37	25.15
DR-1.5C-65-41	25.30
DR-1.5C-65-39	15.15
DR-1.5C-65-37	14.66
DR-1.5P-60-41	44.08
DR-1.5P-60-39	25.99
DR-1.5P-60-37	19.39
DR-1.0P-60-41	18.46
DR-1.0P-60-39	23.10
DR-1.0P-60-37	17.18
DR-1.0C-60-41	69.57
DR-1.0C-60-39	55.71
DR-1.0C-60-37	61.81
DR-1.0C-65-41	172.93
DR-1.0C-65-39	180.69
DR-1.0C-65-37	230.99
DR-1.5C-60-39†	22.66
DR-1.5C-60-37†	34.75
DR-1.0C-60-39†	43.22
DR-1.0C-60-37†	39.67

Mix ID	Specific Work (in)
RC-1.5C-60-41	19.69
RC-1.5C-60-39	18.18
RC-1.5C-60-37	17.60
RC-1.5C-65-41	31.60
RC-1.5C-65-39	20.45
RC-1.5C-65-37	20.57
RC-1.5P-60-41	15.03
RC-1.5P-60-39	15.85
RC-1.5P-60-37	18.01
RC-1.0P-60-41	22.12
RC-1.0P-60-39	21.45
RC-1.0P-60-37	27.67
RC-1.0C-60-41	34.01
RC-1.0C-60-39	24.11
RC-1.0C-60-37	36.95
RC-1.0C-65-41	69.08
RC-1.0C-65-39	63.81
RC-1.0C-65-37	65.21

†Tested in accordance with the modified mixing protocol (Section 3.2)

3.3 Measured Hardened Concrete Properties

The hardened concrete was tested to evaluate compressive strength, flexural strength, and freeze-thaw durability. Preparation of the concrete testing specimens was done according to ASTM C 192-07: “Standard Practice for Making and Curing Concrete Test Specimens in the Laboratory” (ASTM 2009). Testing for compressive strength, flexural strength, and freeze-thaw durability was performed in accordance with the following ASTM standards (ASTM 2009):

- ASTM C39: “Standard Test Method for Compressive Strength of Cylindrical Concrete Specimens”
- ASTM C78: “Standard Test Method for Flexural Strength of Concrete”
- ASTM C215: “Standard Test Method for Fundamental Transverse, Longitudinal, and Torsional Resonant Frequencies of Concrete Specimens” and ASTM C666: “Standard Test Method for Resistance of Concrete to Rapid Freezing and Thawing”

3.3.1 Compressive Strength

Standard 6- by 12-inch concrete cylinders were prepared and tested for compressive strength. All concrete cylinders were moist cured. The compressive strength was measured at 7 and 28 days. Three cylinders of each mix were tested at each age. The measured average compressive strength for each mix is shown in Table 3.10 and Table 3.11 for the limestone and quartzite aggregate mixes, respectively.

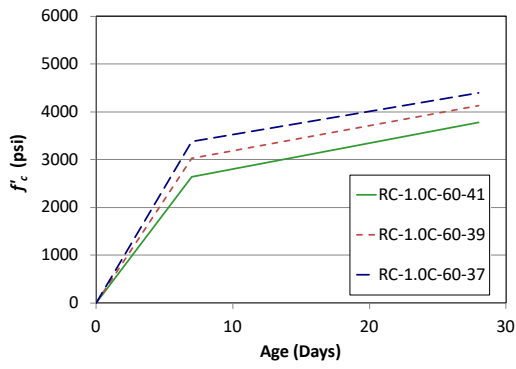
Table 3.11 Average Compressive Strength for the Limestone Aggregate Mixes

Mix ID	Average Compressive Strength (psi)	
	7-Day	28-Day
RC-1.5C-60-41	2134.3	3354.0
RC-1.5C-60-39	3112.4	4179.3
RC-1.5C-60-37	4073.2	5566.9
RC-1.5C-65-41	2481.6	3275.5
RC-1.5C-65-39	2718.6	3660.6
RC-1.5C-65-37	2782.3	3699.9
RC-1.0P-60-41	3253.8	4556.5
RC-1.0P-60-39	3961.2	5523.3
RC-1.0C-60-41	2636.1	3777.3
RC-1.0C-60-39	3020.4	4132.1
RC-1.0C-60-37	3371.7	4391.5
RC-1.0C-65-41	2688.0	3943.5
RC-1.0C-65-39	3153.6	4303.1
RC-1.0C-65-37	4250.0	5670.6

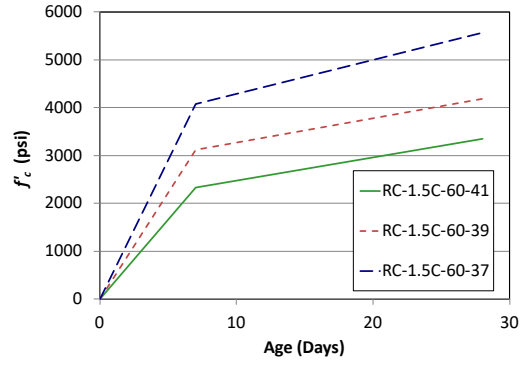
Table 3.12 Average Compressive Strength for the Quartzite Aggregate Mixes

Mix ID	Average Compressive Strength (psi)	
	7-Day	28-Day
DR-1.5C-60-41	2731.8	3624.8
DR-1.5C-60-39	3436.2	4305.7
DR-1.5C-60-37	4070.7	5018.3
DR-1.5C-65-41	2451.2	3373.6
DR-1.5C-65-39	3477.1	4528.8
DR-1.5C-65-37	3408.2	4460.1
DR-1.5P-60-41	1513.7	2162.3
DR-1.5P-60-39	2053.9	2808.4
DR-1.5P-60-37	3688.3	4885.4
DR-1.0P-60-41	3439.9	4377.7
DR-1.0P-60-39	3598.5	4730.7
DR-1.0P-60-37	4130.4	5415.3
DR-1.0C-60-41	2272.4	3029.8
DR-1.0C-60-39	2451.2	3513.0
DR-1.0C-60-37	4726.7	6293.7
DR-1.0C-65-41	2745.4	3858.0
DR-1.0C-65-39	3247.9	4239.7
DR-1.0C-65-37	3978.9	5326.4

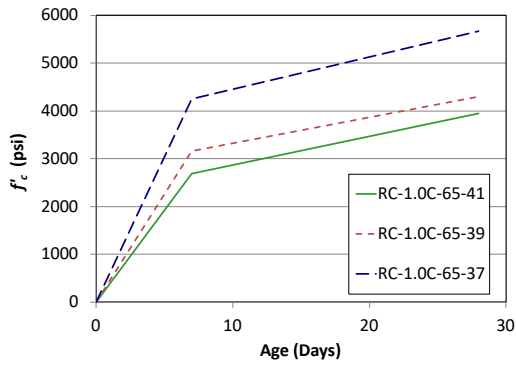
Plots of the average compressive strength gain with age for the limestone and the quartzite aggregate mixes are shown in Figure 3.17 and Figure 3.18, respectively. These plots, which are based on only two data points, the 7- and 28-day strengths, do not represent the exact strength gain profile; however, they provide a good visual tool to compare and verify trends of the compressive strength of the different mixtures. For each of the concrete mix combinations tested in this study, concrete strength increased with a decrease in w/c.



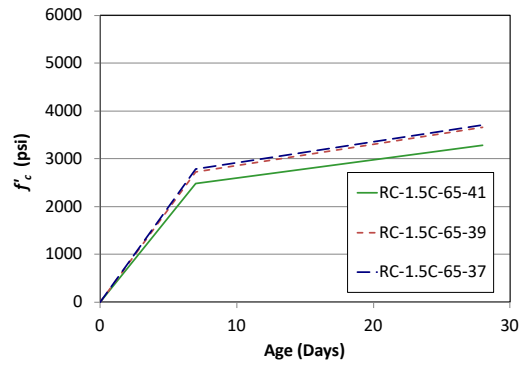
RC-1.0C-60



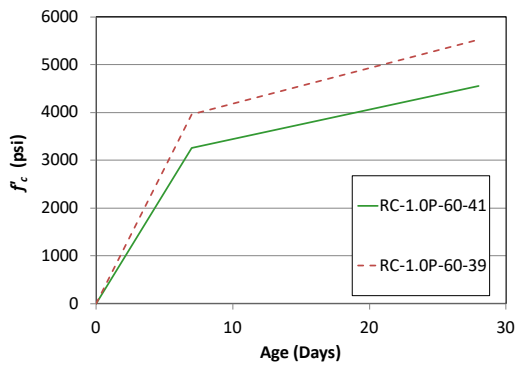
RC-1.5C-60



RC-1.0C-65

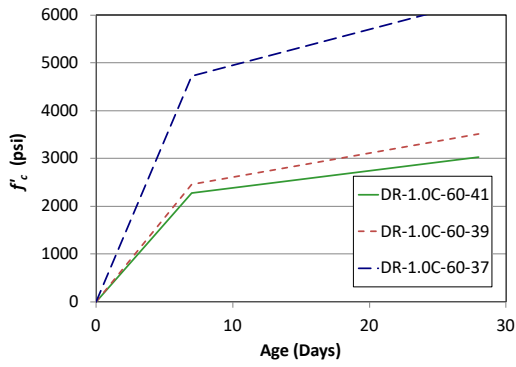


RC-1.5C-65

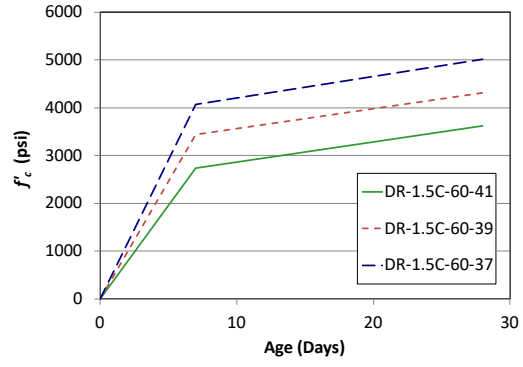


RC-1.0P-60

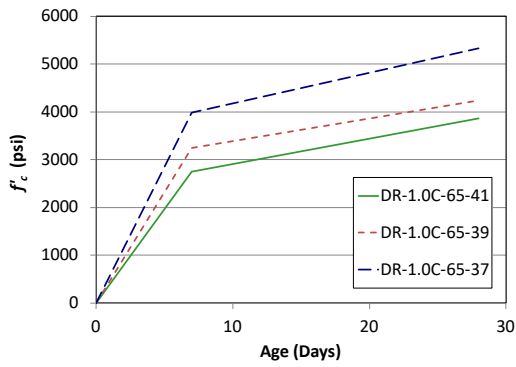
Figure 3.22 Measured Strength Gain of the Limestone Aggregate Concrete Mixes



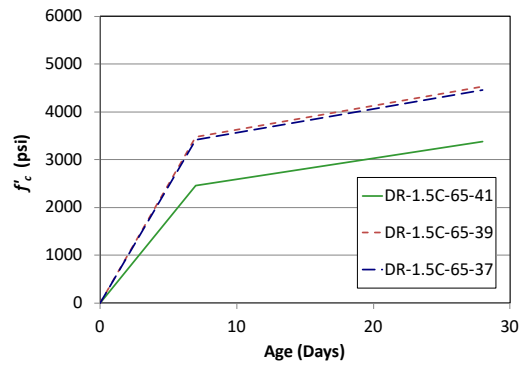
DR-1.0C-60



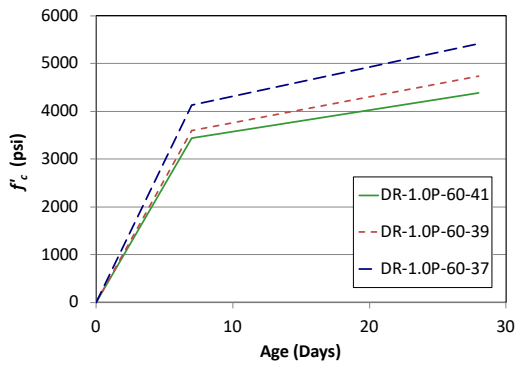
DR-1.5C-65



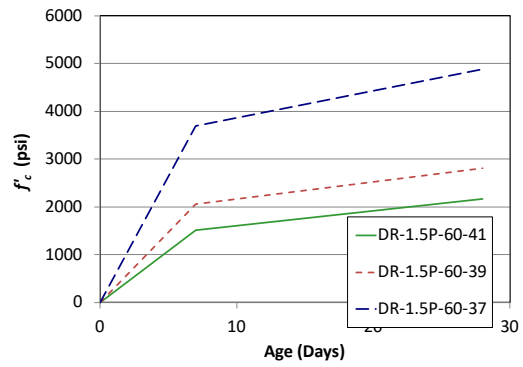
DR-1.0C-65



DR-1.5C-65



DR-1.0P-60



DR-1.5P-60

Figure 3.23 Measured Strength Gain of the Quartzite Aggregate Concrete Mixes

3.3.2 Flexural Strength (Modulus of Rupture)

Standard 6" x 6" x 22" concrete beams were prepared and tested for flexural strength. All the beam specimens were moist cured. The flexural strength was measured at 28 days. Three beams of each mix were tested at each age. The measured average flexural strength is shown in Table 3.12 and Table 3.13 for the limestone and quartzite aggregate mixes, respectively.

Table 3.13 Average Flexural Strength for the Limestone Aggregate Mixes

Mix ID	28-Day Average Flexural Strength (psi)
RC-1.5C-60-41	730.9
RC-1.5C-60-39	809.4
RC-1.5C-60-37	901.2
RC-1.5C-65-41	639.8
RC-1.5C-65-39	727.4
RC-1.5C-65-37	769.9
RC-1.0P-60-41	879.4
RC-1.0P-60-39	908.1
RC-1.0C-60-41	690.5
RC-1.0C-60-39	729.3
RC-1.0C-60-37	882.1
RC-1.0C-65-41	842.3
RC-1.0C-65-39	869.9
RC-1.0C-65-37	970.5

Table 3.14 Average Flexural Strength for the Quartzite Aggregate Mixes

Mix ID	28-Day Average Flexural Strength (psi)
DR-1.5C-60-41	576.8
DR-1.5C-60-39	718.8
DR-1.5C-60-37	754.1
DR-1.5C-65-41	606.1
DR-1.5C-65-39	707.5
DR-1.5C-65-37	718.9
DR-1.5P-60-41	382.9
DR-1.5P-60-39	474.3
DR-1.5P-60-37	719.8
DR-1.0P-60-41	550.5
DR-1.0P-60-39	567.7
DR-1.0P-60-37	690.5
DR-1.0C-60-41	606.1
DR-1.0C-60-39	648.2
DR-1.0C-60-37	790.1
DR-1.0C-65-41	638.8
DR-1.0C-65-39	670.2
DR-1.0C-65-37	702.9

3.3.3 Freeze-Thaw Durability

Standard 3" x 4" x 16" concrete beams were prepared and tested for resistance to rapid freeze-thaw cycles. The specimens were moist cured for 14 days before they were placed in the freeze-thaw cabinet for testing. Figure 3.19 shows beam specimens placed in the freeze-thaw cabinet.



Figure 3.24 Beam Specimens in the Freeze-Thaw Cabinet

The fundamental transverse resonant frequency of the beam specimens was measured using a sonometer. Prior to subjecting a specimen to freeze-thaw cycles, the specimen's initial fundamental frequency was measured. Subsequent frequency measurements were made on specimens in thawed condition at intervals not exceeding 36 freeze-thaw cycles. The fundamental transverse frequency of those specimens that were expected to experience rapid deterioration (i.e. specimens with pea rock) was measured at intervals of 10 freeze-thaw cycles. Figure 3.20 shows one of the beam specimens being tested with a sonometer.

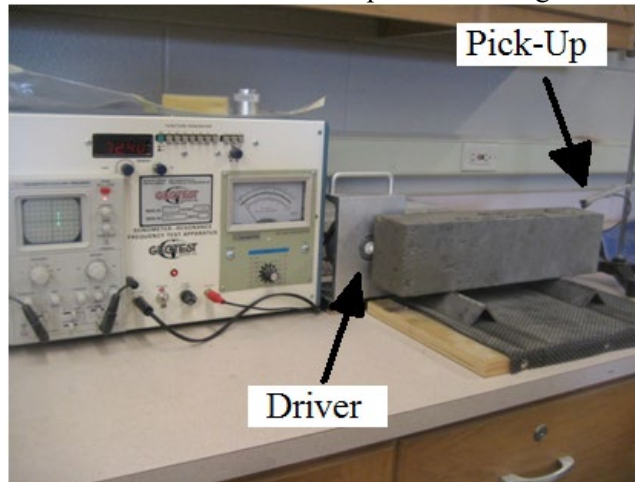


Figure 3.25 Measurement of Concrete Fundamental Frequency Using a Sonometer

Using the fundamental transverse frequency and the test freeze-thaw cycle limits set for the specimen, the relative dynamic modulus and durability factor were calculated using Equation 3.1 and Equation 3.2, respectively.

$$P_c = \left(\frac{n_1^2}{n^2} \right) \times 100 \quad \text{Equation 3.1}$$

where

- P_c = Percent relative dynamic modulus, after c cycles of freezing and thawing.
- n = Fundamental transverse frequency at 0 cycles of freezing and thawing.
- n_1 = Fundamental transverse frequency after c cycles of freezing and thawing

and

$$DF = \frac{P \times N}{M} \quad \text{Equation 3.2}$$

where

- DF = Durability factor of the test specimen.
- P = Percent relative dynamic modulus of elasticity at N cycles.
- N = Number of cycles when P reaches 60 percent of the initial value or the specified number of cycles, whichever is less.
- M = Specified number of cycles at which the exposure to freeze-thaw is to be terminated.

The test duration for specimens with pea rock was limited to 300 cycles or until a specimen's relative dynamic modulus of elasticity reaches 60 percent of the initial modulus, whichever occurred first. For specimens without pea rock, the test duration was limited to 150 cycles since previous durability testing on concrete that did not incorporate pea rock showed good freeze-thaw resistance. The experimental relative dynamic modulus and durability factor values are summarized in Table 3.14 and Table 3.15 for the limestone and the quartzite aggregate mixes.

Table 3.15 Average Relative Dynamic Modulus and Durability Factor for the Limestone Aggregate Mixes

Mix ID	Average Relative Dynamic Modulus						Durability Factor
	25 cycles	50 cycles	75 cycles	100 cycles	125 cycles	150 cycles	
RC-1.5C-60-41	98	94	99	98	98	94	94
RC-1.5C-60-39	105	97	96	98	93	90	90
RC-1.5C-60-37	96	91	94	94	92	93	93
RC-1.5C-65-41	102	99	97	101	98	96	96
RC-1.5C-65-39	94	95	95	94	93	90	90
RC-1.5C-65-37	97	98	105	96	98	94	94
RC-1.0P-60-41	100	80	78	75	64	58	58
RC-1.0P-60-39	98	97	95	86	83	77	77
RC-1.0C-60-41	94	98	97	94	94	93	93
RC-1.0C-60-39	97	96	95	94	92	93	93
RC-1.0C-60-37	105	97	92	98	96	92	92
RC-1.0C-65-41	104	98	94	90	92	90	90
RC-1.0C-65-39	101	99	96	96	94	92	92
RC-1.0C-65-37	105	90	93	95	92	93	93

Table 3.16 Average Relative Dynamic Modulus and Durability Factor for the Quartzite Aggregate Mixes

Mix ID	Average Relative Dynamic Modulus						Durability Factor
	25 cycles	50 cycles	75 cycles	100 cycles	125 cycles	150 cycles	
DR-1.5C-60-41	98	102	100	97	95	96	96
DR-1.5C-60-39	98	97	95	99	96	95	95
DR-1.5C-60-37	100	100	96	95	96	93	93
DR-1.5C-65-41	96	106	102	91	102	96	96
DR-1.5C-65-39	105	98	95	95	97	95	95
DR-1.5C-65-37	90	90	95	96	89	91	91
DR-1.5P-60-41	76	60	65	45	51	45	45
DR-1.5P-60-39	85	80	82	66	77	66	66
DR-1.5P-60-37	90	80	79	77	78	67	67
DR-1.0C-60-41	98	102	97	95	95	94	94
DR-1.0C-60-39	100	100	93	91	93	91	91
DR-1.0C-60-37	95	99	96	94	88	93	93
DR-1.0C-65-41	98	97	101	93	95	93	93
DR-1.0C-65-39	101	105	98	95	96	94	94
DR-1.0C-65-37	96	99	98	96	95	95	95
DR-1.0P-60-41	95	99	94	77	82	80	80
DR-1.0P-60-39	105	103	100	85	76	49	49
DR-1.0P-60-37	92	96	68	53	40	38	38

3.4 Analysis of Experimental Results

The experimental data was analyzed to determine the parameters that may affect concrete workability, compressive strength, and durability under freeze-thaw cycles. In addition, the measured concrete compressive strength growth and flexural strength were compared to results obtained from empirical equations reported in the literature.

3.4.1 Concrete workability

The workability test results were analyzed to determine if any correlations exist between specific work, as a measure of concrete workability, and other mix parameters. The fresh properties considered in the analysis were slump and air content. The concrete mix parameters considered in the analysis were maximum aggregate size and coarse-to-fine aggregate ratio. The number of specimens tested in this study was not sufficient to control for and determine if the effect of each of the mix parameters on concrete workability was statistically significant; however, some noteworthy trends were observed and reported. Since the correlation between workability and slump was being assessed, it was important to verify that the measured slump values were consistent with the expected trend that slump increases with an increase in w/c ratio. The experimental data plotted in Figure 3.21 shows that the slump followed the expected trend. The linear regression of the data points has a correlation coefficient R of 0.540, which indicates a moderate strength correlation between slump and w/c ratio.

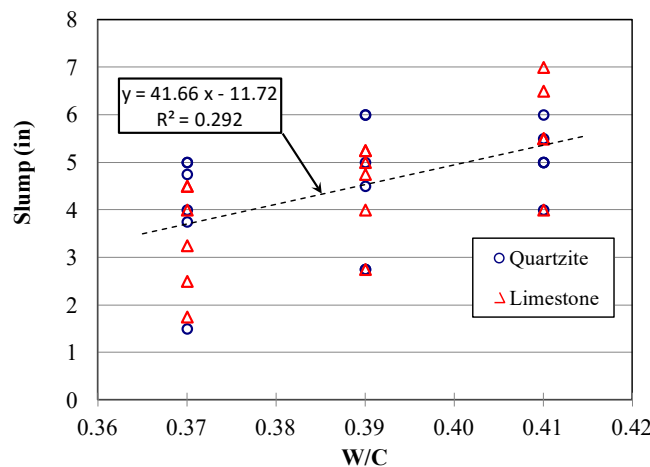


Figure 3.26 Slump vs. W/C Ratio

3.4.1.1 Workability versus Slump

A plot of the specific work versus slump is presented in Figure 3.22. Also shown in the figure is the best fit line. In constructing the best fit line, data from mixes DR-1.0C-65-41, -39, -37, which exhibited significantly higher specific work than the other mixes, were excluded from the analysis to avoid skewing the results. The best fit line shows that as slump increases, the specific work decreases; however, the correlation coefficient R of -0.422 indicates a weak negative correlation between specific work and slump. Moreover, the extremely high specific work values exhibited by the DR-1.0C-65 mixes could not be explained by the corresponding slump values. Thus, workability is highly influenced by factors other than slump.

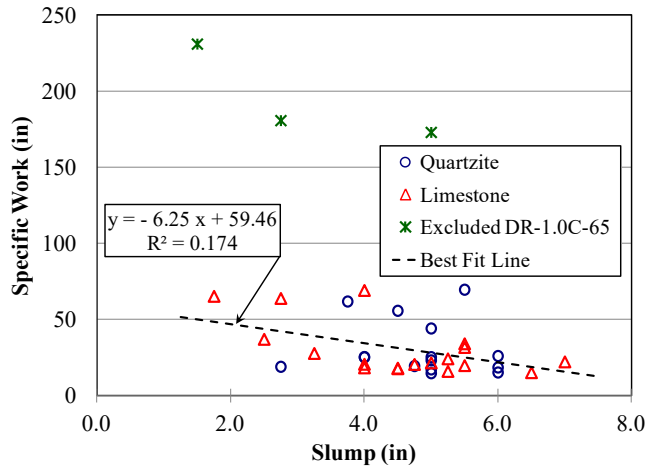


Figure 3.27 Specific Work vs. Slump

3.4.1.2 Workability versus Air Content

Figure 3.23 shows a plot of specific work versus air content. The best fit line does not include the data from mixes DR-1.0C-65, which exhibited significantly higher specific work than the other mixes. The correlation coefficient R of 0.07 indicates that there is no correlation between specific work and slump.

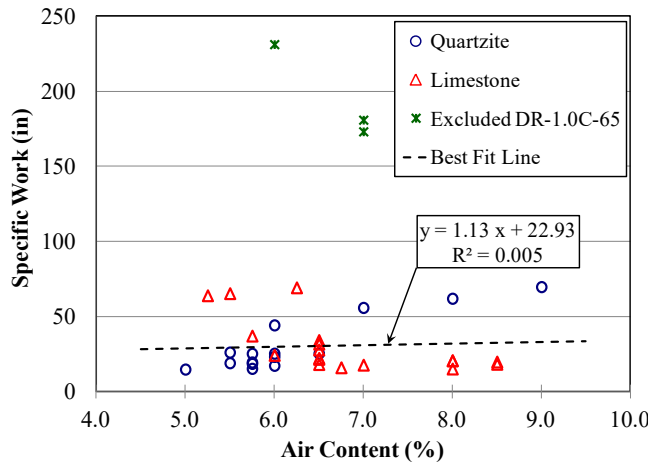


Figure 3.28 Specific Work vs. Air Content

3.4.1.3 Effect of Aggregates on Workability

To determine the effect of the aggregate top size, type, amount and blending aggregate on the specific work, the data was stratified into 15 groups. Each group consisted of mixes having identical parametric values except for the aggregate top size. Plots of the measured specific work for the limestone and quartzite aggregate mixes are presented in Figure 3.24 and Figure 3.25, respectively. Except for the quartzite mixes with pea rock blending aggregates, mixes with 1.0" aggregate top size consistently exhibited higher specific work than their counterpart mixes with 1.5" aggregate top size. This effect is much more prominent in mixes with 65/35 coarse-to-fine aggregate ratio—in limestone and quartzite aggregate mixes. When pea rock was used as the blending aggregate with the quartzite mixes, the 1.5" maximum aggregate size mixes exhibited specific work higher than their 1.0" maximum aggregate size counterpart mixes.

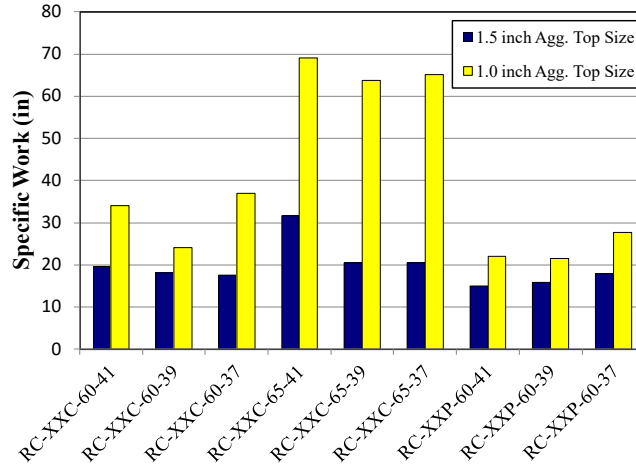


Figure 3.29 Specific Work for the Limestone Aggregate Mixes

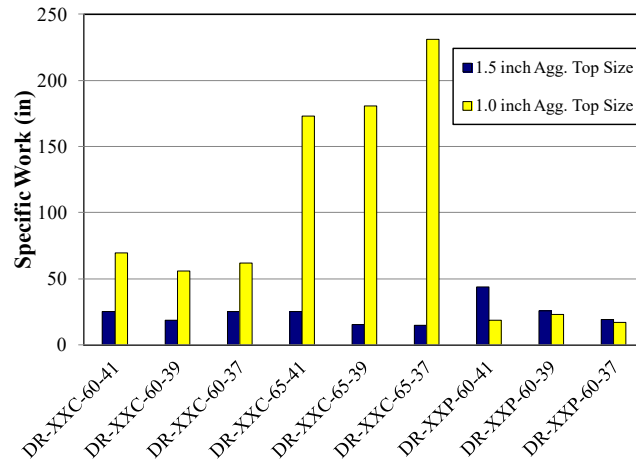


Figure 3.30 Specific Work for the Quartzite Aggregate Mixes

The ratios of the averaged measured specific work for the mixes with 1.0 inch aggregate top size to that of identical mixes but with 1.5-inch aggregate top size are presented in Table 3.16. The ratio for those mixes with chip limestone or quartzite aggregate ranged between 1.71 and 10.59. For mixtures with 65/35 coarse-to-fine aggregate ratio, the use of 1.0-inch instead of 1.5-inch top aggregate size resulted in substantial increase in the specific work; for the limestone aggregate mixes, the specific work of the 1.0-inch top aggregate mixes was on average 2.73 times that of the 1.5-inch top aggregate mixes, while for the quartzite aggregate mixes the specific work of the 1.0-inch top aggregate mixes was on average 10.59 times that of the 1.5-inch top aggregate mixes. Therefore, mixes with 65/35 coarse-to-fine aggregate ratio and 1.0-inch top aggregate size exhibit high specific work and would be unsuitable for concrete pavement applications.

Table 3.17 Ratio of Average Specific Work of Identical Mixes with Different Coarse Aggregate Top Size

Mix ID	Average Sp. Work (in)	Ratio of (a) to (b)
(a) DR-1.0C-60-XX (b) DR-1.5C-60-XX	62.4 23.1	2.7
(a) RC-1.0C-60-XX (b) RC-1.5C-60-XX	31.7 18.5	1.71
(a) DR-1.0C-65-XX (b) DR-1.5C-65-XX	194.9 18.4	10.59
(a) RC-1.0C-65-XX (b) RC-1.5C-65-XX	66.0 24.2	2.73
(a) DR-1.0P-60-XX (b) DR-1.5P-60-XX	19.6 29.8	0.66
(a) RC-1.0P-60-XX (b) RC-1.5P-60-XX	23.75 16.29	1.46

3.4.2 Concrete Compressive Strength

The concrete strength test data were analyzed to verify that test results were consistent with expected trends. The number of specimens tested in this study was not sufficient to control for and determine if the effect of each of the mix parameters on concrete strength was statistically significant.

3.4.2.1 28-Day Compressive Strength versus W/C Ratio

Figure 3.26 shows a plot of the measured 28-day compressive strength (f'_c) versus w/c ratio. Data from mixes with pea gravel is not reflected in the plot because the pea gravel mixes exhibited poor freeze-thaw durability and, therefore, the respective strength test data were of no significant value. Also shown on the figure is the linear regression line with a correlation coefficient R of -0.764. The linear regression analysis indicates a moderately strong negative correlation between the 28-day compressive strength and w/c ratio.

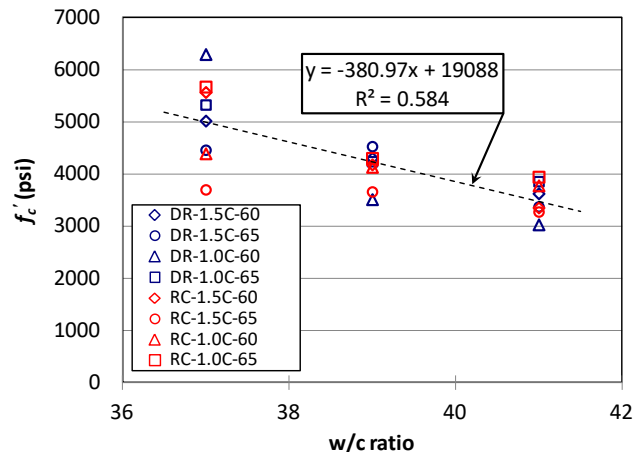


Figure 3.31 28-Day Compressive Strength versus W/C Ratio

3.4.2.2 Compressive Strength Gain Rate

The rate of strength gain was analyzed using a model developed by Branson (1977). The concrete strength at a given age t , where t is in days, is given by

$$f'_{ct} = \frac{t}{\alpha + \beta t} f'_c \quad \text{Equation 3.3}$$

where

f'_{ct}	=	compressive strength at time t
f'_c	=	28-day compressive strength
α	=	factor based on cement type and curing method
β	=	factor based on curing method and curing method

For moist-cured Type I cement, α is 4.0 and the β is 0.85.

The measured compressive strength data, theoretical seven day compressive strength values, and the measured-to-theoretical ratio can be seen in Table 3.17. The measured seven day values were slightly higher than the theoretical values from Equation 3.3. The limestone mixes compressive strengths were on average 3.1 percent higher than the predicted seven day values. The quartzite mixes averaged a compressive strength 6.9 percent higher than the predicted values at seven days. The difference between the theoretical and measured value is relatively small and indicates that the prediction model provides a good estimate for the experimental results.

Table 3.18 Measured and Theoretical Seven-Day Compressive Strength

Mix ID [†]	Measured 7-Day Comp. Strength (psi)	Theoretical 7-Day Comp. Strength (psi)	Measured-to- Theoretical Ratio
DR-1.5C-60-41	2732	2550	1.07
DR-1.5C-60-39	3436	3029	1.13
DR-1.5C-60-37	4071	3530	1.15
DR-1.5C-65-41	2451	2373	1.03
DR-1.5C-65-39	3477	3186	1.09
DR-1.5C-65-37	3408	3138	1.09
DR-1.5P-60-41	1514	1521	1.00
DR-1.5P-60-39	2054	1976	1.04
DR-1.5P-60-37	3688	3437	1.07
DR-1.0C-60-41	2272	2132	1.07
DR-1.0C-60-39	2451	2471	0.99
DR-1.0C-60-37	4727	4428	1.07
DR-1.0C-65-41	2745	2714	1.01
DR-1.0C-65-39	3248	2983	1.09
DR-1.0C-65-37	3979	3747	1.06
DR-1.0P-60-41	3440	3080	1.12
DR-1.0P-60-39	3599	3328	1.08
DR-1.0P-60-37	4130	3810	1.08
RC-1.5C-60-41	2134	2360	0.90
RC-1.5C-60-39	3112	2940	1.06
RC-1.5C-60-37	4073	3916	1.04
RC-1.5C-65-41	2482	2304	1.08
RC-1.5C-65-39	2719	2575	1.06
RC-1.5C-65-37	2782	2603	1.07
RC-1.0C-60-41	2636	2657	0.99
RC-1.0C-60-39	3020	2907	1.04
RC-1.0C-60-37	3372	3089	1.09
RC-1.0C-65-41	2866	2774	0.97
RC-1.0C-65-39	3154	3027	1.04
RC-1.0C-65-37	4250	3989	1.07
RC-1.0P-60-41	3254	3206	1.02
RC-1.0P-60-39	3961	3886	1.02

[†]RC-1.5P-60-41, RC-1.5P-60-39, RC-1.5P-60-37, and RC-1.0P-60-37 were not tested

A plot of the theoretical versus measured seven-day compressive strengths for quartzite and limestone mixes is presented in Figure 3.27. In the plot, the theoretical equation is represented by the 1:1 solid line ($y = x$) and the measured results are represented by data points scatter. The coefficient of correlation R of best fit line is 0.970. This indicates a strong correlation between the theoretical and measured results. The experimental and theoretical values predicted by Equation 3.3 also are in excellent agreement—the slope of the linear best fit line of 0.941 is only 5.9% less than 1.

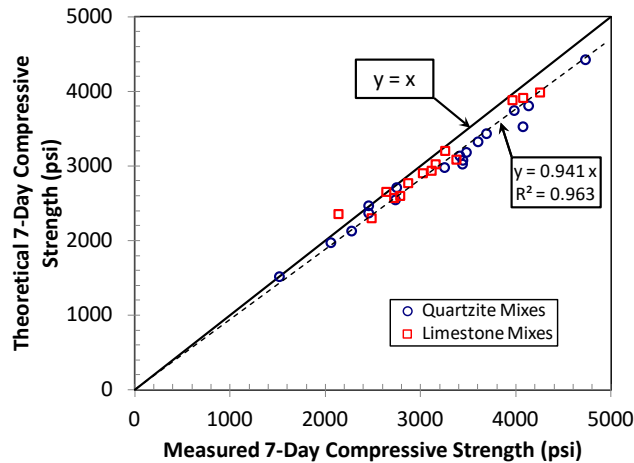


Figure 3.32 Seven-Day Theoretical and Measured Compressive Strength

3.4.3 Concrete Flexural Strength (Modulus of rupture)

Plots of the measured modulus of rupture f_r versus $\sqrt{f'_c}$ for the limestone and quartzite aggregate mixes are presented in Figure 3.28 and Figure 3.29, respectively.

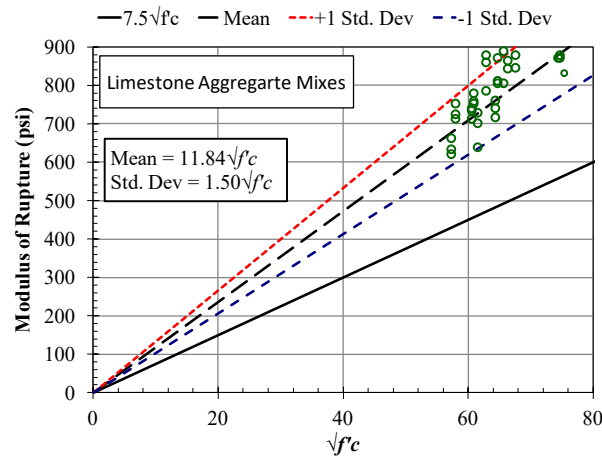


Figure 3.33 Measured f_r versus $\sqrt{f'_c}$ for the Limestone Aggregate Mixes

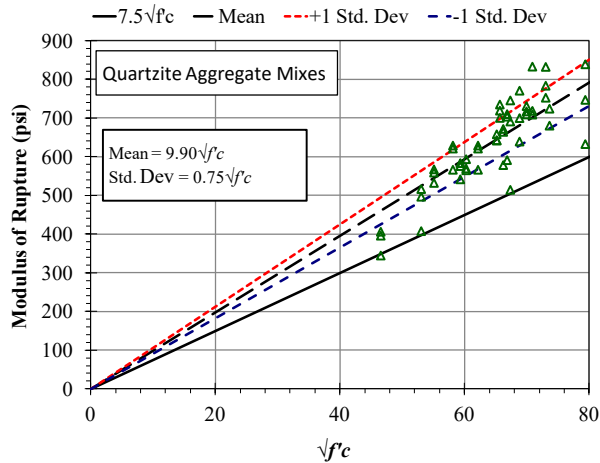


Figure 3.34 Measured f_r versus $\sqrt{f'_c}$ for the Quartzite Aggregate Mixes

The mean f_r for the limestone mixes is $11.84\sqrt{f'_c}$ with a standard deviation of $1.5\sqrt{f'_c}$. The mean f_r for the quartzite mixes is $9.90\sqrt{f'_c}$ with a standard deviation of $0.75\sqrt{f'_c}$. Both means are above the value obtained from the code empirical equation of $7.5\sqrt{f'_c}$ (ACI 2008). However, the flexural strength of concrete has been reported to vary between $7.5\sqrt{f'_c}$ and $13.0\sqrt{f'_c}$ (Park and Paulay 1975). Therefore, the experimental values fell within the expected range. The standard deviations indicate that data of the quartzite mixes had a tighter scatter than that of the limestone mixes.

3.4.4 Concrete Durability-Resistance to Rapid Freezing and Thawing

The freeze-thaw durability test results were compared to a durability factor (DF) of 85. A DF of 85 has been used as a standard for good freeze-thaw durability performance in previous research applications (Wong et al. 2000). The variation of the DF with the number of freeze-thaw cycles is shown in Figure 3.30 and Figure 3.31 for the mixes with and without pea rock, respectively.

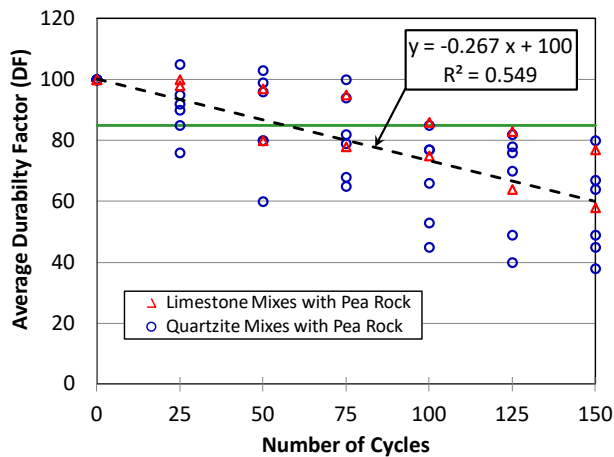


Figure 3.35 Durability Factor Change with Number of Freeze-Thaw Cycles-Mixes with Pea Rock

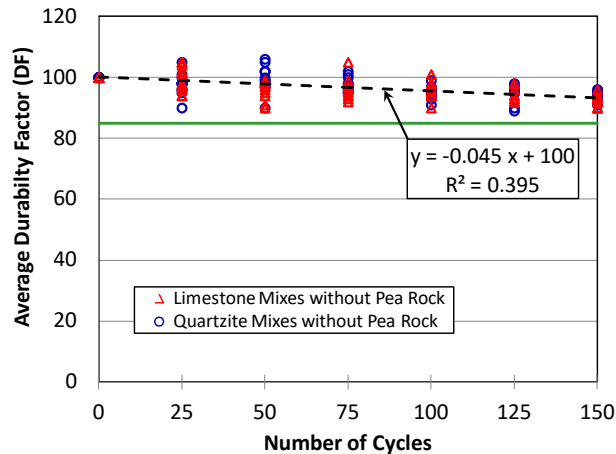


Figure 3.36 Durability Factor Change with Number of Freeze-Thaw Cycles-Mixes without Pea Rock

Mixes with pea rock exhibited rapid durability degradation with increased number of freeze-thaw cycles, whereas those without pea rock showed mild durability degradation. Based on the best fit lines for the DF degradation, the DF degradation rate of the mixes with pea rock was more than 5.9 times that of the mixes that did not contain pea rock. At the end of 150 freeze-thaw cycles, all mixes with pea rock had a DF less than the acceptable limit of 85, with most of them significantly below 85. On the other hand, all mixes that did not contain pea rock had a DF higher than 85.

The final DF values for the different mixes at 150 freeze-thaw cycles are shown in Figure 3.32 and Figure 3.33 for the limestone and quartzite aggregate mixes, respectively. Variation in the DF among the mixes that did not contain pea rock was insignificant. When the pea rock mixes are excluded, the average DF for the 1.5-inch and 1.0-inch limestone mixes is 92.8 and 92.2, respectively, and that for the 1.5-inch and 1.0-inch quartzite mixes was 94.3 and 93.3, respectively. The DF varied between 90 and 96 for the limestone mixes, and between 91 and 96 for the quartzite mixes. The narrow range of variation in the DF indicates that when pea rock was not used, the DF values were insensitive to the aggregate type, aggregate top size, w/c ratio, or fine-to-coarse aggregate ratio.

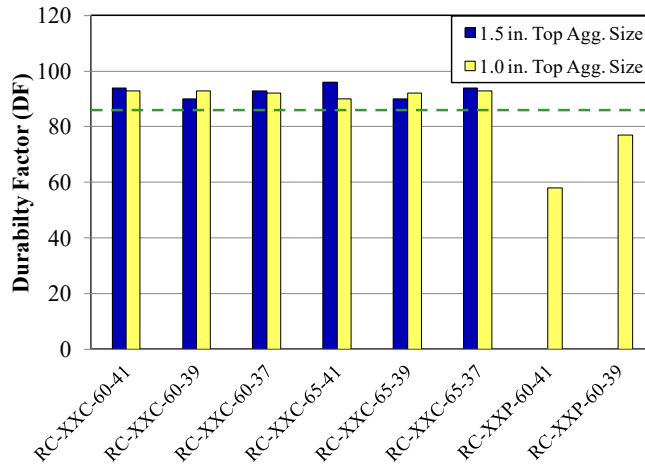


Figure 3.37 Durability Factor for Limestone Aggregate Mixes

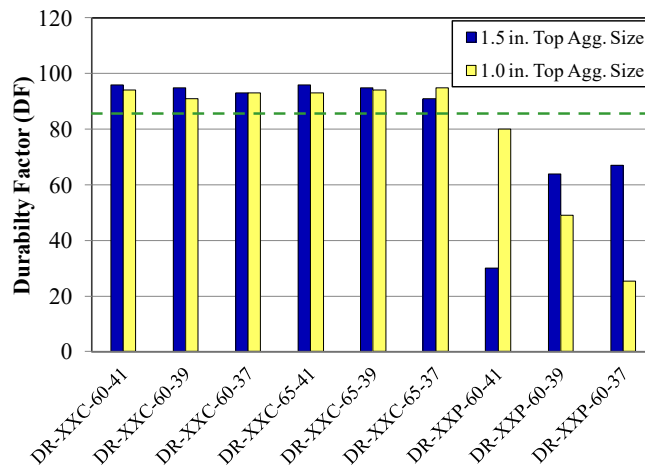


Figure 3.38 Durability Factor for the Quartzite Aggregate Mixes

4. EVALUATION OF NEW JPC PAVEMENT IN SOUTH DAKOTA

This section covers experimental and analytical work done in this study to evaluate the performance of different newly constructed JPC pavement. The evaluation was performed at four test sites across the state of South Dakota. Each test site consisted of multiple test sections. The parameters were the transverse contraction joint type, the curing compound application rate, and the dowel bar configuration (number of bars and arrangement) and the corresponding transverse contraction joints spacing. The experimental work entailed collecting data from various in situ tests that were performed on the JPC pavement test sections. The purpose for the tests was to gather relevant data over an extended time period to evaluate concrete surface strain near the transverse joints, transverse joint movement, moisture ingress at the transverse joints, faulting at the transverse joints, load transfer efficiency (LTE) at the transverse joints, and the International Roughness Index (IRI) of the pavement. Statistical analyses were performed on the collected data in order to determine the influence of the different parameters on the performance of JPC pavement.

4.1 Testing Parameters

The parameters selected in this study were the transverse contraction joint type, the curing compound application rate, and the dowel bar configuration and the corresponding transverse contraction joint spacing.

4.1.1 Transverse Contraction Joint Type

The transverse joint sealant type may affect the amount of moisture ingress into the base material and the infiltration of incompressible material into the joint crack. Three transverse joint types were incorporated into the test sections: silicone sealed, unsealed (saw-cut only with no sealant), and hot-pour sealed. Figure 4.1 shows details of the three joint types. The silicone sealed joint, which is the standard transverse joint type specified by SDDOT, is saw cut in two runs. In the first run, the cut is made 1/8-inch to 1/4-inch wide and one-quarter the pavement thickness deep. In the second run, approximately the top two-thirds portion of the cut depth is widened to 3/8 inches to allow for the placement of a backer rod and the silicone sealant. The silicone sealant is placed approximately 3/16- to 5/16-inch deep into the joint and is finished at 1/8- to 1/4-inch below the surface of the pavement. The unsealed joint is cut to 1/8-inch wide by one-quarter the pavement thickness deep. The hot-pour joint is cut to approximately 1/8- to 1/4-inch wide by one-quarter the pavement thickness deep, and then filled with a hot-pour sealant up to a maximum of 1/8 inch from the top of the pavement.

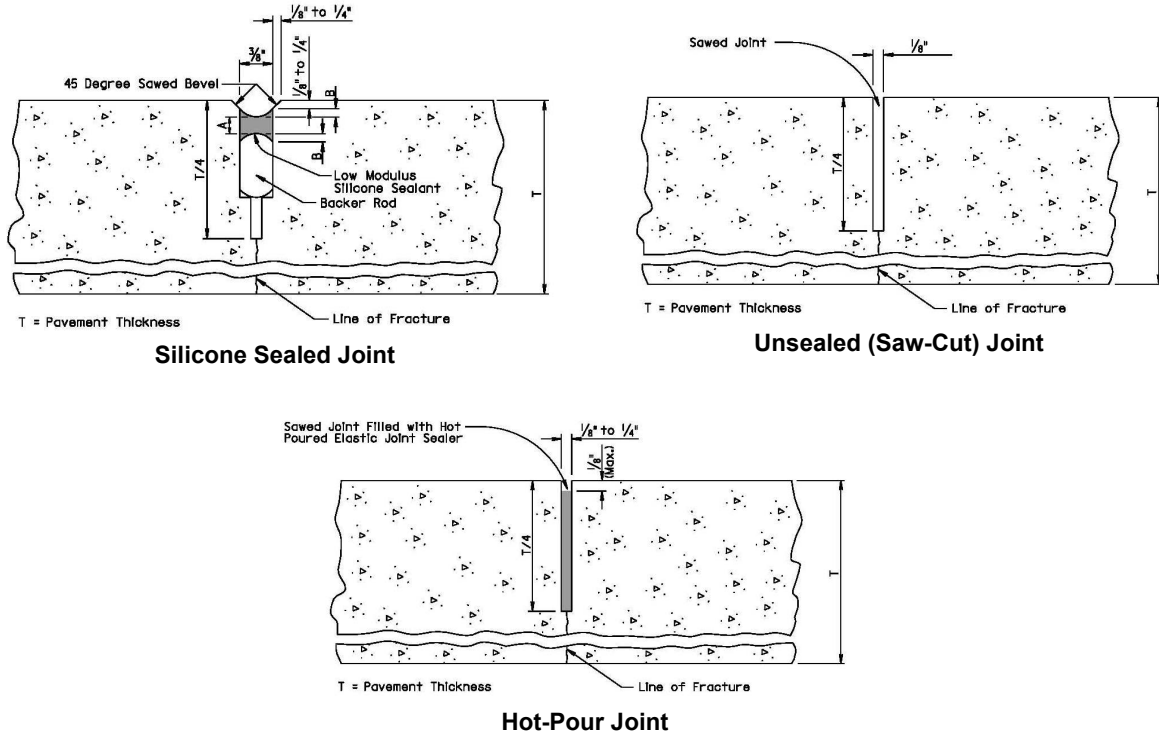


Figure 4.39 Types of Transverse Contraction Joints Considered in the Study

4.1.2 Curing Compound Application Rate

Curing of the pavement concrete included in this study was accomplished by spraying a film of water-base, wax-base, concrete curing compound on the pavement surface. The curing compound conformed to ASTM C 309, Type 2, Class A (ASTM 2009). The reported curing compound normal application rate for the pavement sections included in this study was approximately 150 ft²/gal. To study the effect of the curing compound application rate on the development of pavement surface roughness, a select number of test sections were treated with 1.5 times the normal curing compound application rate.

4.1.3 Dowel Bar Configuration and Corresponding Transverse Contracting Joint Spacing

In this study, the performance of a standard dowel configuration at a transverse joint spacing of 20 feet and a reduced number of dowel bar configuration at a 15-foot transverse joint spacing was investigated. The standard dowel bar configuration used for 10 inches or thicker JPC pavement in South Dakota consists of 12 dowel bars placed within a 12-foot wide lane. Figure 4.2 shows the arrangement of a normal dowel bar configuration. With a standard dowel bar arrangement, the first dowel bar at each edge of the lane is placed at 6 inches from the edge of the lane and the dowels are spaced at 12 inches on center. The standard transverse contraction joint spacing that corresponds to a 10-inch or thicker JPC pavement is 20 feet.

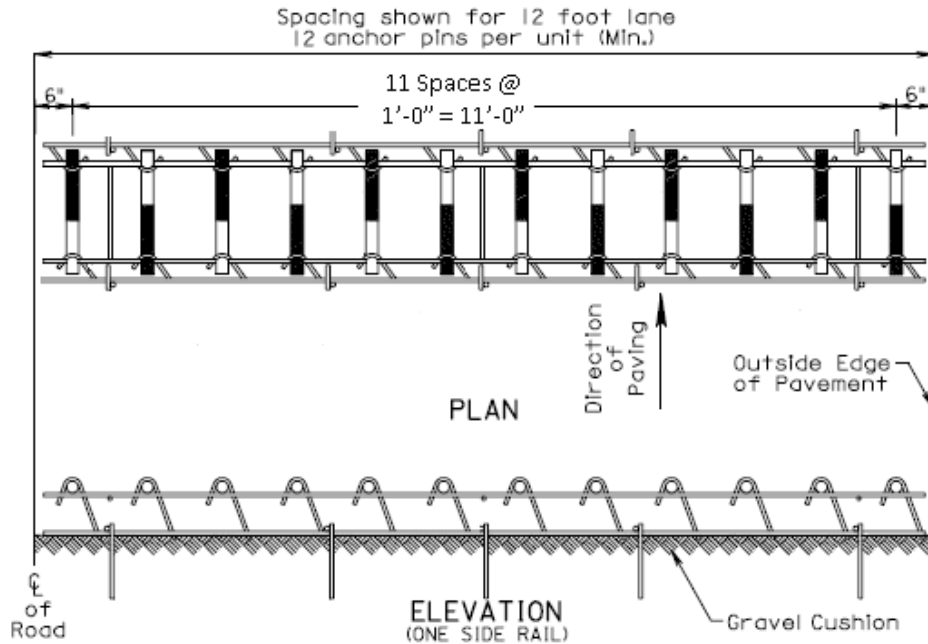


Figure 4.40 Typical Standard SDDOT Dowel Bar Configuration for 12' Lanes

The reduced dowel bar configuration used for 8- to 9-inch thick JPC pavement in South Dakota consists of nine dowel bars placed within a 12-foot wide lane. Figure 4.3 shows the reduced dowel bar configuration where five bars and four bars are placed on the outside edge and the inside edge of the pavement, respectively. Similar to the standard dowel bar arrangement, the first dowel bar at each edge of the lane is placed at 6 inches from the edge of the lane and the dowels are spaced at 12 inches on center. The standard transverse contraction joint spacing that corresponds to 8- to 9.5-inches thick JPC pavement is 15 feet.

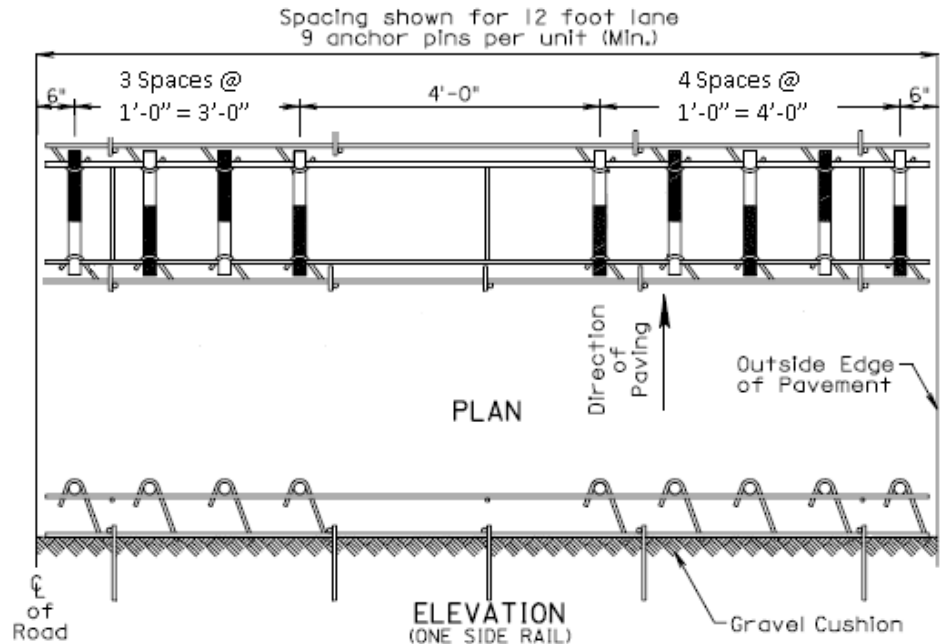


Figure 4.41 Typical Reduced Dowel Bar Configuration for 12' Lanes

The standard dowel bar sizes specified by SDDOT are 1¼" x 18" for pavements 8- to 10-inches thick, and 1½" x 18" for pavements 10½- to 12-inches thick.

4.2 Test Sites and Test Sections

4.2.1 Test Sites

JPC pavement data were collected from four test sites in South Dakota. The site selection was based on availability of newly constructed JPC pavement. The four test sites were:

- I-29 north of Brookings in Brookings County
- US 212 west of Belle Fourche in Butte County
- SD 50 west of Vermillion in Yankton County
- I-29 south of Vermillion in Union County

The location of the four test sites is shown in Figure 4.4. The test site numbering in the figure corresponds to numbering of the test site list shown above.

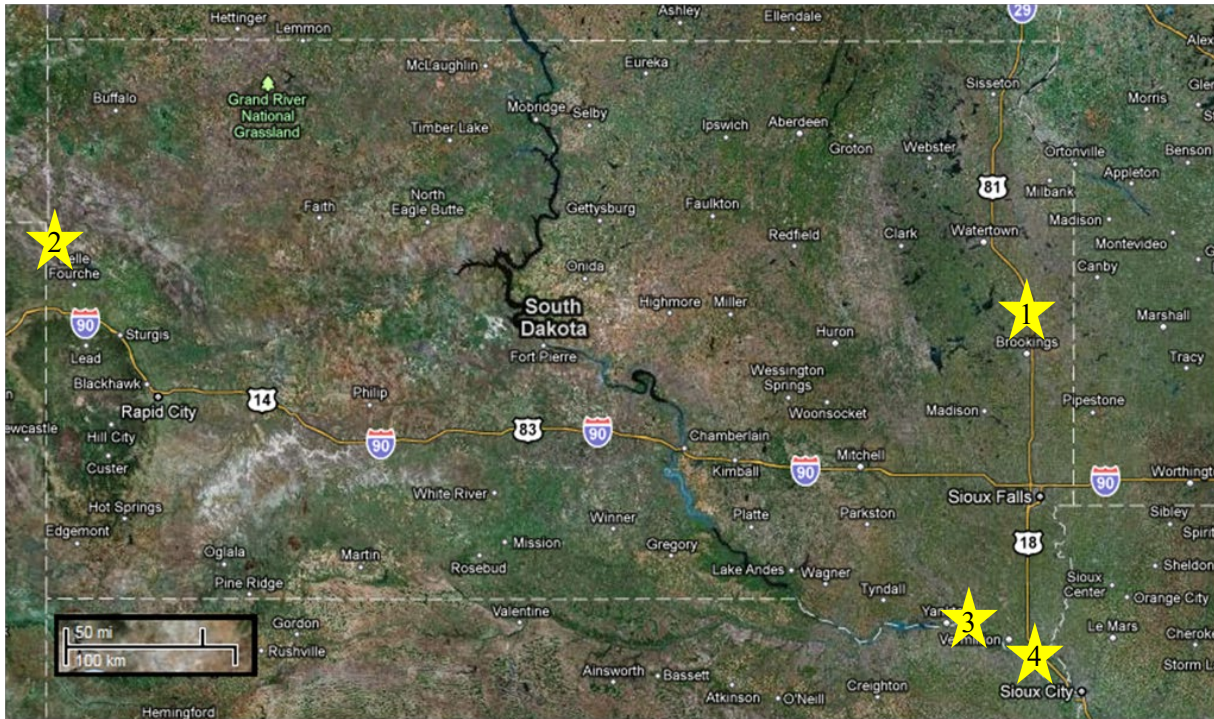


Figure 4.42 Map of Test Site Locations in South Dakota (Google Maps)

The JPC pavement of the I-29 site in Brookings County was constructed in August 2008. The pavement was 11 inches thick, was supported on 5-inch thick granular base (gravel), and was fitted with standard dowel bar configuration at the joints. The highway consisted of four lanes (divided). The test site was limited to the northbound lanes only. At the year of construction, the northbound average daily traffic (ADT) was 9010 and the average daily truck traffic (ADTT) was 1496. Data collected from this site was used to evaluate faulting, LTE, IRI, concrete surface strain, and joint movement.

The JPC pavement of the US 212 site in Butte County was constructed in June 2009. The pavement was 8-inches thick, supported on a 5-inch thick asphalt base, and fitted with reduced dowel bar configuration at the joints. The highway consisted of two lanes (undivided). The test site was limited to the westbound lane only. At the year of construction, the westbound ADT was 1464 and the ADTT was 593. The data collected from this site was used to evaluate faulting, LTE, IRI, concrete surface strain, and joint movement.

The JPC pavement of the SD 50 site in Yankton County was constructed in November 2009. The pavement was 9 inches thick, supported on 5-inch thick granular base (gravel), and fitted with reduced dowel bar configuration at the joints. The highway consisted of four lanes (divided). The test site was limited to the eastbound lanes only. At the year of construction, the eastbound ADT was 4500 and the ADTT was 855. The data collected from this site was used to evaluate faulting, LTE, IRI, concrete surface strain, and joint movement.

The JPC pavement of the I-29 site in Union County was constructed in October 2010. The pavement was 11 inches thick, supported on 5-inch thick granular base (gravel), and fitted with standard dowel bar configuration at the joints. The highway consisted of four lanes (divided). The test site was limited to the northbound lanes only. At the year of construction the northbound ADT was 10590 and the ADTT was 2616. The data collected from this site was used for the evaluation of moisture ingress only.

Table 4.1 presents a summary of the characteristics of and the pavement performance data considered at each test site.

Table 4.19 Summary of the Test Sites

Test Site	Year Constructed	No. of Lanes	ADT/ADTT [†]	Pavement Thickness	Base	Dowel Bar Configuration	Performance Data
I-29 Brookings County	Aug. 2008	4 Divided	9010/1496 (Northbound)	11"	5" Gravel	Standard	Faulting; LTE; IRI; Strain; Joint Movement
US 212 Butte County	Jun. 2009	2 Undivided	1464/593 (Westbound)	8"	5" Asphalt	Reduced	Faulting; LTE; IRI; Strain; Joint Movement
SD 50 Yankton County	Nov. 2009	4 Divided	4500/855 (Eastbound)	9"	5" Gravel	Reduced	Faulting; LTE; IRI; Strain; Joint Movement
I-29 Union County	Oct. 2010	4 Divided	10590/2616 (Northbound)	11"	5" Gravel	Standard	Moisture Ingress

[†]Corresponding to year of construction

4.2.2 Test sections

A test section represents a highway segment, within a test site, where data was collected periodically. Two types of test sections were used in this study. The first type, referred to as “1½ Applications of Curing Compound” (or simply Curing Compound) test section, was used to study the effect of increased curing compound application rate on the pavement performance. The second type, referred to as “Joint” test section, was used to study the effect of joint type on the pavement performance. Only the standard SDDOT silicone sealed joints were used within a Curing Compound test section, whereas all three joint types (silicone sealed, hot-pour sealed, and unsealed) were used within a joint test section. Joint test sections were treated with the curing compound regular application rate. Thus, there was no overlap between a curing compound test section and a joint test section.

Except for the test section at the Union County test site, a typical joint test section incorporated one group of four successive unsealed (saw-cut) joints, one group of four successive hot-pour sealed joints, and one group of multiple successive silicone sealed joints placed over a minimum of 100 feet of highway length separation between the unsealed and the hot-pour sealed joints. Outside the test section, all the joints were silicone-sealed. This layout allowed for collecting data from the two interior joints of each joint group to minimize any interactive effects that might exist between two adjacent joints of different types. The joint spacing was 20 feet for test sections in the Brookings County test site and 15 feet for test sections in the Butte County and Yankton County test sites. Figure 4.5 shows a schematic view of a typical Joint test section layout.

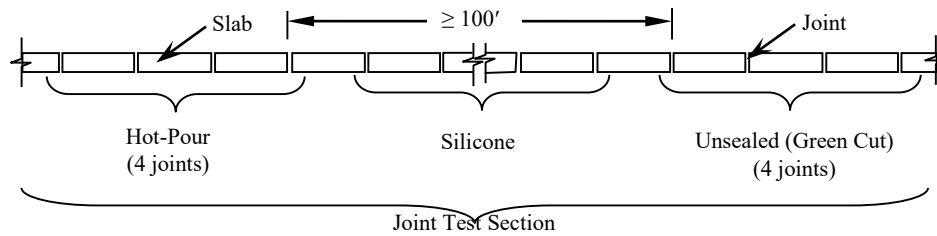


Figure 4.43 Schematic View of a Typical Joint Test Section (Brookings, Butte, and Yankton Test Sites)

Layout of the Joint test section at the Union County test site was slightly different than that at the other test sites. It was instrumented with moisture sensors placed under the joints. To minimize the length of wiring needed between the sensors and the data acquisition system, the hot-pour sealed and the unsealed joint groups were placed next to each other, and the silicone-sealed joints were placed everywhere else. Figure 4.6 shows the modified Joint test section layout used at the Union County test site.

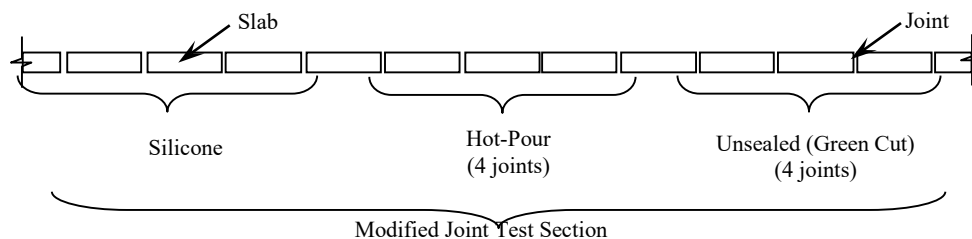


Figure 4.44 Schematic View of a Modified Joint Test Section (Union County Test Site)

To reduce bias in the collected data resulting from variations in the subgrade soil type and conditions, precipitation, and other factors in the same test site, data was collected from multiple test sections at each of the Brookings County, Butte County, and Yankton County test sites where faulting, LTE, IRI, surface strain, and joint movement were being investigated.

Only one Joint test section was considered at the Union County test site since moisture ingress into the base was the only joint-related property being investigated. Moisture ingress depends mainly on precipitation and the joint type. Therefore, moisture ingress would be less sensitive to variations in other factors within a test site.

Five Joint test sections and two Curing Compound test sections were incorporated at each of the Brookings County, Butte County, and Yankton County test sites. The Union County test site incorporated only one Joint test section. Length of the Curing Compound test section was approximately one mile at the Brookings County and the Butte County test sites, and approximately 500 feet at the Yankton County test site. Figure 4.7 through Figure 4.10 show the locations of the test sections within each of the test sites.

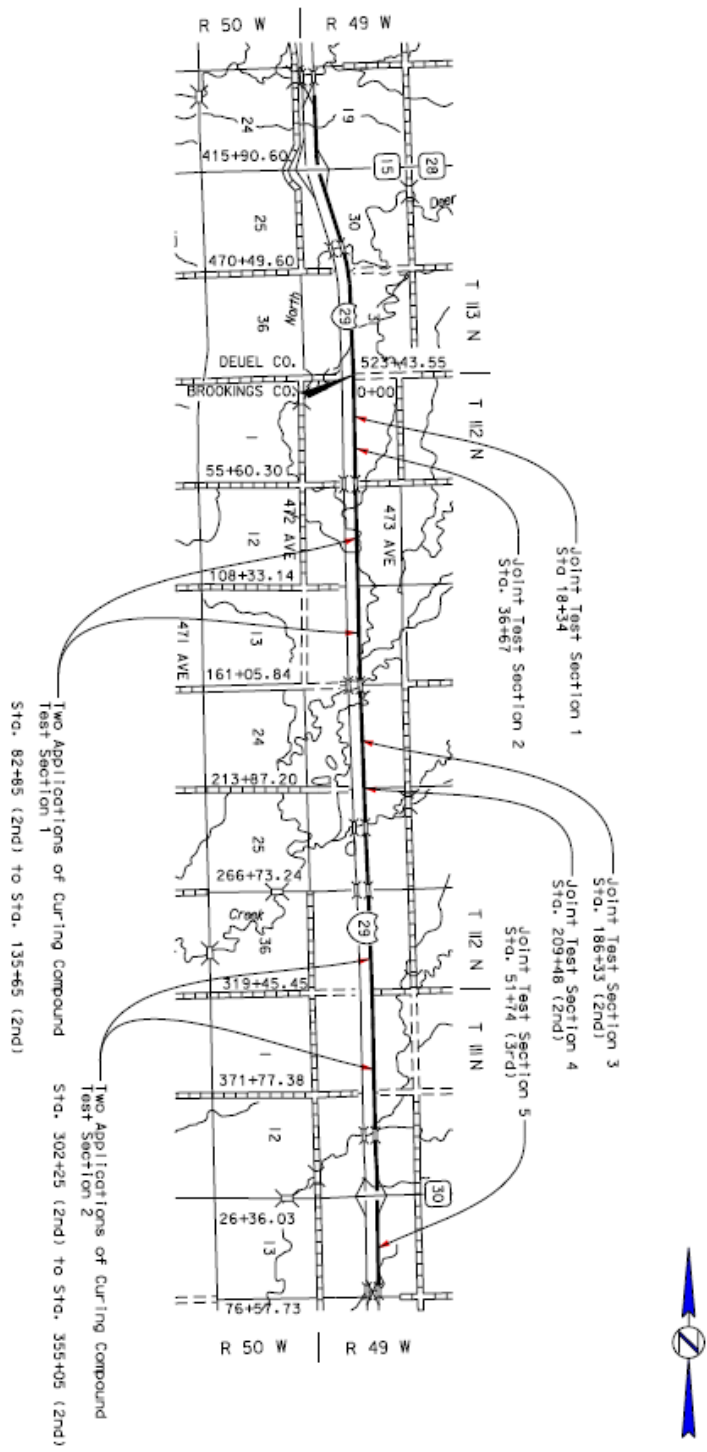


Figure 4.45 Location of Test Sections at the Brookings County Test Site

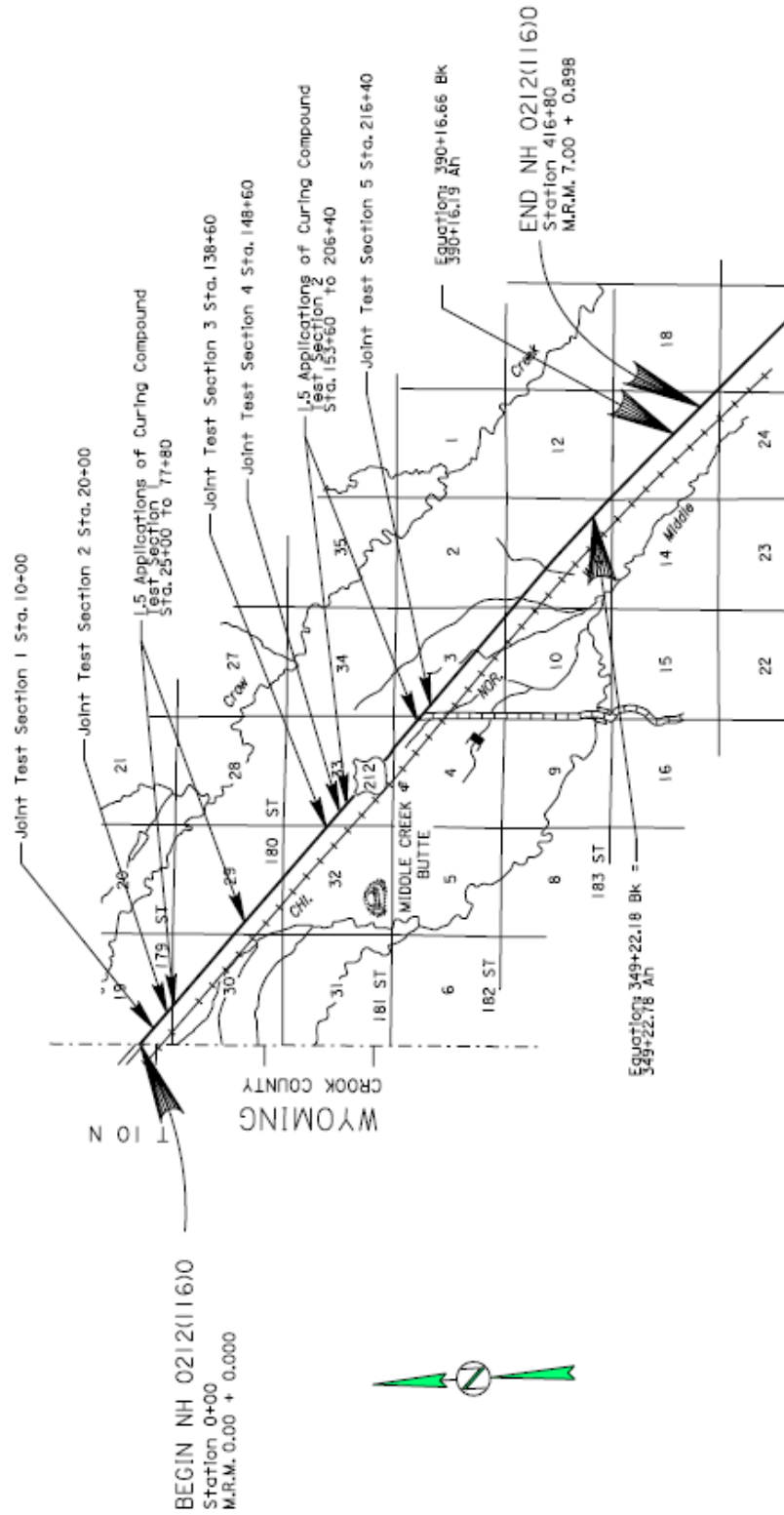


Figure 4.46 Location of Test Sections at the Butte County Test Site

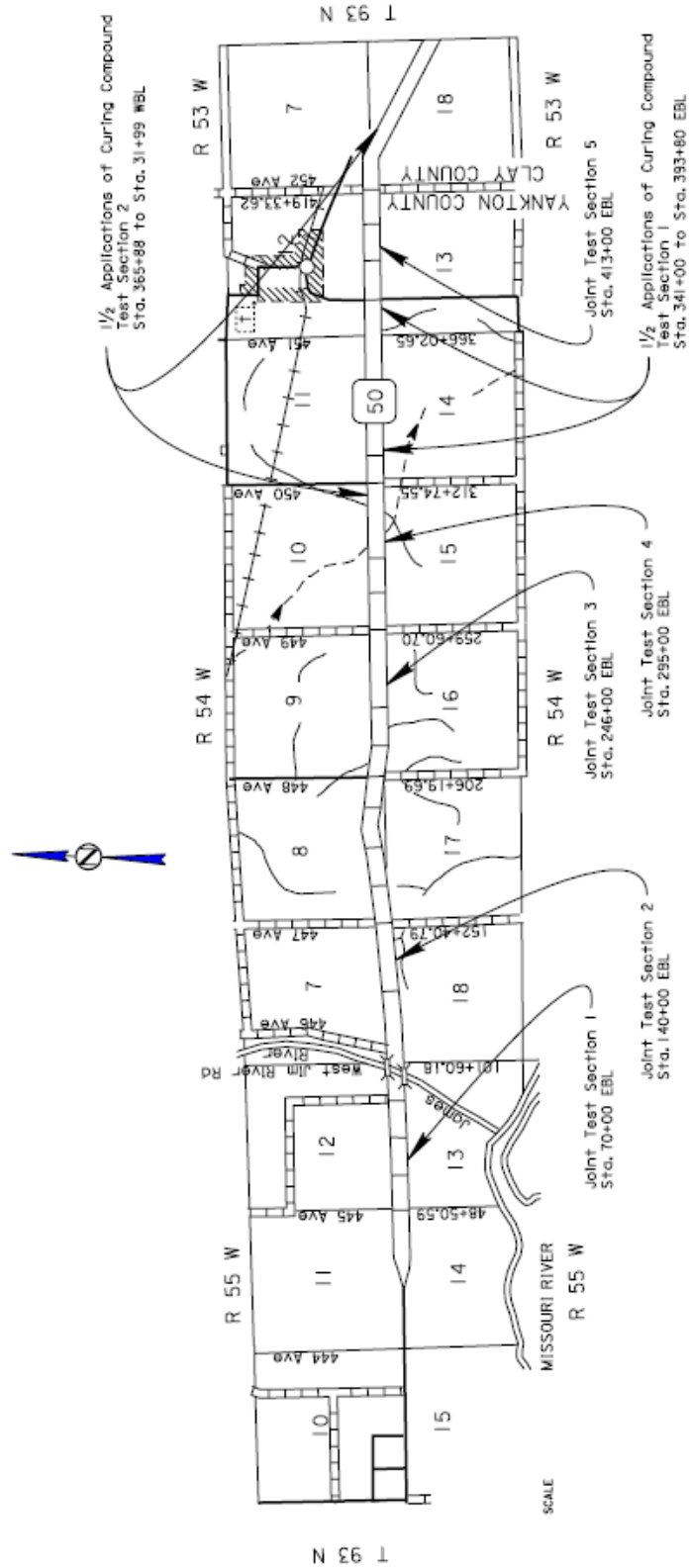


Figure 4.47 Location of Test Sections at the Yankton County Test Site

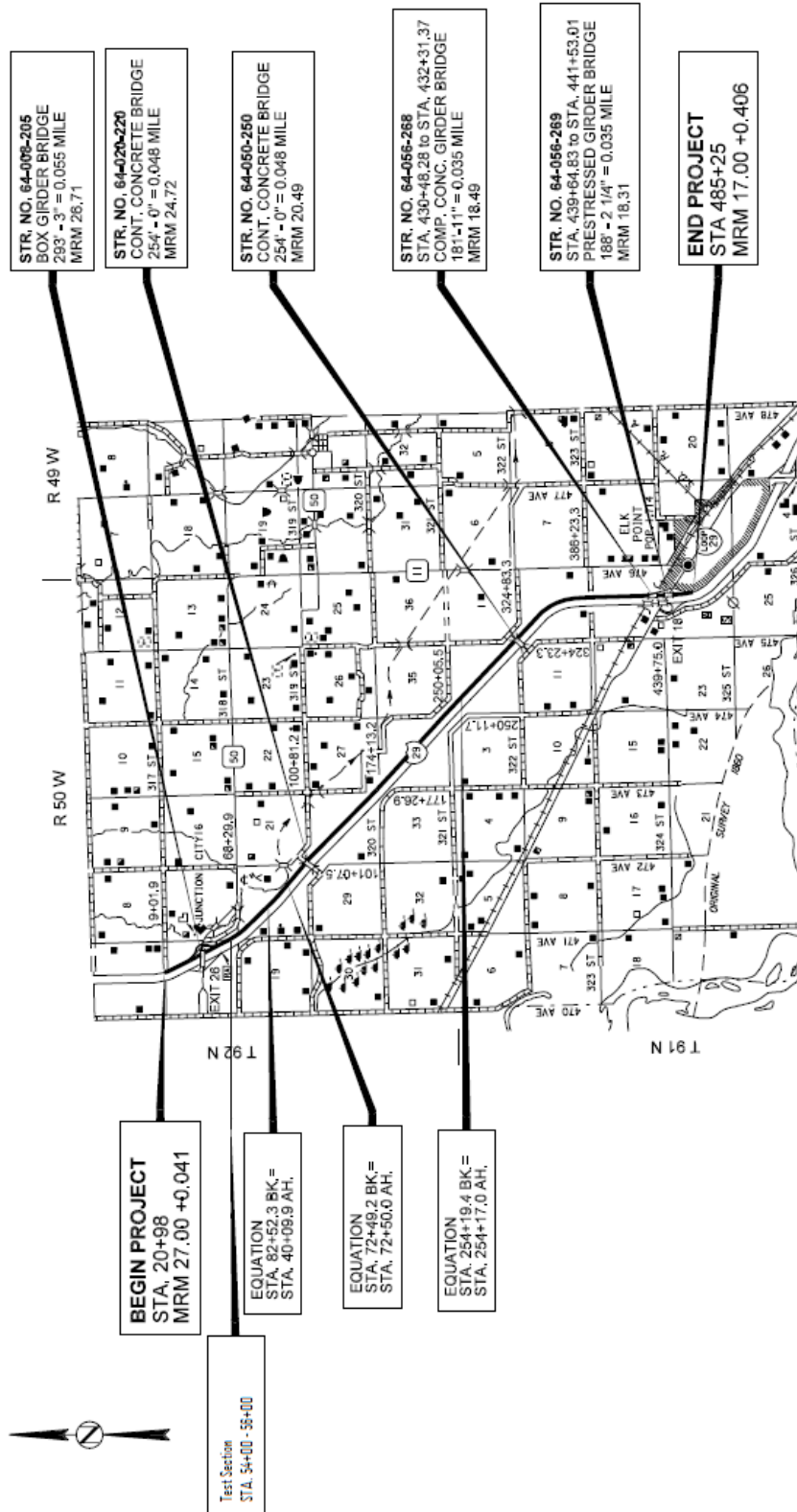


Figure 4.48 Location of Test Sections at the Union County Test Site

4.3 Test Methods and Protocols

The experimental program followed in this study was designed to evaluate concrete surface strain near the transverse joints, transverse joint movement, moisture ingress at the transverse joints, faulting at the transverse joints, load transfer efficiency (LTE) at the transverse joints, and the International Roughness Index (IRI) of the pavement. Test methods and protocols used to collect the relevant data are described in this section.

4.3.1 Pavement Surface Strain and Transverse Joint Movement

The pavement concrete surface strain next to the transverse joint and the joint movement were measured using the same measurement set up. The set up consisted of installing on the pavement surface a set of eight permanent reference points with four placed on each side of the joint. Figure 4.11 shows a plan view of the square grid pattern used for placing the eight reference points across a transverse joint. The specified spacing (gauge length) of the reference points was 4-inches in both directions and the pattern was to be centered at the joint. By making gauge length measurements between the reference points periodically, the change in surface strain and the joint movement could be determined.

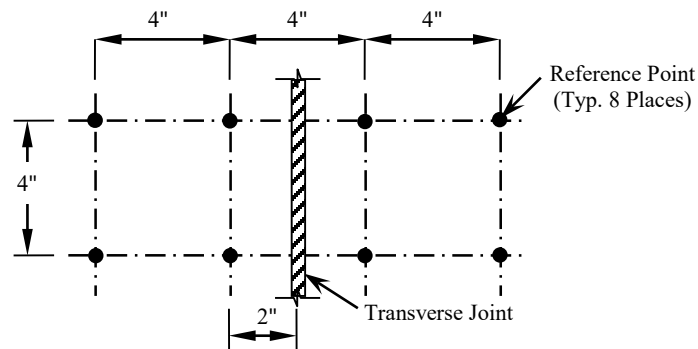


Figure 4.49 Plan View of the Pavement Reference Points Pattern

Permanent reference points on the pavement surface were marked on $\frac{1}{4} \times 1\frac{1}{4}$ -inch stainless steel hex bolts. Using a shop press drill, a $\frac{1}{64}$ -inch tapered indentation was pre-drilled in each bolt head to mark the reference point. A bolt and the drill bit used to form the indentation are shown in Figure 4.12. To accurately mark the location of the reference points' pattern on the pavement, an aluminum template with holes arranged in a pattern similar to that of the reference points was fabricated in the shop. The template was used to drill pilot holes in the pavement. Figure 4.13 shows the pattern template.



Figure 4.50 ¼ x 1¼-inch Stainless Steel Hex Bolt and Bit



Figure 4.51 Reference Points Pattern Template

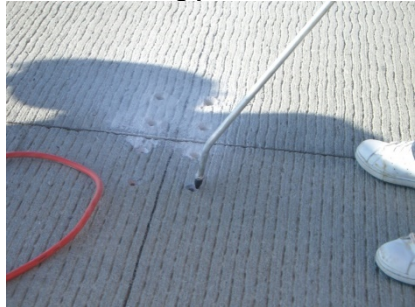
Vertical 5/16-inch diameter holes were drilled in the pavement at the pilot holes. The indented bolts were then epoxy glued inside the drilled vertical holes such that the top of the hex head was flush with or slightly below the pavement surface. The epoxy adhesive used to anchor the bolts was Hilti-HIT-RE 500. The epoxy adhesive data sheet is presented in Appendix C. Figure 4.14 shows the sequence of the installation process.



Drilling pilot holes



Drilling 5/16-inch diameter holes



Air blowing concrete dust



Checking hole depth



Filling holes with epoxy adhesive



Setting stainless steel bolts inside holes

Figure 4.52 Installation of Reference Points on Pavement

The instrumented joints were each fitted with three sets of reference points at the Brookings County test site and two sets of reference points at the Butte County and the Yankton County test sites. Figure 4.15 shows the placement of the reference points across an instrumented transverse joint. The first set was centered at approximately 6 inches from the edge of the pavement and the second set was centered at the middle of the driving lane. The third set, which was installed at the Brookings County test site only, was centered at the longitudinal joint.

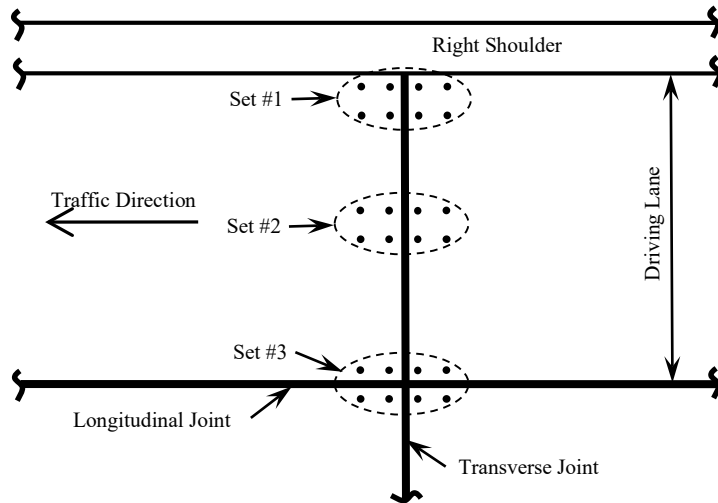


Figure 4.53 Placement of Reference Points along a Transverse Joint

At each Joint test section, two joints of each type were instrumented. Figure 4.16 shows the selection of the instrumented joints.

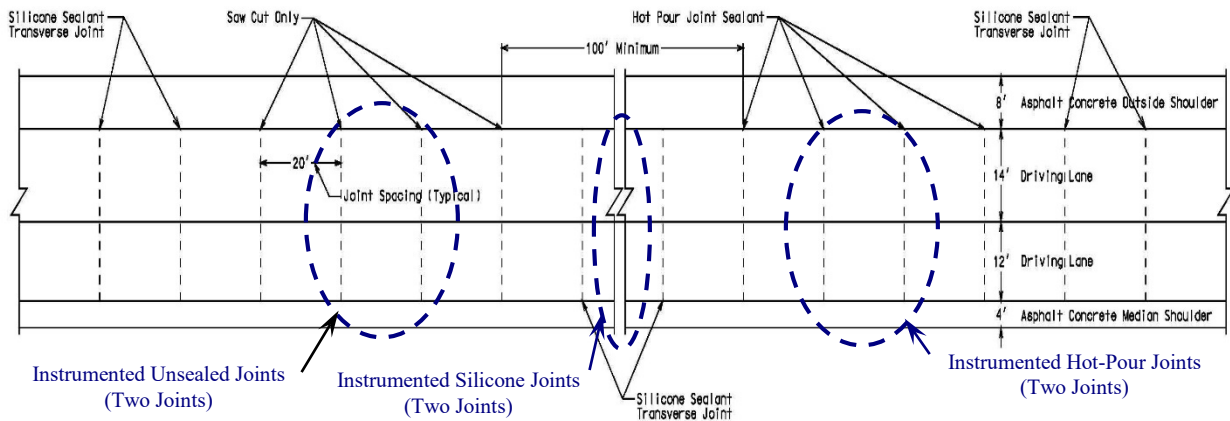


Figure 4.54 Instrumented Joints in a Joint Test Section

The gauge length between the reference points was measured using calipers capable of measurements to the nearest 1/10,000. Initially, 10 gauge lengths were to be measured at each reference points set as is shown in Figure 4.17. However, only measurements of gauge lengths 1, 2, 3, 4, 5, and 6 were recorded. Measurements of gauge lengths 1, 3, 4, and 6 were used to determine the surface strain in the two adjacent slabs, while measurements of gauge lengths 2 and 5 were used to determine the joint movement. The measurement of each gauge length was repeated three times and the average value was recorded. Initial measurements were made soon after the epoxy adhesive had cured. Other measurements were made periodically to document the changes in strain and joint movement. The change in strain was determined as the change in gauge length divide by the initial gauge length. A positive change in strain indicates extension and a negative change in strain indicates contraction. A positive change in the joint movement indicates widening of the joint gap, while a negative change in the joint movement indicates

narrowing of the joint gap. The pavement surface temperature was measured with an infrared thermometer and recorded for each round of gauge length measurements.

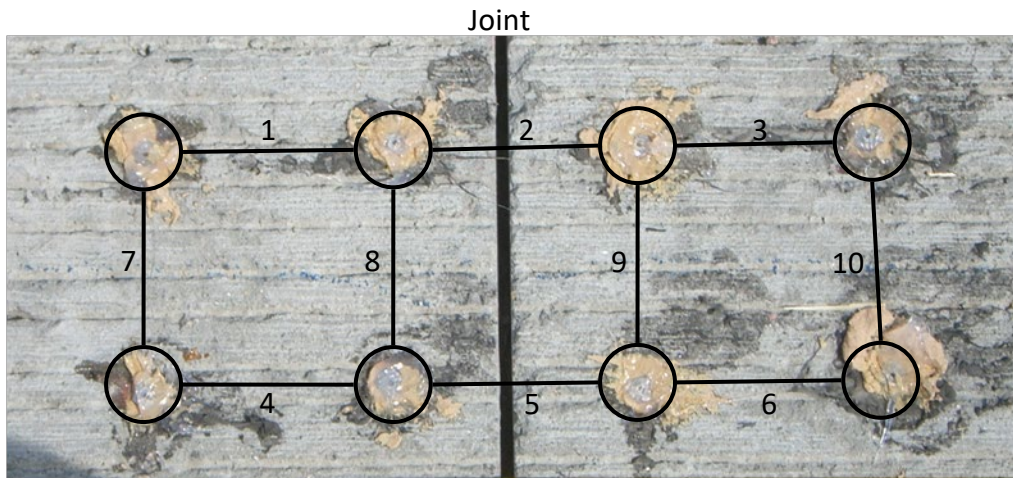


Figure 4.55 Distance Measurements between Reference Points

4.3.2 Moisture Ingress

Effectiveness of the different joint types in reducing moisture ingress through the joint was assessed by measuring the moisture content of the pavement subgrade at the joint. Water content reflectometers, simply called moisture sensors, and a datalogger were used to collect the moisture content data. The sensors and datalogger were Campbell Scientific Model CS616 and Model CR1000, respectively. Figure 4.18 shows the sensor and the datalogger types used in this project.



Figure 4.56 Moisture Sensor and Datalogger (after Campbell Scientific)

The moisture ingress data was collected from the test section at the Union County test site. The subgrade under one silicone sealed joint, one hot-pour sealed joint, and one unsealed joint was instrumented with moisture sensors. For each joint, sensors were placed at three locations: at the exterior edge of the driving lane, the middle of the pavement between the driving lane and the passing lane, and the middle of the passing lane. Figure 4.19 shows a schematic diagram of the instrumentation plan.

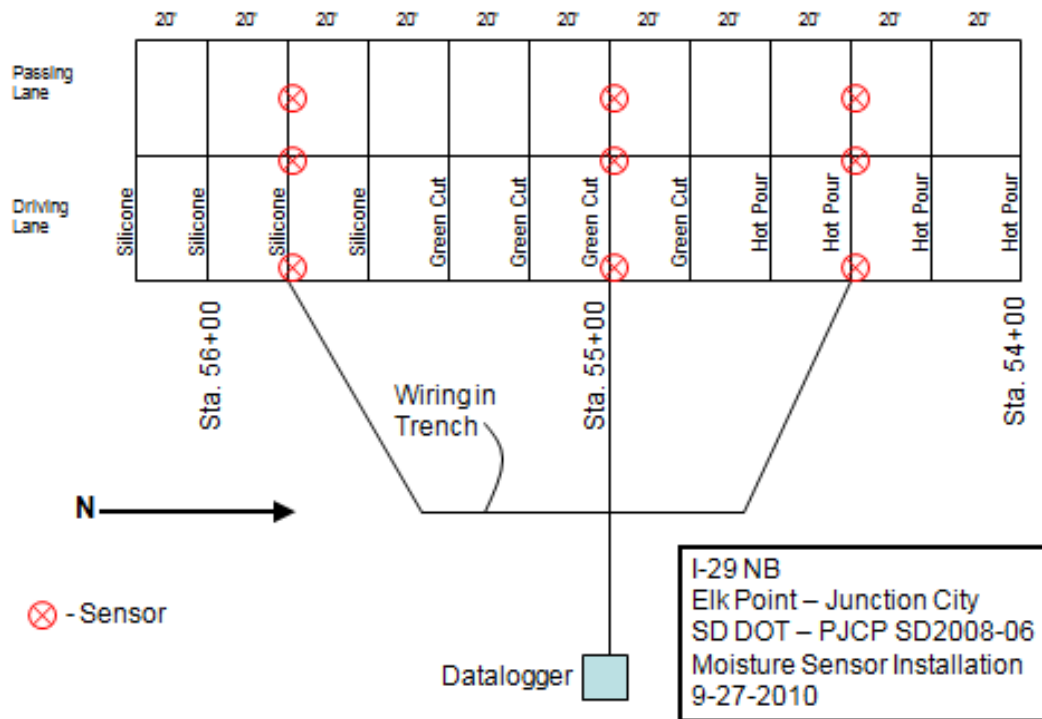


Figure 4.57 Moisture Content Instrumentation Plan

Installation of moisture sensors and wiring were completed prior to the compaction of the subbase and the subsequent placement of the pavement concrete. The uncompacted subbase was first trenched to allow for placement of the sensors and wiring. Moisture sensors were buried horizontally at approximately 12 inches deep into the uncompacted subbase and wiring was laid inside polyvinyl chloride (PVC) conduits to prevent damaging the wires during compaction. Wiring was connected to the datalogger which was positioned at the side of the road. The datalogger and solar panel providing power to the system were mounted on a steel pole. After the sensor installation and wiring were completed, trenches were backfilled and the subbase was subsequently compacted. Figure 4.20 shows pictures of the installation process.



Trenching the subbase



Placement of the Moisture Sensor



Datalogger Box

Figure 4.58 Installation of the Moisture Instrumentation

The moisture instrumentation system was installed at the end of September 2010 and the concrete pavement was completed in October 2010. Due to inclement weather conditions soon after the paving was completed, sealing of the joints was not performed until April of 2011. Collection of moisture data did not

start until after the joints were sealed. Therefore, the effect of not sealing the joints on moisture ingress from October 2010 to April 2011 was not a concern. Moisture measurements in the form of volumetric water content in the subbase were sampled and stored at a frequency of one reading per hour.

4.3.3 Load Transfer Efficiency

The load transfer efficiency (LTE) across the transverse contraction joints was determined using the falling weight deflectometer (FWD) apparatus owned and operated by SDDOT. The FWD apparatus used in this study is shown in Figure 4.21. FWD measurements across a transverse joint can be used to assess the efficiency of the dowel bars to transmit wheel loads across the joint.



Figure 4.59 FWD Apparatus

The FWD test involves dropping a weight on the pavement surface and measuring the resulting deflections at several points along a line parallel to the direction of traffic. Figure 4.22 shows the deflection sensors arrangement of the FWD apparatus used in this study. Arrows marked by the letter “S” followed by a number represent locations where deflection measurements are made. The number following the “S” indicates the order of the proximity of the deflection sensor to the falling weight. The falling weight is dropped between S1 and S2 and deflection measurements are made at locations S1 through S7. For the purpose of determining the LTE, only the S2 and S3 measurements are needed. When testing for LTE, the first deflection sensor, S3, is placed on the “Approach” slab while the other deflection sensors are placed on the “Leave” or “Departing” slab. Figure 4.23 shows FWD test at a joint.

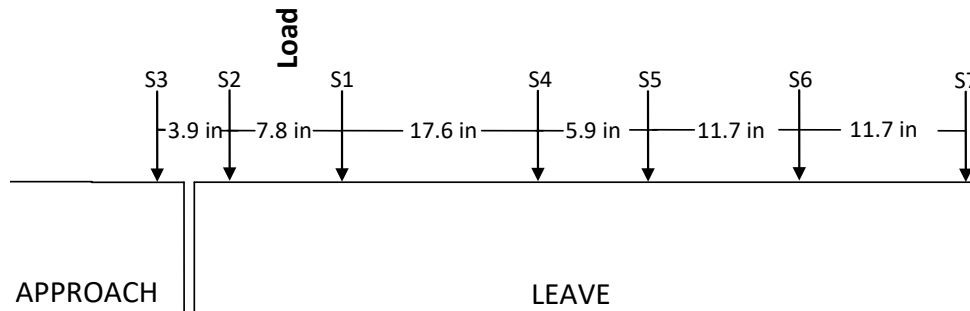


Figure 4.60 FWD Sensors Arrangement



Figure 4.61 FWD Test at a Transverse Joint

The degree of mechanical interlock between adjacent slab panels affects the FWD readings. As the pavement temperature increases, the joint between the slabs closes and the mechanical interlock increases. When the joint gap closes, the joint is said to be “locked.” When the joint gap opens, the joint becomes “unlocked.” A joint will exhibit higher LTE when it is locked. The unlocked condition occurs when the ambient temperature is between 50°F and 70°F. Unlocked LTE is a better indicator of the dowel bars efficiency, while locked LTE provides a better idea of the existence of voids under a slab.

The FWD tests were limited to the driving lane. For each joint tested, FWD readings were performed at two locations; one location was at approximately 2 to 3 feet from the right shoulder and the other was at the mid width of the driving lane. At each location, the FWD test was repeated twice. The average of the four sets of readings per sensor was used for determining the LTE according to the following equation:

$$\text{LTE (\%)} = \left(\frac{\text{Delection of S3}}{\text{Delection of S2}} \right) \times 98 \quad \text{Equation 4.4}$$

Based on recommendation of the FWD apparatus manufacturer, the LTE deflection ratio in Equation 4.1 is multiplied by a factor of 98, rather than 100, to adjust for the effect of the relatively short distance (approximately 4 inches) between sensors S2 and S3 on the FWD test readings.

4.3.3 International Roughness Index (IRI)

The International Roughness Index is a measure of the pavement’s quality of ride IRI values are obtained from profile measurements of the pavement surface. A profilometer is used to measure the surface profile of the pavement, which would indicate surface profile roughness including slab curling and warping. IRI values can theoretically range from 0 inch/mile for absolutely perfect pavement profile to 1,200 inches/mile for rough unpaved roads (Sayers and Karamihas 1998). Figure 4.24 shows a plot of the IRI ranges for different pavement surface conditions. In this study, the IRI values for the test sites were used to determine effects of the increased amount of curing compound on reducing pavement surface roughness.

In this study, the profilometer readings and the resulting IRI values were provided by SDDOT. The laser profilometer used by SDDOT does not provide accurate readings below freezing. Therefore, all pavement profiles were done when the ambient temperature was above 32°F. The profilometer was run along the

left and right wheel paths. An average IRI for each 0.1 miles was determined by SDDOT personnel using a program called ProVAL 3.0.

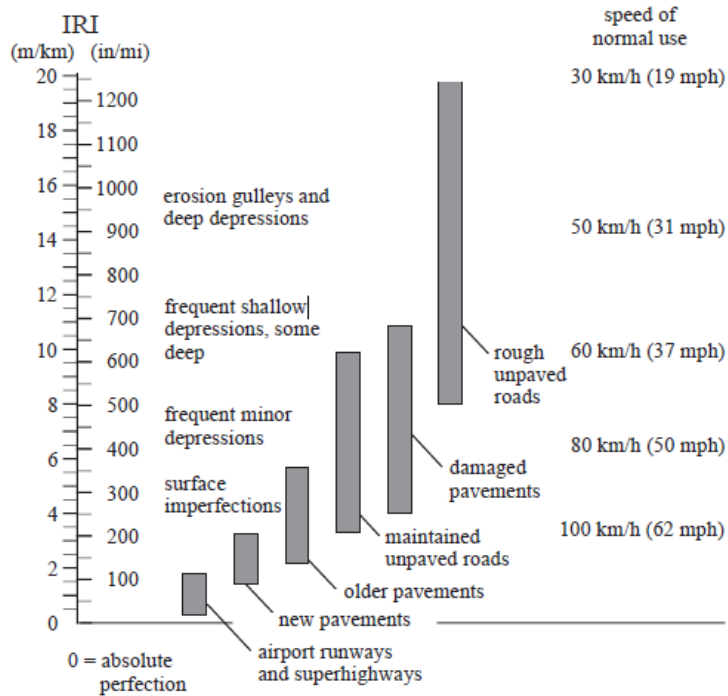


Figure 4.62 Ranges for IRI Values (Sayers and Karamihas 1998)

4.3.4 Joint Faulting

Joint faulting was evaluated using rod-and-level measurements. The relative change in the pavement surface level on both sides of the joint was measured periodically. The measurements were always made at the same location along the joint. The sign of the reported values indicates the movement of the “approach” slab relative to the “departure” slab in the direction of traffic. A positive sign indicates that the approach slab is higher than the departure slab at the joint while a negative sign indicates the opposite relative movement.

The Paver Concrete Distress Manual (US Army Corps of Engineers 1997) defines three levels of faulting severity: Low (L), Medium (M), and High (H). Table 4.2 shows the range of the difference in elevation for each severity level.

Table 4.20 Levels of Faulting Severity

Severity Level	Difference in Elevation
L	> 3 and < 10 mm (> 1/8 and < 3/8 in.)
M	> 10 and < 20 mm (> 3/8 and < 3/4 in.)
H	> 20 mm (> 3/4 in.)

4.3.5 Data Collection History

Except for moisture content, data was collected at different times of the year to capture the pavement performance under different weather and temperature conditions. The moisture content data was collected continuously at a frequency of one reading per hour year round. The original data collection plan was to collect data over a two-year period. However, due to factors such as changes in construction schedules and availability of SDDOT FWD truck and profilometer, data collection was performed at time intervals as permitted by the prevailing conditions. The data collection history for the test sites at I-29 Brookings County, US 212 Butte County, and SD 50 Yankton County are presented in Table 4.3, Table 4.4, and Table 4.5, respectively. The first pin measurements were used as reference readings for determining surface strain and change in joint width. The moisture content data was collected continuously from April through November 2011.

Table 4.21 Data Collection History for the I-29 Brookings County Test Site

	2009	2010	2011
Conc. Strain and Joint Movement	June; October	February; May; August	April
Rod-and-Level	October	February; May; August	April
Profilometer	November	July	March
FWD		October	June; November

Table 4.22 Data Collection History for the US 212 Butte County Test Site

	2009	2010	2011
Conc. Strain and Joint Movement	June; October	February; May; August	Apr
Rod-and-Level	October	February; May; August	Apr
Profilometer	November	July	March
FWD		October	November

Table 4.23 Data Collection History for the SD 50 Yankton County Test Site

	2009	2010	2011
Conc. Strain and Joint Movement		June; August	March; August; October
Rod-and-Level		June; August	March; August; October
Profilometer			
FWD		October	June; November

4.4 Data Analysis

The data collected in this study were analyzed statistically to determine influence of the different parameters (independent variables) on concrete surface strain near the transverse joints, transverse joint movement, moisture ingress at the transverse joints, faulting at the transverse joints, load transfer efficiency (LTE) at the transverse joints, and the International Roughness Index (IRI) of the pavement.

4.4.1 Statistical Methods

Three statistical methods (tests) were applied to the field data. The three methods were the Analysis of Variance (ANOVA), the Tukey HSD Test, and linear regression.

ANOVA performs a t -test to compare the means of two data sets to determine whether the two data sets are statistically different (i.e. if the data sets are from two different populations). For two data sets labeled 1 and 2, having means of μ_1 and μ_2 the null hypothesis, H_0 , tested with ANOVA is as follows:

$$H_0 : \mu_1 = \mu_2 \quad \text{Equation 4.5}$$

If the p -value from the t -test is larger than the preset significance level, α , the null hypothesis is not rejected and therefore, it cannot be concluded that the two data sets have statistically different means. If the p -value is smaller than the preset significance level, the null hypothesis is rejected and therefore, the two data sets have statistically different means.

The Tukey HSD test compares the means of three or more data sets to determine which ones are statistically different. The Tukey HSD test simply performs ANOVA for all possible two-set combinations. As with ANOVA, each comparison has a null hypothesis in which the means of the two data sets are equal. Each comparison is assigned a p -value that is compared to the preset significance level. In addition, output from a Tukey HSD test includes a lettering system to illustrate the differences between data sets. Each data set is assigned to one or more letter groups. Data sets not in the same letter group have means that are significantly different.

Linear regression is used to determine the extent to which dependent variable(s) affect an independent variable. For n independent variables x_1, x_2, \dots, x_n , with coefficients $\beta_1, \beta_2, \dots, \beta_n$, the equation relating the dependent variable to the independent variables is:

$$Y = \beta_0 + \beta_1 x_1 + \beta_2 x_2 + \dots + \beta_n x_n \quad \text{Equation 4.6}$$

There are $(n + 1)$ null hypotheses associated with Equation 4.3 as follows:

$$\begin{aligned} (H_0)_0 &: \beta_0 = 0 \\ (H_0)_1 &: \beta_1 = 0 \\ (H_0)_2 &: \beta_2 = 0 \\ &\vdots \\ &\vdots \\ &\vdots \\ (H_0)_n &: \beta_n = 0 \end{aligned} \quad \text{Equation 4.7}$$

A test is done for each independent variable. As with ANOVA, each test results in a p -value compared to the preset significance level. If the null hypothesis is not rejected, then the independent variable does not have a significant effect on the dependent variable. In this case, the independent variable term can be dropped from Equation 4.3. If the null hypothesis is rejected, then the independent variable does have a significant effect the dependent variable.

The statistical analysis was performed using the statistical analysis software JMP (SAS 2012).

4.4.2 Pavement Surface Strain and Transverse Joint Movement

The pavement longitudinal strain, and consequently the joint movement, is a complex mechanism that involves drying shrinkage, thermal strains and frictional drag under the concrete slab (Pittman and McCullough 1997). In addition, the infiltration of incompressible materials into the joint gap may also affect joint movement and, consequently, surface strain close to the joint. This study was not designed to develop predictive equations for surface strain and joint movement, but rather to statistically determine the significance of the influence of joint type and test site on surface strain and joint movement.

The initial pavement surface temperatures corresponding to the initial gauge length measurements are summarized in Table 4.6. The pavement surface temperatures for the subsequent gauge length measurements were recorded to determine the change in pavement temperatures corresponding to the change in surface strain and joint width. It should be noted that due to construction scheduling, the pin installation and reference gauge length measurements were made following one winter season after construction for the I-29 Brookings County and SD 50 Yankton County test sites, and immediately after construction for the US 212 Butte County test site.

Table 4.24 Measured Pavement Surface Temperature at Initial Gauge Length Measurements

	Measured Initial Surface Temperature (°F)				
	Test Section 1	Test Section 2	Test Section 3	Test Section 4	Test Section 5
I-29	85	86	89	91	89
US 212	89	88	86	83	82
SD 50	79	82	82	84	83

4.4.2.1 Surface Strain

The measured change in surface strain, ($\Delta\epsilon$) at the I-29 Brookings County, US 212 Butte County, and SD 50 Yankton County test sites are shown in Figure 4.25 and summarized in Table 4.7. Positive and negative values of $\Delta\epsilon$ indicate extension and contraction, respectively relative to the initial gauge length measurement. The change in surface temperature (ΔT) for the different data sets is also plotted in Figure 4.25. Positive and negative ΔT values indicate increase and decrease in surface temperature, respectively relative to the initial measured surface temperature.

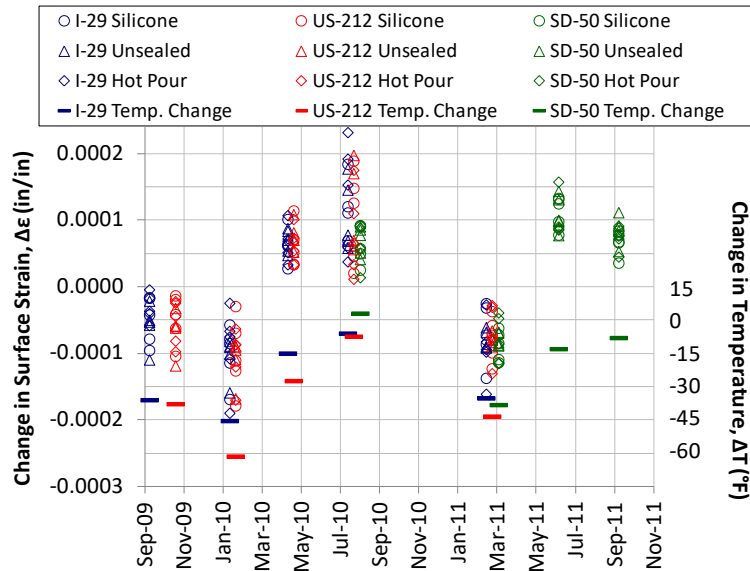


Figure 4.63 Measured Change in Surface Strain

Table 4.25 Summary of Change in Surface Strain Data

Data Group	Change in Surface Strain			
	Minimum	Maximum	Mean	Standard Deviation
I-29	-0.000190	0.000230	-0.000009	-0.000106
US-212	-0.000180	0.000200	-0.000014	-0.000108
SD-50	-0.000120	0.000160	0.000042	-0.000122
Unsealed	-0.000170	0.000200	0.000003	-0.000107
Silicone	-0.000180	0.000190	0.000003	-0.000109
Hot Pour	-0.000190	0.000230	0.000004	-0.000107

The measured strain versus change in pavement surface temperature is plotted in Figure 4.26. The best fit linear relationships between $\Delta\varepsilon$ and ΔT stratified for test site and joint type are also shown in Figure 4.26. The characteristics of the best fit linear relationships are presented in Table 4.8. The coefficient of variation (R^2) values ranged between 0.607 and 0.874, indicating strong correlations between surface strain and surface temperature for all cases.

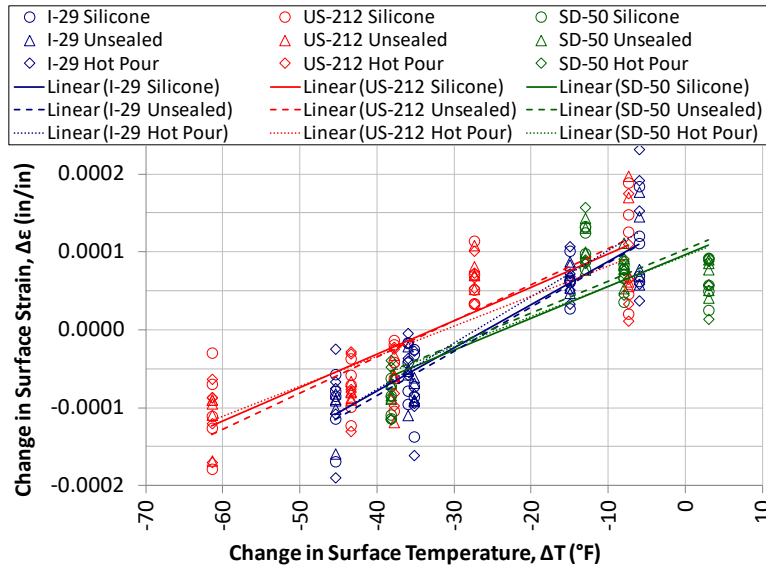


Figure 4.64 Change in Surface Strain vs. Change in Surface Temperature

Table 4.26 Characteristics of $\Delta\epsilon - \Delta T$ Best Fit Lines Stratified for Test Site and Joint Type

Data Group	Slope	Y-Intercept	R ²
I-29, Silicone	0.0000055	0.0001424	0.822
I-29, Unsealed	0.0000057	0.0001432	0.874
I-29, Hot Pour	0.0000059	0.0001606	0.726
US 212, Silicone	0.0000043	0.0001403	0.694
US 212, Unsealed	0.0000046	0.0001507	0.745
US 212, Hot Pour	0.0000039	0.0001204	0.668
SD 50, Silicone	0.0000041	0.0000961	0.615
SD 50, Unsealed	0.0000041	0.0001032	0.654
SD 50, Hot Pour	0.0000039	0.0000943	0.607

A Tukey HSD test was performed to determine whether the joint type had a significant influence on surface strain. The joint type was set as the independent variable and surface strain was set as the dependent variable. A significance level of $\alpha = 0.05$ was used. Table 4.9 presents the results of the analysis for each pair of joint types. In all three cases, the p -value was much greater than 0.05, indicating that the joint type did not have a significant influence on surface strain close to the joint.

Table 4.27 Tukey HSD Test Results for Change in Surface Strain by Joint Type

Comparison	<i>p</i> -value*	Conclusion
Unsealed vs. Hot Pour	0.9988	Insignificant difference
Unsealed vs. Silicone	1.0000	Insignificant difference
Hot Pour vs. Silicone	0.9983	Insignificant difference

*Significance level: $\alpha = 0.05$

A Tukey HSD test was also performed to determine if the test site location has a significant influence on surface strain. The test site location reflects variation in slab thickness and subbase material and thickness. The site location was set as the independent variable, and surface strain was set as the dependent variable. All the strain change values were shifted by 0.0002 to eliminate the effect of negative values on the statistical analysis results. A significance level of $\alpha = 0.05$ was used. The results of the statistical test are shown in Table 4.10. The results indicate that the measured change in surface strain values at the SD 50 test site were significantly different from those at the I-29 and US 212 test sites, while the difference in results between I-29 and US 212 was not significant. The reasons behind these statistical results are unclear; both I-29 and US 212 pavements were placed on a 5-inch gravel subbase, while the SD 50 was placed on a 5-inch asphalt subbase; the pavement thickness was 11, 9, and 8 inches at the I-29, SD 50, and US 212, respectively. Therefore, there seems to be no association between surface strain on one hand and the subbase material and the pavement thickness on the other.

Table 4.28 Tukey HSD Test Results for Change in Surface Strain by Test Site

Comparison	<i>p</i> -value*	Conclusion	Comments
I-29 vs. SD 50	0.0035	Significantly different	SD-50 yielded the highest change in surface strain.
I-29 vs. US 212	0.9285	Insignificant difference	
US-212 vs. SD 50	0.0011	Significantly different	

*Significance level: $\alpha = 0.05$

4.4.2.2 Joint Width

The measured change in the joint width (Δw) at the different test sites (I-29, US 212, and SD 50) are shown in Figure 4.27 and are summarized in Table 4.11. Positive and negative values of Δw indicate joint gap opening and closing, respectively relative to the initial gauge length measurement. The change in surface temperature (ΔT) for the different data sets is also plotted in Figure 4.27.

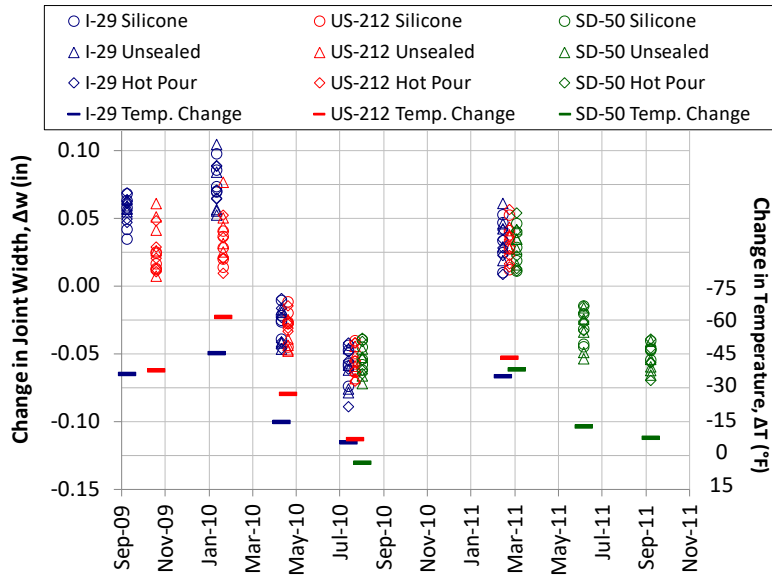


Figure 4.65 Measured Change in Joint Gap Width

Table 4.29 Summary of Joint Gap Width Data

Data Group	Change in Joint Gap Width (in)			
	Minimum	Maximum	Mean	Standard Deviation
I-29	-0.406	0.406	0.016	-0.440
US-212	-0.172	0.224	0.001	-0.456
SD-50	-0.224	0.094	-0.027	-0.460
Unsealed	-0.406	0.406	0.001	-0.440
Silicone	-0.179	0.224	0.002	-0.450
Hot Pour	-0.181	0.188	0.001	-0.449

The measured strain versus change in the joint gap width temperature is plotted in Figure 4.28. The best fit linear relationships between Δw and ΔT stratified for test site and joint type are also shown in Figure 4.28. The characteristics of the best fit linear relationships are presented in Table 4.12. The coefficient of variation (R^2) values ranged between 0.671 and 0.874, indicating strong correlations between change in joint width and surface temperature.

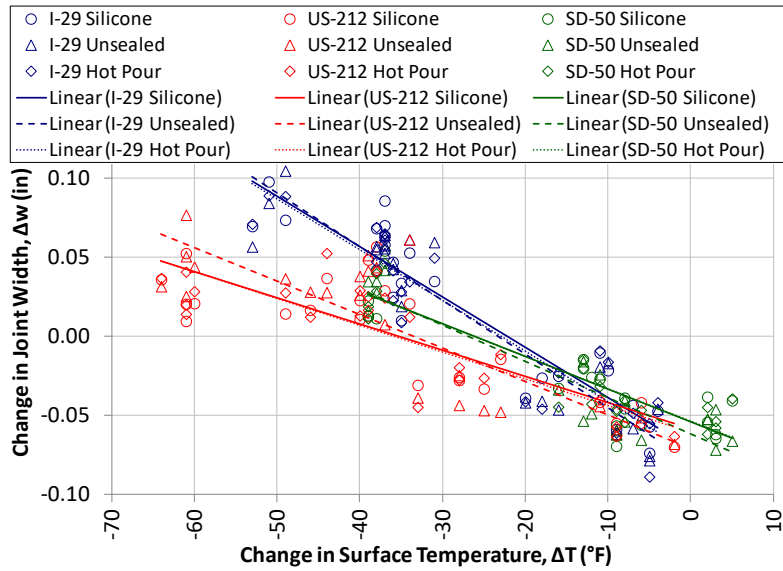


Figure 4.66 Change in Joint Gap Width vs. Change in Surface Temperature

Table 4.30 Characteristics of $\Delta w - \Delta T$ Best Fit Lines Stratified for Test Site and Joint Type

Data Group	Slope	Y-Intercept	R ²
I-29, Silicone	-0.0032	-0.0703	0.874
I-29, Unsealed	-0.0034	-0.0790	0.874
I-29, Hot Pour	-0.0032	-0.0734	0.863
US 212, Silicone	-0.0017	-0.0584	0.671
US 212, Unsealed	-0.0021	-0.0708	0.709
US 212, Hot Pour	-0.0017	-0.0606	0.726
SD 50, Silicone	-0.0021	-0.0542	0.801
SD 50, Unsealed	-0.0023	-0.0618	0.861
SD 50, Hot Pour	-0.0020	-0.0536	0.846

A Tukey HSD test was performed to determine whether the joint type had a significant influence on joint gap width. The joint type was set as the independent variable and the change in joint gap width was set as the dependent variable. A significance level of $\alpha = 0.05$ was used. Table 4.13 presents the results of the analysis for each pair of joint types. In all three cases, the p -value was much greater than 0.05, indicating that the joint type did not have a significant influence on the joint gap width.

Table 4.31 Tukey HSD Test Results for Change in Joint Gap Width by Joint Type

Comparison	<i>p</i> -value*	Conclusion
Unsealed vs. Hot Pour	0.9993	Insignificant difference
Unsealed vs. Silicone	0.9451	Insignificant difference
Hot Pour vs. Silicone	0.9563	Insignificant difference

*Significance level: $\alpha = 0.05$

A Tukey HSD test was also performed to determine if the test site location has a significant influence on the joint gap width. The test site location reflects the variation in slab thickness and subbase material and thickness. The site location was set as the independent variable, and change in the joint gap width was set as the dependent variable. All the joint gap width change values were shifted by 0.5 to eliminate effect of the negative values on the statistical analysis results. A significance level of $\alpha = 0.05$ was used. Results of the statistical test are shown in Table 4.14. Results indicate that the test site had a significant influence on the measured change in joint gap width. The test site at I-29 exhibited the greatest, while the test site at SD 50 exhibited the least change in joint gap width. Results indicate that the thicker slab exhibited greater change in joint gap width than the thinner slab; I-29 was thicker than SD 50 by 2 inches, but the subbase material was substantially identical at the two sites. Results also indicate that asphalt underlayment allows for greater joint movement than gravel subbase; the 9-inch thick pavement at SD 50 was placed on gravel subbase while the 8-inch thick pavement at US 212 was placed on an asphalt underlayment.

Table 4.32 Tukey HSD Test Results for Change in Joint Gap Width by Test Site

Comparison	<i>p</i> -value*	Conclusion	Comments
I-29 vs. SD 50	< 0.0001	Significantly different	I-29 yielded the largest and SD-50 yielded the lowest changes in Joint width.
I-29 vs. US 212	< 0.0001	Significantly different	
US-212 vs. SD 50	< 0.0001	Significantly different	

*Significance level: $\alpha = 0.05$

Theoretically, a negative change in surface temperature will result in contraction of the concrete (contraction strain) and opening (widening) of the joint. A positive change in surface temperature will cause extension of the concrete and closing (tightening) of the joint up to the point when the joint gap closes completely. Following joint closure, any additional increase in temperature will not cause significant change in the joint gap gauge length, but the surface extension strain will start to reduce and eventually turn into contraction strain as a result of the compressive stress build up at the closed joint gap. At sufficiently high temperatures, the compressive strain could potentially reach the concrete's ultimate compressive strain (approximately 0.003 to 0.004) corresponding to crushing of the concrete. Figure 4.29 shows a graphical representation of relationships between change in temperature and changes in joint gap width and concrete surface strain. The qualitative relationships shown in Figure 4.29 do not take into account the effects of temperature gradient along the depth of the pavement, drying shrinkage strain, swelling of concrete due to moisture absorption, or frictional drag stresses. Except for one data set from SD 50 during the summer of 2010, the collected data corresponded to negative change in surface temperature relative to the initial temperature (see Figure 4.27). Therefore, the data range obtained in this

study was insufficient to experience cases of joint gap full closure and determine the effect of incompressible material infiltration into the joint gap. For SD 50, the change in the two data clusters corresponding to surface temperature change between approximately -9°F and $+6^{\circ}\text{F}$ (Figure 4.28) appear to cause no significant change in the joint gap width. This could be indicative of joint gap closure, but the data is too limited to draw any conclusions regarding the effect of joint sealing method on infiltration of incompressible materials.

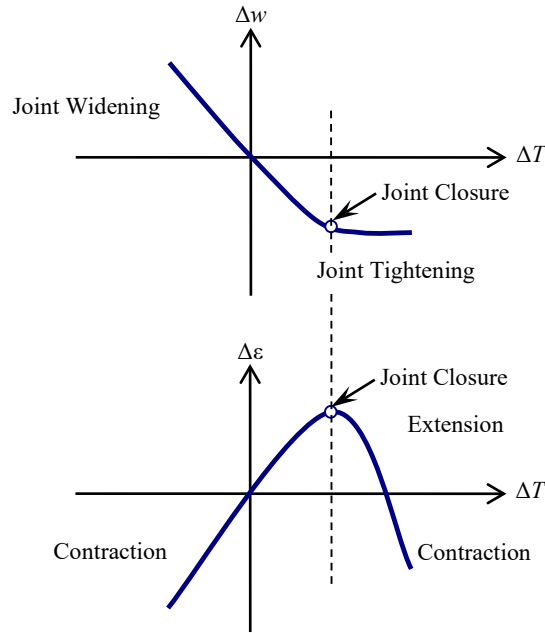


Figure 4.67 Theoretical relationships between ΔT , Δw and $\Delta \epsilon$

4.4.3 Moisture Ingress

The moisture content hourly readings from the three moisture sensors under each joint type were averaged and analyzed. Figure 4.30 shows a plot of the moisture content versus time for the three joint types. The similar trends followed by all three curves signify that readings from all sensors were being influenced by the same factor, which most probably was precipitation. Although precipitation was not measured at the test section, precipitation in the spring and summer of 2011, during which elevated moisture readings were recorded, was relatively high. The data clearly indicate that the unsealed joints allowed the most, while the silicone sealed joints allowed the least moisture ingress. Table 4.15 presents a summary of the moisture ingress data. On average, the moisture ingress at the unsealed joint and the hot-pour sealed joint was 34.5% and 14.2% higher than that at the silicone sealed joint.

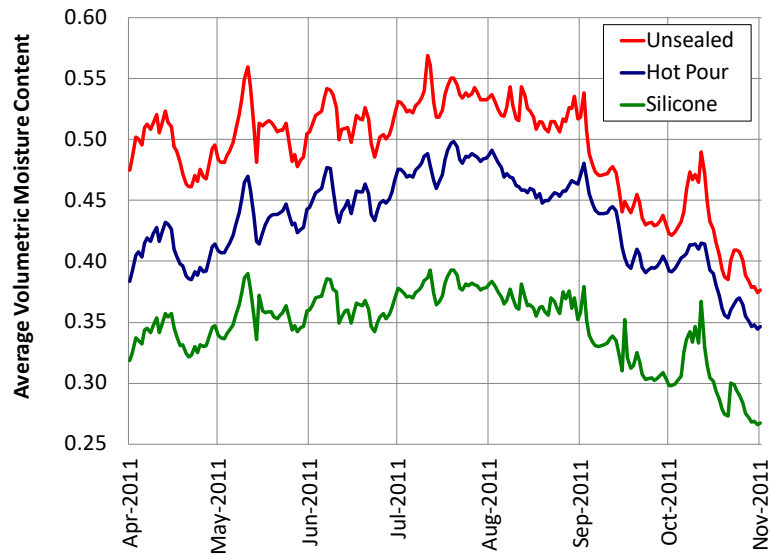


Figure 4.68 Moisture Ingress versus Time

Table 4.33 Summary of Moisture Ingress Data

Data Group	Volumetric Moisture Content			
	Minimum	Maximum	Mean	Standard Deviation
All	0.112	0.679	0.367	0.118
Silicone	0.112	0.535	0.316	0.095
Unsealed	0.153	0.679	0.424	0.123
Hot Pour	0.141	0.568	0.360	0.108

A Tukey HSD test was performed to determine whether the joint type had a significant influence on moisture ingress. The joint type was set as the independent variable and moisture ingress was set as the dependent variable. A significance level of $\alpha = 0.05$ was used. Table 4.16 presents the results of the analysis for each pair of joint types. In all three cases, the p -value was less than 0.0001, indicating that the joint type had a significant influence on moisture ingress.

Table 4.34 Tukey HSD Test Results for Moisture Ingress by Joint Type

Comparison	p -value*	Conclusion
Unsealed vs. Silicone	< 0.0001	Significantly different
Unsealed vs. Hot Pour	< 0.0001	Significantly different
Hot Pour vs. Silicone	< 0.0001	Significantly different

*Significance level: $\alpha = 0.05$

4.4.4 Load Transfer Efficiency

The LTE for the locked and unlocked conditions were analyzed separately. The unlocked LTE results at the three different test sites are presented in Figure 4.31 and summarized in Table 4.17. The unlocked LTE values ranged between a minimum of 0.508 and a maximum of 0.980. The average unlocked LTE for the test sites at Vermillion County (SD 50) and Butte County (US 212) was 25.2% and 16.9% higher than that at Brookings County (I-29). This result was not surprising. The FWD was performed more than two years after construction at the I-29 site, more than one year after construction at the US 212 site, and almost right after construction at the SD 50 site. Newer pavements exhibit higher LTE than older pavement. Moreover, the 5-inch asphalt subbase at the US 212 site helps support the wheel load and reduce the deflection of the departure slab, thereby resulting in higher LTE values.

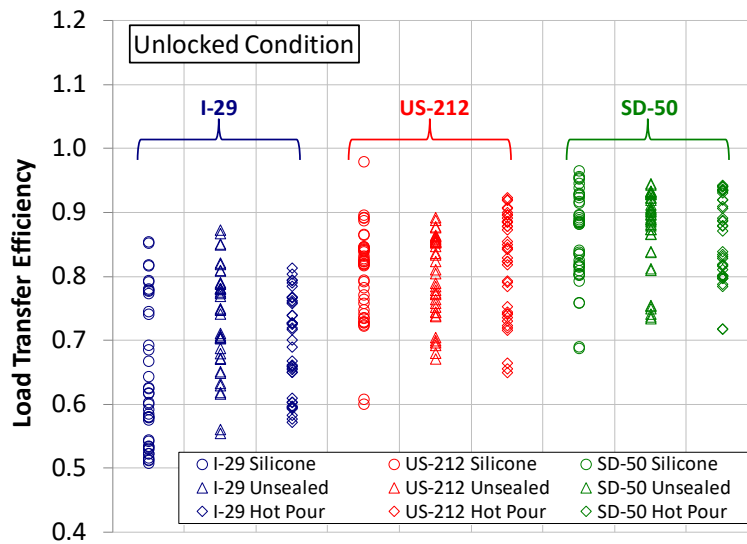


Figure 4.69 LTE for the Unlocked Condition

Table 4.35 Summary of LTE Values for the Unlocked Condition

Data Group	LTE (Unlocked Condition)			
	Minimum	Maximum	Mean	Standard Deviation
All	0.508	0.980	0.788	0.108
I-29	0.508	0.873	0.691	0.097
US 212	0.601	0.980	0.808	0.074
SD 50	0.688	0.966	0.865	0.066
Silicone	0.508	0.980	0.769	0.127
Unsealed	0.555	0.946	0.804	0.091
Hot Pour	0.572	0.943	0.791	0.101
I-29, Silicone	0.508	0.855	0.643	0.112
I-29, Unsealed	0.555	0.873	0.734	0.081
I-29, Hot Pour	0.572	0.814	0.695	0.075
US 212, Silicone	0.601	0.980	0.802	0.074
US 212, Unsealed	0.672	0.893	0.802	0.066
US 212, Hot Pour	0.650	0.923	0.821	0.080
SD 50, Silicone	0.688	0.966	0.862	0.070
SD 50, Unsealed	0.734	0.946	0.874	0.064
SD 50, Hot Pour	0.718	0.943	0.859	0.065

The locked condition LTE values are shown in Figure 4.32 and summarized in Table 4.18. The locked LTE values ranged between a minimum of 0.614 and a maximum of 0.980. The average locked LTE values followed a trend similar to that of the unlocked values; the Vermillion County (SD 50) average locked LTE was the highest and the Brookings County average locked LTE was the lowest. The average locked LTE for the test sites at Vermillion County (SD 50) and Butte County (US 212) was 15.4% and 11.2% higher than that at Brookings County (I-29). It was also observed that average LTE for the locked condition is higher than the respective LTE for the unlocked condition; the average locked LTE values at the SD 50, US 212, and I-29 sites were 16.5%, 10.8%, and 7.4% higher than the respective average unlocked LTE values.

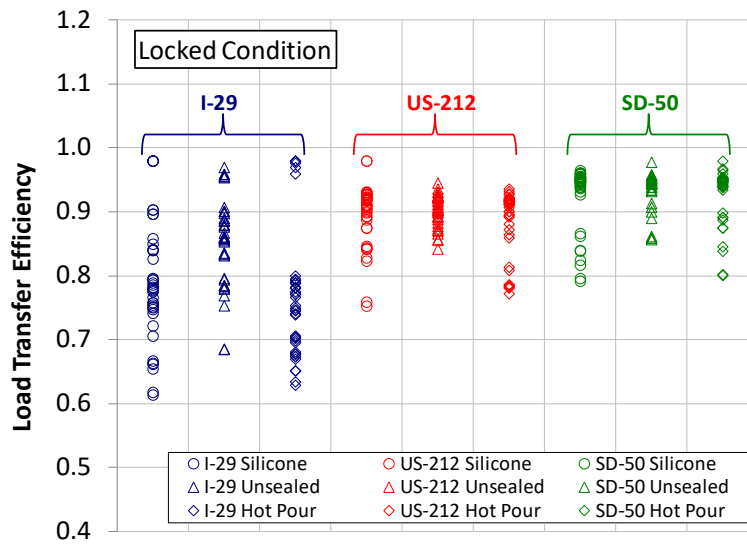


Figure 4.70 LTE for the Locked Condition

Table 4.36 Summary of LTE Values for the Locked Condition

Data Group	LTE (Locked Condition)			
	Minimum	Maximum	Mean	Standard Deviation
All	0.614	0.980	0.876	0.084
I-29	0.614	0.980	0.805	0.097
US 212	0.753	0.980	0.895	0.043
SD 50	0.792	0.980	0.929	0.042
Silicone	0.614	0.980	0.872	0.088
Unsealed	0.685	0.978	0.898	0.056
Hot Pour	0.629	0.980	0.859	0.099
I-29, Silicone	0.614	0.980	0.794	0.096
I-29, Unsealed	0.685	0.970	0.855	0.069
I-29, Hot Pour	0.629	0.980	0.764	0.102
US 212, Silicone	0.753	0.980	0.897	0.048
US 212, Unsealed	0.842	0.946	0.904	0.024
US 212, Hot Pour	0.773	0.936	0.885	0.052
SD 50, Silicone	0.792	0.965	0.925	0.050
SD 50, Unsealed	0.857	0.978	0.935	0.030
SD 50, Hot Pour	0.801	0.980	0.928	0.044

A Tukey HSD test was performed to determine if the test site location has a significant influence on LTE. The test site location reflects the dowel bar arrangement and subbase material used at the site. Using the pooled LTE data from all joint types, the site location was set as the independent variable, and LTE was set as the dependent variable. A significance level of $\alpha = 0.05$ was used. The results of the statistical test are shown in Table 4.19. The results show that for locked and unlocked joint conditions, the test site location had a significant influence on LTE.

Table 4.37 Tukey HSD Test Results for LTE by Location, All Joint Types

Joint Type	LTE Condition	Comparison	<i>p</i> -value*	Conclusion	Comments
All Types	Unlocked	I-29 vs. SD-50	< 0.0001	Significantly different	SD-50 yielded the highest average LTE values and I-29 yielded the lowest average LTE values.
		I-29 vs. US-212	< 0.0001	Significantly different	
		US-212 vs. SD-50	< 0.0001	Significantly different	
	Locked	I-29 vs. SD-50	< 0.0001	Significantly different	
		I-29 vs. US-212	< 0.0001	Significantly different	
		US-212 vs. SD-50	0.0002	Significantly different	

*Significance level: $\alpha = 0.05$

The influence of the site location was also assessed for each joint type individually. A Tukey HSD test was performed and the results are shown in Table 4.20. The site location was found to have significant influence on LTE for each joint type with two exceptions: the influence of the site location was statistically insignificant between US 212 and SD 50 for the locked silicone joint and the unlocked hot pour joint cases.

Table 4.38 Tukey HSD Test Results for LTE by Location for each Joint Type

Joint Type	LTE Condition	Comparison	p-value*	Conclusion	Comments
Silicone	Unlocked	I-29 vs. SD-50	< 0.0001	Significantly different	SD 50 yielded the highest average LTE values and I-29 yielded the lowest average LTE values. I-29 yielded significantly lower average LTE values than US 212 and SD 50.
		I-29 vs. US-212	< 0.0001	Significantly different	
		US-212 vs. SD-50	0.0065	Significantly different	
	Locked	I-29 vs. SD-50	< 0.0001	Significantly different	
		I-29 vs. US-212	< 0.0001	Significantly different	
		US-212 vs. SD-50	0.1611	Insignificant difference	
Hot Pour	Unlocked	I-29 vs. SD-50	< 0.0001	Significantly different	I-29 yielded significantly lower LTE values than US 212 and SD 50. SD 50 yielded the highest average LTE values, and I-29 yielded the lowest average LTE values.
		I-29 vs. US-212	< 0.0001	Significantly different	
		US-212 vs. SD-50	0.0588	Insignificant difference	
	Locked	I-29 vs. SD-50	< 0.0001	Significantly different	
		I-29 vs. US-212	< 0.0001	Significantly different	
		US-212 vs. SD-50	0.0220	Significantly different	
Unsealed	Unlocked	I-29 vs. SD-50	< 0.0001	Significantly different	SD 50 yielded the highest average LTE values, and I-29 yielded the lowest average LTE values. SD 50 yielded the highest average LTE values, and I-29 yielded the lowest average LTE values.
		I-29 vs. US-212	0.0001	Significantly different	
		US-212 vs. SD-50	< 0.0001	Significantly different	
	Locked	I-29 vs. SD-50	< 0.0001	Significantly different	
		I-29 vs. US-212	< 0.0001	Significantly different	
		US-212 vs. SD-50	0.0073	Significantly different	

*Significance level: $\alpha = 0.05$

In general, the test site location had a statistically significant effect on LTE. The effect of the site location on LTE may not necessarily be result of the dowel bar arrangement, but rather is reflective of the pavement’s age and stiffness of the subbase. However, the LTE at US 212 and SD 50 where the reduced dowel bar arrangement was used were relatively high. Therefore, the initial load transfer provided by the reduced dowel bar arrangement seems to be adequate.

4.4.5 International Roughness Index

The IRI data for test sections with standard and increased curing compound application rate are presented in Figure 4.33 and Figure 4.34, respectively. The data points in these two figures are grouped into three test sites and are plotted against the dates when the profilometer measurements were made. Lower IRI values correspond to smoother driving surfaces. The IRI data is also summarized in Table 4.21. The data in Table 4.21 are presented under various data group combinations. The data groups reflected in Table 4.21 are test site, curing compound application rate, test site and curing compound application rate, and pavement age and curing compound application rate. When all the data points are considered, IRI values varied between a minimum of 43.8 and a maximum of 183.0. These IRI values were well within the range for new pavement, as shown in Figure 4.24.

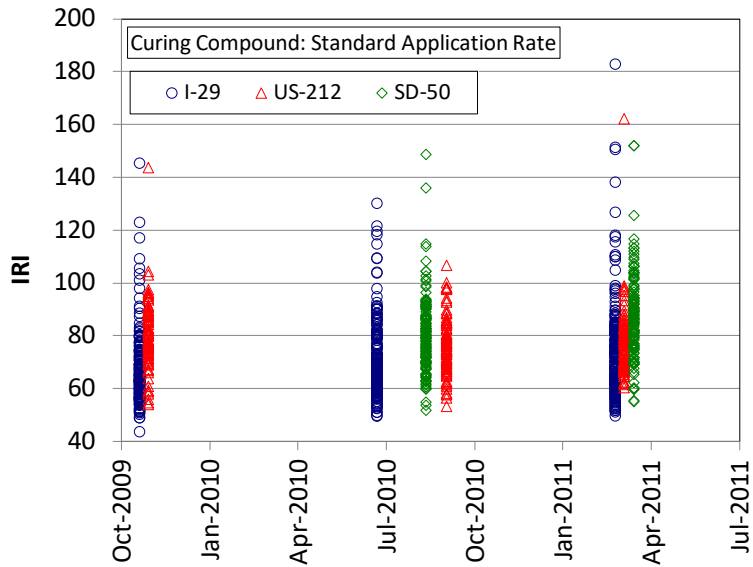


Figure 4.71 IRI Values – Standard Curing Compound Application Rate

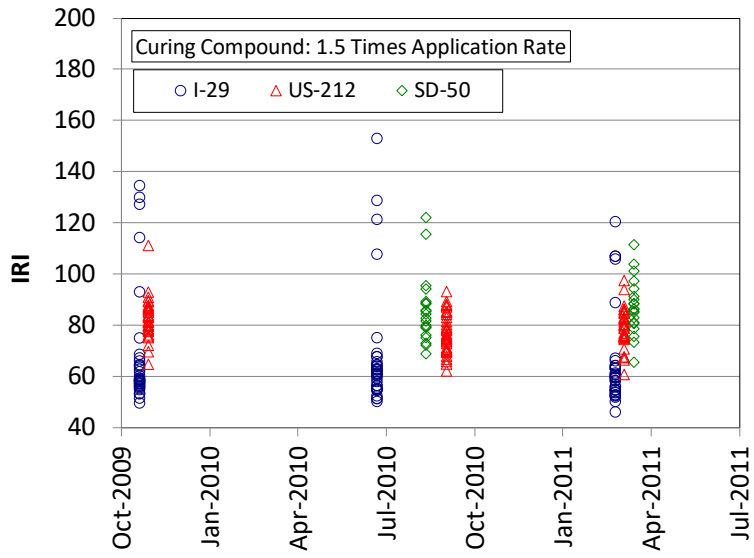


Figure 4.72 IRI Values – Increased Curing Compound Application Rate

Table 4.39 Summary of IRI Values for Various Data Group Combinations

Data Group	IRI			
	Minimum	Maximum	Mean	Standard Deviation
All	43.8	183.0	75.6	15.9
I-29	43.8	183.0	70.4	16.4
US-212	53.4	162.3	78.5	11.2
SD-50	51.9	152.1	84.5	15.1
Standard	43.8	183.0	75.6	15.7
1.5 Times*	46.4	153.2	75.8	17.0
I-29, Standard	43.8	183.0	70.8	15.4
I-29, α -methylstyrene	46.4	153.2	67.4	21.5
US-212, Standard	53.4	162.3	78.1	12.2
US-212, 1.5 Times*	61.0	111.4	79.4	8.0
SD-50, Standard	51.9	152.1	84.1	15.5
SD-50, 1.5 Times	65.8	122.3	86.9	12.0
2009, Standard	43.8	145.5	71.7	14.5
2010, Standard	49.7	148.8	75.0	14.0
2011, Standard	49.8	183.0	78.7	17.3
2009, 1.5 Times*	49.9	134.8	75.8	18.3
2010, 1.5 Times*	50.5	153.2	75.8	17.4
2011, 1.5 Times*	46.4	120.7	75.7	15.8

4.4.4.5 Comparison of IRI Values at the Different Test Sites

A Tukey HSD test was performed to determine whether the three test sites yield different levels of surface roughness. IRI data associated with each curing compound application rate were analyzed separately. The test site was set as the independent variable, and IRI was set as the dependent variable. A significance level of $\alpha = 0.05$ was used. The results of the test analysis are shown in Table 4.22. The differences between IRI readings from the three sites for both application rate cases were all statistically significant. I-29 yielded the lowest IRI readings (smoothest surface), and SD-50 yielded the highest IRI readings (roughest surface). Because the test site location has a significant effect on IRI, the differences between application rates is analyzed for each location individually.

Table 4.40 Tukey HSD Test Results for IRI by Location and Curing Compound Application Rate

Application Rate	Comparison	<i>p</i> -value*	Conclusion	Comments
Standard	US 212 vs. I-29	< 0.0001	Significantly different	SD 50 yielded the highest and I-29 yielded the lowest IRI values.
	US 212 vs. SD 50	< 0.0001	Significantly different	
	SD 50 vs. I-29	< 0.0001	Significantly different	
1.5 Times	US 212 vs. I-29	< 0.0001	Significantly different	SD-50 yielded the highest and I-29 yielded the lowest IRI values.
	US 212 vs. SD 50	0.0262	Significantly different	
	SD 50 vs. I-29	< 0.0001	Significantly different	

*Significance level: $\alpha = 0.05$

4.4.4.6 Influence of Curing Compound Application Rate on Change of IRI Values with Time

A Tukey HSD test was performed to determine how IRI changes over time for each of the two curing compound application rates. The objective was to determine effectiveness of an application rate in maintaining surface smoothness over time. IRI data from all three locations were pooled and labeled based on the year in which the profilometer measurement was made. Year was set as the independent variable and IRI was set as the dependent variable. A significance level of $\alpha = 0.05$ was used. Results are presented in Table 4.23. For the locations where the standard application rate was used, the IRI increased each year (i.e. the surfaces became rougher). The changes in IRI with time were all statistically significant. For locations where 1.5 times the application rate was used, the IRI did not increase significantly from one year to the next. The surfaces that were treated with 1.5 times the curing compound normal application rate maintained their original smoothness, while the surfaces treated with the standard application rate did not.

Table 4.41 Tukey HSD Test Results for IRI by Year – All Test Site Locations

Test Site	Application Rate	Comparison	<i>p</i> -value*	Conclusion	Comments
All Sites	Standard	2009 vs. 2010	0.0140	Significantly different	2011 yielded the highest and 2009 yielded the lowest IRI values.
		2010 vs. 2011	0.0011	Significantly different	
		2009 vs. 2011	< 0.0001	Significantly different	
	1.5 Times	2009 vs. 2010	0.9999	Insignificant Difference	Insignificant change in IRI over time.
		2010 vs. 2011	0.9982	Insignificant Difference	
		2009 vs. 2011	0.9976	Insignificant Difference	

*Significance level: $\alpha = 0.05$

4.4.5 Joint Faulting

The rod-and-level instruments used for measuring faulting at the joints allowed for measurements in increments of 0.06 inches. Measurements were made at eight locations across each joint. All the faulting measurements made in this study were 0.00, 0.06, or 0.12 inches in absolute value. Therefore, the joint faulting for all joints included in this study was either close to the lower limit or below the low severity faulting level reported in Table 4.2. The averaged absolute faulting values versus time are shown in Figure 4.35 and the faulting data is summarized in Table 4.24. Because the faulting values were insignificant, no further analysis was performed on the faulting data.

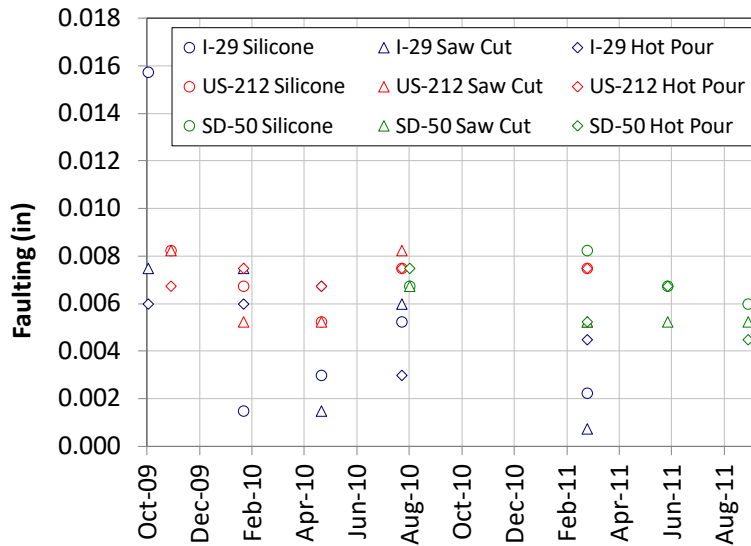


Figure 4.73 Average Absolute Faulting Values versus Time

Table 4.42 Summary of Faulting Values for Various Data Group Combinations

Data Group	LTE (Locked Condition)			
	Minimum	Maximum	Mean	Standard Deviation
All	0.00	0.12	0.0061	0.0207
I-29	0.00	0.12	0.0052	0.0201
US 212	0.00	0.12	0.0070	0.0218
SD 50	0.00	0.12	0.0062	0.0200
Silicone	0.00	0.12	0.0066	0.0215
Unsealed	0.00	0.12	0.0056	0.0198
Hot Pour	0.00	0.12	0.0062	0.0207
I-29, Silicone	0.00	0.12	0.0056	0.0212
I-29, Unsealed	0.00	0.12	0.0047	0.0191
I-29, Hot Pour	0.00	0.12	0.0053	0.0199
US 212, Silicone	0.00	0.12	0.0074	0.0219
US 212, Unsealed	0.00	0.12	0.0065	0.0217
US 212, Hot Pour	0.00	0.12	0.0072	0.0217
SD 50, Silicone	0.00	0.12	0.0069	0.0214
SD 50, Unsealed	0.00	0.12	0.0056	0.0181
SD 50, Hot Pour	0.00	0.12	0.0060	0.0204
Normal Dowel Bars	0.00	0.12	0.0052	0.0201
Reduced Dowel Bars	0.00	0.12	0.0066	0.0210

5. SUMMARY, CONCLUSIONS, RECOMMENDATIONS, AND IMPLEMENTATION

5.1 Summary

The South Dakota Department of Transportation has not reviewed design and construction methods of JPC pavements for many years. Research was needed to review the current design and construction procedures, and examine joint performance as related to ride quality and overall pavement performance. The overall goal is optimizing current joint design and sealing practices while enhancing pavement smoothness, minimizing costs and improving quality.

This report is part of SDDOT Research Project SD2008-06, “Jointed Plain Concrete Pavement Design and Construction Review.” The objectives of this research were to: 1) review available literature and field performance of various concrete pavement designs, especially with regard to joint and sealant systems, to determine any possible beneficial changes to current practice, 2) develop optimized concrete mix designs incorporating larger top size aggregate and pea gravel to provide good workability at lower cement contents and resist thermal effects, and 3) construct and evaluate appropriate JPC test sections to resolve any performance issues with regard to potential changes in design or construction.

Research covered in this report included experimental studies of optimized concrete mixtures for JPC pavements and field evaluation of newly constructed JPC pavement sections along South Dakota highways.

Concrete mixtures with reduced cement content and 36 combinations of coarse aggregate types (quartzite and limestone), aggregate top sizes (1.5 and 1.0 inches), blending aggregate types (3/8-inch aggregate in quartzite chip, limestone chip, and pea rock), coarse-to-fine aggregate ratios (60/40 and 65/35), and water/cementitious materials (w/cm) ratios (0.41, 0.39, and 0.37) were tested to develop an optimized mix for use in JPC pavement applications. Freeze-thaw durability, workability (consolidation ability), and mechanical properties of the mixes were measured and evaluated. A new energy-based experimental method for assessing the workability of concrete was devised. The method introduces a performance parameter, called “Specific Work,” to compare the workability of different concrete mixes.

Four newly constructed JPC pavement sites on South Dakota highways were selected for instrumentation, monitoring, and data collection. The four sites were located on I-29 north of Brookings in Brookings County, US 212 west of Belle Fourche in Butte County, SD 50 west of Vermillion in Yankton County, and I-29 south of Vermillion in Union County. The parameters considered in the study included the transverse joint sealant type, dowel bar configuration at the transverse joints, and amount of curing compound. Three different transverse joint sealing types were incorporated in the pavement at each test site: hot-pour sealant, epoxy sealant, and green cut with no sealant (unsealed). Two dowel bar configurations at the transverse joints were included in the study. I-29 sites were provided with normal dowel bar configuration (12 dowels per lane), whereas the US 212 and the SD 50 sites were provided with reduced dowel bar configuration (9 dowels per lane). Test sections at the test sites in Brookings, Butte, and Yankton counties were treated with increased amount of curing compound (1.5 times the normal amount).

The test site in Union County was used to only measure moisture content of the subbase under the transverse joints through the use of moisture sensors. The data collected from the Brookings County, Butte County, and Yankton County test sites were:

- Pavement surface gauge length measurements to determine change in pavement surface strain and transverse joint width.
- Falling weight deflectometer (FWD) to assess the load transfer efficiency (LTE) at the transverse joint.
- Profilometer measurements to evaluate the pavement ride quality through the International Roughness Index (IRI).
- Rod-and-level measurements to determine faulting at the transverse joints

5.2 Conclusions

Based on the experimental and analytical work performed in this study, many conclusions have been drawn regarding the fresh and hardened properties of concrete pavement mix designs and the performance of newly constructed concrete pavements.

A byproduct of this study was development of a new apparatus and testing method for comparative evaluation of concrete workability. The method measures the “specific work” of a fresh concrete sample. The specific work is the work per unit weight needed to displace and consolidate a concrete sample. Lower specific work values correspond to higher concrete workability.

Following are the conclusions made in this study.

5.2.1 Concrete Mixtures Optimization

5.2.1.1 Plastic Concrete Behavior

- The specific work method provides a rigorous approach in a laboratory setting for comparative evaluation of concrete workability.
- There is a weak negative correlation between specific work and slump. Workability is highly influenced by factors that could not be captured in the slump test.
- There is no correlation between specific work and air content.
- For concrete mixtures with 3/8-inch limestone or quartzite chip aggregates, the use of 1.5-inch instead of 1-inch aggregate top size increases the workability of concrete mixtures. Except for the quartzite mixes with pea rock blending aggregates, mixes with 1-inch aggregate top size consistently exhibited higher specific work (lower workability) than their counterpart mixes with 1.5-inch aggregate top size.
- Mixes with 65/35 coarse-to-fine aggregate ratio and 1-inch top aggregate size exhibited high specific work. Therefore, mixes with 65/35 coarse-to-fine aggregate ratio would be unsuitable for concrete pavement applications.
- When pea rock was used as the blending aggregate with the quartzite mixes, the 1.5-inch maximum aggregate size mixes exhibited specific work higher than their 1-inch maximum aggregate size counterpart mixes.

5.2.1.2 Hardened Concrete Behavior

- The compressive strength gain of the concrete mixes in this study could be predicted with reasonable accuracy using the Branson equation. The limestone mixes compressive strengths were on average 3.1 percent higher than the predicted seven day values. The quartzite mixes averaged a compressive strength 6.9 percent higher than the predicted values at seven days
- The measured modulus of rupture was higher than the value obtained from the ACI code empirical equation. The mean f_r for the limestone mixes is $11.84\sqrt{f'_c}$ with a standard deviation of

$1.5\sqrt{f'_c}$. The mean f_r for the quartzite mixes is $9.90\sqrt{f'_c}$ with a standard deviation of $0.75\sqrt{f'_c}$. Both means are above the value obtained from the code empirical equation of $7.5\sqrt{f'_c}$.

- Mixes with pea rock exhibited rapid durability degradation with increased number of freeze-thaw cycles, whereas those without pea rock showed mild durability degradation. At the end of 150 freeze-thaw cycles, all of the mixes with pea rock had a durability factor (DF) less than the acceptable limit of 85, with most of them significantly below 85. On the other hand, all of the mixes that did not contain pea rock had a DF higher than 85.

5.2.2 Performance of Newly Constructed JPC Pavements

- The joint type did not show significant influence on the concrete surface strain close to the joint. However, one test site (SD 50) exhibited significantly higher surface strains than the other two test sites (I-29 and US 212). It was unclear why the surface strain at one test site was significantly different than those at the other two sites because no association between surface strain on one hand and the subbase material and the pavement thickness on the other could be established.
- The joint type did not have a significant influence on the joint gap width. However, the test site location, which reflects the variation in slab thickness and subbase material and thickness, had a significant influence on the measured change in joint gap width. For the identical subbase material and thickness, increasing the slab thickness resulted in increase in the change of the joint gap width. For practically similar slab thicknesses, gravel subbase results in lower change in joint gap width than asphalt subbase.
- The joint type had a significant influence on moisture ingress. On average, the moisture ingress at the unsealed joint and the hot-pour sealed joint was 34.5% and 14.2% higher than that at the silicone sealed joint.
- The pavement test sections in this study did not allow for comparison of the performance of different dowel bar arrangements under otherwise identical pavement conditions. In general, test sections with reduced dowel bar arrangement exhibited higher LTE than test sections with standard dowel bar arrangement. However, the effect of the dowel bar arrangement on LTE may not necessarily be the result of the dowel bar arrangement, but rather is reflective of the age of the pavement and the stiffness of the subbase.
- The LTE at US 212 and SD 50 where the reduced dowel bar arrangement was used were relatively high. Therefore, the initial load transfer provided by the reduced dowel bar arrangement seems to be adequate.
- These IRI values of the test sections were all well within the range for new pavement. However, pavement surfaces that were treated with 1.5 times the curing compound normal application rate maintained their original smoothness over time, while the surfaces treated with the standard application rate exhibited statistically significant reduction in smoothness (increase in IRI).
- The joint faulting for all of the joints included in this study was either close to the lower limit or below the low severity faulting level as specified by the U.S. Army Corps of Engineers paver distress manual.
- For the duration of this study, no joint spalling was observed at any of the test sections of this study.

5.3 Recommendations

Based on the results of this study, the following recommendations are made:

Number	Recommendation	Reason/Benefit of Recommendation
1	It is recommended that SDDOT prohibit the use of pea rock for the production of pavement concrete mixtures in South Dakota.	Mixes with pea rock exhibited rapid durability degradation with increased number of freeze-thaw cycles, whereas those without pea rock showed mild durability degradation. The experimental work conducted in this study showed that at the end of 150 freeze-thaw cycles, all of the mixes with pea rock had a durability factor (DF) less than the acceptable limit of 85, with most of them significantly below 85. On the other hand, all of the mixes that did not contain pea rock had a DF higher than 85.
2	It is recommended that SDDOT increase the maximum aggregate size from 1 to 1.5-inch for concrete mixes of jointed plain concrete pavement.	Previous studies show that increasing the maximum aggregate size will increase the surface area of the coarse aggregate. An increased surface area results in lower cement quantities necessary to obtain a given water-to-cement ratio. A lower cement quantity will yield cost savings on projects. The tests conducted in this study show that the hardened properties of concrete mixtures with an increased maximum aggregate size of 1.5 inches had no adverse effects on the compressive and flexural strength of the hardened concrete. At the same time, the experimental results showed that for concrete mixtures with 3/8-inch limestone or quartzite chip blending aggregates, the use of 1.5-inch instead of 1-inch aggregate top size increases the workability of concrete mixtures. Except for the quartzite mixes with pea rock aggregates, mixes with 1-inch aggregate top size consistently exhibited higher specific work (i.e. lower workability) than their counterpart mixes with 1.5-inch aggregate top size.
3	It is recommended that SDDOT conduct additional research to determine the effect of increasing the coarse-to-fine aggregate ratio on fresh concrete properties.	Previous studies show that increasing the coarse aggregate surface area results in lower cement quantities necessary to obtain a given water-to-cement ratio. A lower cement quantity will yield cost savings on projects. One way to increase

Number	Recommendation	Reason/Benefit of Recommendation
		<p>aggregate surface area in a concrete mixture is to increase the coarse-to-fine aggregate ratio.</p> <p>The experimental results in this study showed that the compressive and flexural strengths of mixes with increased 65/35 coarse-to-fine aggregate ratio were comparable to those mixes having the 60/40 coarse-to-fine aggregate ratio currently specified by SDDOT. However, the testing method developed in this study for determining the workability of the concrete mixes showed variability in the results. Some test results showed that increasing the coarse-to-fine ratio could result in a significant increase in the amount of effort required to consolidate concrete (i.e. reduced workability). The results obtained in this study are not conclusive.</p>
4	<p>It is recommended that SDDOT implement the two proposed mix designs presented in Appendix A (one with limestone aggregates and one with quartzite aggregates) in trial test sections and assess mix workability and the short and long term performance of those test sections.</p>	<p>The experimental work showed that among the 36 different concrete mixes tested in this study, the two recommended mix designs (presented in Appendix A) were economical (least amount of cement) and most workable concrete mixtures. However, concrete workability, which was based on laboratory batches, should be verified in the field through batch plant production of the two concrete mixes and placing and finishing of full-scale jointed plain concrete pavement sections.</p>
5	<p>It is recommended that SDDOT change the specified curing compound (ASTM C 309, Type 2, Class A) application rate from 150 ft²/gallon to 100 ft²/gallon.</p>	<p>The IRI values of the test sections were well within the range for new pavement. However, pavement surfaces of the test sections that were treated 1.5 times the SDDOT specified curing compound normal application rate maintained their original smoothness over time, while the surfaces treated with the SDDOT specified curing compound at the standard application rate exhibited statistically significant reduction in smoothness (increase in IRI). Although the time window for data collection was narrow (maximum of 16 months), the difference in the change in IRI values for the two curing compound application rates indicates that increasing the curing compound</p>

Number	Recommendation	Reason/Benefit of Recommendation
		application rate leads to better pavement performance over time.
6	It is recommended that SDDOT continue to use silicone sealant for transverse joints in plain jointed concrete pavement.	The moisture ingress at the unsealed and the hot-pour sealed transverse joints was significantly higher than that at the silicone-sealed joints. Although the long-term effect of higher moisture ingress was not evaluated in this study, it is believed that higher moisture ingress will lead to increased pumping at the joint. Therefore, it is recommended that SDDOT maintains the use of silicone sealant for transverse joints.
7	It is recommended that SDDOT fund a study to develop limits for acceptable workability measurements using the laboratory method that was developed in this study.	A byproduct of this study was the development of a new apparatus and testing method for comparative evaluation of concrete workability. The method measures the “specific work” of a fresh concrete sample. The specific work is the work per unit weight needed to displace and consolidate a concrete sample. Lower specific work values correspond to higher concrete workability. However, this study did not develop limits for acceptable workability measurements. Therefore, a study is needed to quantify “specific work” numbers that correspond to acceptable workability in the field.

5.4 Implementation

The following actions are recommended for future implementation.

- Update the SDDOT Standard Specifications for Roads and Bridges as per the applicable recommendations listed above.
- Construct and monitor the performance over time of two JPC pavement sections (one with quartzite and one with limestone aggregates) using the optimized concrete mix designs presented in Appendix A.
- A future study should be designed to compare the performance of normal and reduced dowel bar arrangements in identical JPC pavements.

REFERENCES

- Allen, H. (1948). "Final Report of Project Committee No. 1, Maintenance of Concrete Pavements as Related to the Pumping Action of Slabs," Proceedings of the Twenty-Eighth Annual Meeting, Highway Research Board, Washington D.C., Vol. 28, December 7-10, 1948, pp. 281-310.
- American Concrete Institute (ACI). (2008). Building code requirements for structural concrete and commentary, ACI 318-08 and ACI 318R-08, ACI, Farmington Hills, Michigan.
- American Concrete Institute (ACI). (2006). Guide to durable concrete, ACI Manual of Concrete, Part 1: Materials and General Properties of Concrete, ACI 201.2R-06, ACI, Farmington Hills, Michigan.
- American Society for Testing and Materials (ASTM). (2009). Annual book of ASTM standards, Section 4 construction, Volume 04.02 concrete and mineral aggregates, ASTM, Philadelphia, Pennsylvania.
- Baker, S. D., and Scholer, C. F. (1973). Effect of variations in coarse aggregate gradation on properties of Portland cement concrete, Highway Research Record 441, Highway Research Board, Washington, D.C., pp 97-110.
- Branson, D.E. (1977). "Deformation of Concrete Structures." McGraw-Hill, New York City, New York.
- Cable, J. K., Wang, K. and Ge, Zhi. (2003). "Investigation into Improved Pavement Curing Materials and Techniques: Part 2 (Phase III)." Center for Portland Cement Concrete Pavement Technology at Iowa State University, Iowa Highway Research Board, Iowa Department of Transportation. pp. 1-24.
- Cordon, W. A. (1966). Freezing and thawing of concrete – Mechanisms and control, American Concrete Association, Farmington Hills, Michigan.
- Cramer, S., Walls, R. A. (2001). "Strategies for enhancing the freeze-thaw durability of Portland cement and concrete pavements." Report No. WI/SPR-06-01, Wisconsin Department of Transportation, Madison, Wisconsin.
- Cramer, S., Hall, M., and Parry, J. (1995). "Effect of optimized total aggregate gradation on Portland cement concrete for Wisconsin pavements." Transportation Research Record 1478, Transportation Research Board, Washington, D.C. pp 100-106.
- Crovetti, J. A. and Bischoff, D. (2001) "Construction and Performance of Alternative Concrete Pavement Designs in Wisconsin." TRB Volume No. 1778. pp. 43-53.
- Federal Highway Administration (FHWA). (2001). "Portland-Cement Concrete Rheology and Workability: Final Report." Publication No. FHWA-RD-00-025. McLean, Virginia.
- Hall, K. T., Crovetti, J. A., Hoerner, T., Smith, K.D., Ioannides, I.M. and Armaghani, J. (2007). "Cost-Effectiveness of Sealing Transverse Contraction Joints in Concrete Pavements – Draft Final Report." Office of Research, Development, and Technology: Federal Highway Administration. Contract No. DTFH61-03-C-00102. pp. 1-201.
- Hall, K. T., and Crovetti, J. A. (2000). "LTPP Data Analysis: Relative Performance of Jointed Plain Concrete Pavement with Sealed and Unsealed Joints." NCHRP Web Document 32 (Project SP20-50[2]). Prepared for the NCHRP, TRB and NRC. pp. 1-98.

- Harrison, P. J. (2004). "For the Ideal Slab-on-Ground Mixture." *Concrete International*, Volume 26, No. 3. PP. 46-55.
- Huang, Yang H. (2004) "Pavement Analysis and Design." Pearson Education, Inc: Pearson Prentice Hall. Upper Saddle River, NJ. pp. 147-182.
- Ioannides, A. M., and Mills, J. C. (2006). Effect of larger sized coarse aggregates on mechanical properties of Portland cement concrete pavement and structures, Report No. FHWA/OH-2006/10A, Ohio Department of Transportation, Columbus, Ohio.
- Janssen, D. J., and Snyder, M. B. (1994). Resistance of concrete to freezing and thawing, Report No. SHRP-C-391, Strategic Highway Research Program, Washington, D.C.
- Kosmatka, S. H., Kerkhoff, B. and Panarese, W. C. (2002). Design and control of concrete mixtures, 14th Ed., Portland Cement Association (PCA), Skokie, Illinois.
- McNally, G. H. (1998). Soil and rock construction materials, 1st Ed., Routledge, New York, New York.
- Miller, J. S. and Bellinger, W. Y. (2003). "Distress Identification Manual for the Long-Term Pavement Performance Program (Fourth Revised Edition)." Office of Infrastructure Research and Development: Federal Highway Administration. Manual. pp. 33-58.
- Mindness, S., Young, J. F., and Darwin, D. (2003). Concrete, 2nd Ed., Prentice-Hall, Inc., Upper Saddle River, New Jersey.
- Morian, D. A., Stoffels, S. (1998). "Joint Seal Practices in the United States Observations and Considerations." *Transportation Research Record* 1627. Paper No. 98-1346. pp. 7-12.
- Neville, A. M. (1996). Properties of concrete, Prentice Hall, Essex, England.
- Park, R. and Paulay, T. (1975). Reinforced Concrete Structures, J. Wiley & Sons, New York, NY.
- Pittman D. W. and McCullough B. F. (1997). "Development of a Roller-Compacted Concrete Pavement Crack and Joint Spacing Model." *Transportation Research Record* No. 1567, Transportation Research Board.
- Rasmussen, R. O., Agosto, A., and Cramer, S. (2007). "Analysis of Concrete Pavement Joints to Predict the Onset of Distress." Wisconsin Department of Transportation. pp. 1-58.
- SAS (2012). *JMP Statistical Discovery Software, Version 10* (Computer software), SAS Institute Inc., Cary, NC, <<http://www.jmp.com/>> (Jul. 9, 2012)
- Sayers, M. W. and Karamihas, S. M. (1998). "The Little Book of Profiling Basic Information about Measuring and Interpreting Road Profiles."
- Shober, S. F. (1996). "The Great Unsealing. A Perspective on PCC Joint Sealing." Wisconsin Department of Transportation. pp. 1-102.
- South Dakota Department of Transportation (SDDOT). (2010). "Concrete Paving Manual." pp. 32-115.

South Dakota Department of Transportation (SDDOT). (2004). Standard Specifications for Roads and Bridges, South Dakota.

State of South Dakota Transportation Inventory Management. (2007).

<http://www.sddot.com/pe/data/pave.asp>. Accessed on August 25, 2010.

US Army Corps of Engineers. (1997). "Pavement Concrete Distress Manual." TR 97/105.

Wong, G.S., Alexander, A.M., Hakins, R., Poole, T.S., Maolone, P.G., and Wakeley, L. (2000). Portland-Cement Concrete Rheology and Workability: Final Report, Report No. FHWA-RD-00-025, Federal Highway Administration, McLean, Virginia.

APPENDIX A: MIX DESIGN RECOMMENDATIONS

SDDOT 2008-6: JPC Design and Construction Review

Mix Design Recommendations

June 4, 2010

Parameters

Following are the potential changes to SDDOT's current jointed plain concrete (JPC) mix design that were investigated in this research project.

- Substituting 3/8-inch chipped aggregate with pea rock
- Incorporating a maximum aggregate size of 1.5 inches instead of the current standard of 1.0 inch maximum size
- Lowering the amount of cement required in the mixture by increasing the coarse-to-fine aggregate ratio. These changes have the possibility to lower the cost of JPC.

Recommendations

Based on the experimental results, the following recommendations are made:

1. Effect of Pea Rock

The research conducted on freeze-thaw durability of the concrete mixtures showed that incorporating pea rock into concrete resulted in an increased rate of deterioration and a much lower durability factor. Based solely on the durability testing results, it is recommended that pea rock not be used in SDDOT jointed plain concrete pavements.

2. Effect of Maximum Aggregate Size

Research shows that increasing the maximum aggregate size will also increase the surface area of the coarse aggregate. The literature shows that an increased surface area results in lower cement quantities necessary to obtain a given water-to-cement ratio. A lower cement quantity will yield cost savings on projects.

The tests conducted in this study on the concrete mixtures with an increased maximum aggregate size of 1.5 inches included compressive strength, flexural strength, workability, and freeze-thaw durability. The test results of the mixtures with an increased maximum aggregate size and those of the current SDDOT standard mix with a maximum size of 1.0 inch show that the maximum aggregate size had no significant effects on the performance of the concrete. Based on the overall performance of the increased aggregate size and the cost benefits of having a larger aggregate surface area, it is recommended that the maximum aggregate size be increased from 1.0 inch to 1.5 inches for SDDOT JPC pavements.

3. Effect of Increasing Coarse-to-Fine Aggregate Ratio

Another way to increase aggregate surface area in a concrete mixture is to increase the coarse-to-fine aggregate ratio. The results for compressive strength, flexural strength, and freeze-thaw durability for these mixtures were comparable to the current mix design. The testing method developed to determine the effort required to consolidate concrete showed variability in the results. Test results showed that

increasing the coarse-to-fine ratio could result in a significant increase in the amount of effort required to consolidate concrete. Therefore, it is recommended additional testing should be performed on the effects of increasing the coarse-to-fine ratio in concrete mixes before making changes to the current SDDOT JPC coarse-to-fine ratio.

In summary, it is recommended that pea rock should not be used in SDDOT concrete due to its poor freeze-thaw durability performance. The maximum aggregate size in JPC pavement can be increased from 1.0 inch to 1.5 inches without negatively affecting the performance. Further testing is needed prior to making changes to the current coarse-to-fine aggregate ratio.

Proposed Optimized Mix Designs

Limestone Aggregate:

Mix design

1.5" Coarse, lb/cu yd	720
1" Coarse, lb/cu yd	535
3/8" Chip, lb/cu yd	591
Fine, lb/cu yd	1230
Cement, lb/cu yd	460
Fly Ash, lb/cu yd	115
W/C ratio	0.41

Quartzite Aggregate:

Mix design

1.5" Coarse, lb/cu yd	848
1" Coarse, lb/cu yd	643
3/8" Chip, lb/cu yd	320
Fine, lb/cu yd	1208
Cement, lb/cu yd	460
Fly Ash, lb/cu yd	115
W/C ratio	0.41

The optimum aggregate gradation for each mix and the sieve analysis for each of the aggregates are presented on the next pages. Note that the 3/8-inch quartzite and limestone aggregates were each separated out at the source for 100% passing the 1/2-inch sieve and retention on the 3/8-inch sieve.

ASTM C 136, "Standard Test Method for Sieve Analysis of Fine and Coarse Aggregates"

Test Sample
1.5 inch - Rapid City Limestone

Sieve	Size (in)	Sieve Wt. Only (kg)	Sieve + Retained Sample Wt. (kg)	Retained Sample Wt. (kg)	Percent Retained on Sieve (%)	Percent Passing Sieve (%)
1.5"	1.5	7.26	7.26	0	0.0	100.0
1.0"	1.0	7.24	19.19	11.95	78.0	22.0
3/4"	0.75	7.22	9.99	2.77	18.1	3.9
1/2"	0.50	7.33	7.43	0.10	0.7	3.3
3/8"	0.375	7.17	7.22	0.05	0.3	2.9
No. 4	0.1870079	7.28	7.64	0.36	2.3	0.6
Pan	0	7.28	7.37	0.09	0.6	0.0

Total Retained 15.32 100.0

ASTM C 136, "Standard Test Method for Sieve Analysis of Fine and Coarse Aggregates"

Test Sample
1.0 inch - Rapid City Limestone

Sieve	Size (in)	Sieve Wt. Only (kg)	Sieve + Retained Sample Wt. (kg)	Retained Sample Wt. (kg)	Percent Retained on Sieve (%)	Percent Passing Sieve (%)
1.5"	1.5	7.26	7.26	0	0.0	100.0
1.0"	1.0	7.24	7.24	0	0.0	100.0
3/4"	0.75	7.22	10.32	3.1	19.7	72.0
1/2"	0.50	7.33	12.39	5.06	32.1	38.0
3/8"	0.375	7.17	11.11	3.94	25.0	13.0
No. 4	0.1870079	7.28	10.20	2.92	18.6	4.0
Pan	0	7.28	8.00	0.72	4.6	0.0

Total Retained 15.74 100.0

ASTM C 136, "Standard Test Method for Sieve Analysis of Fine and Coarse Aggregates"

Test Sample
1.5 inch - Dell Rapids Quartzite

Sieve	Size (in)	Sieve Wt. Only (kg)	Sieve + Retained Sample Wt. (kg)	Retained Sample Wt. (kg)	Percent Retained on Sieve (%)	Percent Passing Sieve (%)
1.5"	1.5	7.26	7.26	0	0.0	100.0
1.0"	1.0	7.24	7.42	0.18	1.2	98.8
3/4"	0.75	7.22	10.8	3.58	23.0	75.8
1/2"	0.50	7.33	14.76	7.43	47.8	28.0
3/8"	0.375	7.17	10.31	3.14	20.2	7.8
No. 4	0.1870079	7.28	8.44	1.16	7.5	0.3
Pan	0	7.28	7.33	0.05	0.3	0.0

Total Retained 15.54 100.0

ASTM C 136, "Standard Test Method for Sieve Analysis of Fine and Coarse Aggregates"

Test Sample
1.0 inch - Dell Rapids Quartzite

Sieve	Size (in)	Sieve Wt. Only (kg)	Sieve + Retained Sample Wt. (kg)	Retained Sample Wt. (kg)	Percent Retained on Sieve (%)	Percent Passing Sieve (%)
1.5"	1.5	7.26	7.26	0	0.0	100.0
1.0"	1.0	7.24	7.24	0	0.0	100.0
3/4"	0.75	7.22	8.63	1.41	19.7	80.3
1/2"	0.50	7.33	9.63	2.30	32.2	48.1
3/8"	0.375	7.17	8.96	1.79	25.0	23.1
No. 4	0.1870079	7.28	8.60	1.32	18.5	4.6
Pan	0	7.28	7.61	0.33	4.6	0.0

Total Retained 7.15 100.0

ASTM C 136, "Standard Test Method for Sieve Analysis of Fine and Coarse Aggregates"

Test Sample: Brookings Sand

Sieve	Size (µm)	Sieve Wt. Only (g)	Sieve + Retained Sample Wt. (g)	Retained Sample Wt. (g)	Percent Retained on Sieve (%)	Percent Passing Sieve (%)	Min. SD DOT % Passing Req't (%)	Max. SD DOT % Passing Req't (%)
3/8"	9500		0	0	0	100.0	100	100
No. 4	4750		0	0	0	100.0	95	100
No. 8	2360	687.99	724.12	36.13	7.12	92.9		
No. 16	1180	648.31	788.28	139.97	27.59	65.3	45	85
No. 30	600	592.69	752.21	159.52	31.45	33.8		
No. 50	300	548.94	665.23	116.29	22.92	10.9	10	30
No. 100	150	522.05	570.03	47.98	9.46	1.5	2	10
No. 200	75	513.6	516.69	3.09	0.61	0.8		
Pan	0	492.43	494.06	1.63				
Wash	0			2.68	0.8	0.0		

Total Sample Weight 507.29 100.0

Sample Wt. Before Washing and Sieving 508

Sieve	Size (µm)	Percent Retained on Sieve (%)	Cumulative Percent Retained on Sieve (%)
3/8"	9500	0	0
No. 4	4750	0	0
No. 8	2360	7.12	7.12
No. 16	1180	27.59	34.71
No. 30	600	31.45	66.16
No. 50	300	22.92	89.08
No. 100	150	9.46	98.54
No. 200	75	0.61	99.15
Pan	0		
Wash	0	0.8	99.95

Fineness Modulus 2.96

APPENDIX B: CEMENT, FLY ASH, AND AIR ENTRAINER DATA

	<p>GCC of America 130 Rampart Way, Suite 205 Denver, CO 80230 Sales (303) 739-5800</p>
<p>Plant: Rapid City 501 N. Saint Onge Street Rapid City, South Dakota</p>	<p>Cement Type: III, Low Alkali</p>
<p>Contact: Larry Paulsen Phone: (605) 721-7100</p>	<p>Date: 2/6/09 Production period ending: 1/17/09 Average of last 10 silos.</p>

STANDARD REQUIREMENTS ASTM C 150-07/AASHTO M-85					
CHEMICAL			PHYSICAL		
Item	Spec. Limit	Test Result	Item	Spec. Limit	Test Result
SiO ₂ (%)	A	20.9	Air content of mortar (volume %)	12 max	7.7
Al ₂ O ₃ (%)	6.0 max.	4.6	Blaine fineness (m ² /kg)	280 min.	384
Fe ₂ O ₃ (%)	6.0 max.	3.1	Autoclave expansion (%)	0.80 max.	0.0
CaO (%)	A	64.5	False set (%)	50 min.	80.3
MgO (%)	6.0 max.	1.2	Compressive strength (MPa)		
SO ₃ (%)	3.0 max.	2.5	1 day, Minimum MPa (psi)	A	
Ignition loss (%)	3.0 max.	2.1	3 day, Minimum MPa (psi)	12 (1740)	29 (4196)
Na ₂ O (%)	A	0.16	7 day, Minimum MPa (psi)	19 (2760)	38 (5507)
K ₂ O (%)	A	0.60	28 day, Minimum MPa (psi)	A	
Equivalent alkalis (%)	B	0.55	Time of setting, Vicat (minutes)		
Insoluble residue (%)	0.75 max.	0.4	Initial	Not less than	45
CO ₂ (%)	A	1.2		Not more than	375
Limestone (%)	5.0 max.	2.8			
CaCO ₃ in limestone (%)	70% min.	93.2			
Potential Compounds (%)					
C ₃ S	A	55.1			
C ₂ S	A	18.4			
C ₃ A	8 max.	6.9			
C ₄ AF	A	9.5			

A Not applicable.
 B Limit not specified by purchaser. Test result provided for information only.

GCC OF AMERICA PORTLAND CEMENT IS WARRANTED TO CONFORM AT THE TIME OF SHIPMENT WITH ASTM C 150-07/AASHTO M-85. NO OTHER WARRANTY IS MADE OR IMPLIED. HAVING NO CONTROL OVER THE USE OF ITS CEMENTS, GCC OF AMERICA DOES NOT GUARANTEE FINISHED WORK. GCC IS NOT RESPONSIBLE FOR ANY ADDITIVES NOT STATED IN THE CERTIFICATE OF COMPLIANCE.

We certify that the above described cement, at the time of shipment, meets the chemical and physical requirements of the ASTM C 150-07/AASHTO M-85.

Signature:  Laboratory Supervisor

ASTM C618-05 / AASHTO M 295-0 Testing of
 Coal Creek Fly Ash

Sample Type:	3200-ton	Report Date:	5/19/2009
Sample Date:	4/1-4/3/09	MTRF ID	500CC
		Sample ID:	

Chemical Analysis	ASTM / AASHTO Limits		ASTM Test Method
	Class F	Class C	
Silicon Dioxide (SiO ₂)	50.85 %		
Aluminum Oxide (Al ₂ O ₃)	14.61 %		
Iron Oxide (Fe ₂ O ₃)	6.62 %		
Sum of Constituents	72.08 %	70.0% min 50.0% min	D4326
Sulfur Trioxide (SO ₃)	0.80 %	5.0% max 5.0% max	D4326
Calcium Oxide (CaO)	14.96 %		D4326
Moisture	0.027 %	3.0% max 3.0% max	C311
Loss on Ignition (AASHTO M 295-00 req.)	0.04 %	6.0% max 5.0% max	C311
Available Alkalies, as Na ₂ O (AASHTO M 295-00 req.)	0.92 %	1.5% max 1.5% max	C311
Physical Analysis			
Fineness, % retained on #325	23.82 %	34% max 34% max	C311, C430
Strength Activity Index - 7 or 28 day requirement 7 day, % of control	88 %	75% min 75% min	C311, C109
28 day, % of control	101 %	75% min 75% min	
Water Requirement, % control	89 %	105% max 105% max	
Autoclave Soundness	0.029 %	0.8% max 0.8% max	C311, C151
True Particle Density	2.48		

Headwaters Resources certifies that, to the best of its knowledge, the test data listed herein was generated by applicable ASTM methods and meets the requirements of ASTM C618-05 for Class F fly ash.


 Robb Bergman
 MTRF Manager



DARAVAIR® 1000 Air-entraining admixture ASTM C260

Product Description

Daravair® 1000 is a liquid air-entraining admixture that provides freeze-thaw resistance, yield control, and finishability performance across the full range of concrete mix designs. Daravair 1000 is a clean, light-orange product designed to generate specification-quality air systems. Based on a high-grade saponified rosin formulation, Daravair 1000 is chemically similar to vinsol-based products, but with increased purity and supply dependability. Daravair 1000 weighs approximately 8.5 lbs/gal (1.02 kg/L). Daravair 1000 does not contain intentionally added chloride.

Uses

Daravair 1000 air-entraining admixture may be used wherever the purposeful entrainment of air is required by concrete specifications. Formulated to perform across the entire spectrum of production mixes, Daravair 1000 generates quality, freeze-thaw resistant air systems in concrete conditions that include the following:

- Low slump
- Paving
- Central mix
- Extruded slip form
- Mixes containing hot water and accelerators
- Precast

Product Advantages

- Rapid air build suitable for short mix cycles
- Can be used in wide spectrum of mix designs

- High cement factor
- Fly ash and slag
- Superplasticizers
- Manufactured sands

Performance

Air is incorporated into the concrete by the mechanics of mixing and stabilized into millions of discrete semi-microscopic bubbles in the presence of a specifically designed air-entraining admixture such as Daravair 1000. These air bubbles act much like flexible ball bearings increasing the mobility, or plasticity and workability of the concrete. This can permit a reduction in mixing water with no loss of slump. Placeability is improved. Bleeding, plastic shrinkage and segregation are minimized.

Through the purposeful entrainment of air, Daravair 1000 markedly increases the durability of concrete to severe exposures particularly to freezing and thawing. It has also demonstrated a remarkable ability to impart resistance to the action of frost and de-icing salts as well as sulfate, sea and alkaline waters.



Addition Rates

There is no standard addition rate for Daravair 1000. The amount to be used will depend upon the amount of air required for job conditions, usually in the range of 4 to 8%. Typical factors which might influence the amount of air-entraining admixture required are temperature, cement, sand gradation, and the use of extra fine materials such as fly ash and microsilica. Typical Daravair 1000 addition rates range from ½ to 3 fl oz/100 lbs (30 to 200 mL/100 kg) of cement. Pretesting of concrete should be performed to confirm dosage rates required to achieve desired concrete performance.

The air-entraining capacity of Daravair 1000 is usually increased when other concrete admixtures are contained in the concrete, particularly water-reducing admixtures and water-reducing retarders. This may allow up to ½ reduction in the amount of Daravair 1000 required.

Mix Adjustment

Entrained air will increase the volume of the concrete making it necessary to adjust the mix proportions to maintain the cement factor and yield. This may be accomplished by a reduction in water requirement and aggregate content.

Compatibility with Other Admixtures and Batch Sequencing

Daravair 1000 is compatible with most Grace admixtures as long as they are added separately to the concrete mix. In general, it is recommended that Daravair 1000 be added to the concrete mix near the beginning of the batch sequence for optimum performance, preferably by “dribbling” on the sand. Different sequencing may be used if local testing shows better performance. Please see Grace

Technical Bulletin TB-0110, *Admixture Dispenser Discharge Line Location and Sequencing for Concrete Batching Operations* for further recommendations. Daravair 1000 should not be added directly to heated water.

Pretesting of the concrete mix should be performed before use, and as conditions and materials change in order to assure compatibility, and to optimize dosage rates, addition times in the batch sequencing and concrete performance. Please consult your Grace representative for guidance.

Packaging & Handling

Daravair 1000 is available in bulk, delivered by metered tank trucks and in 55 gal (210 L) drums. **Daravair 1000 will freeze at about 30°F (-1°C) but its air-entraining properties are completely restored by thawing and thorough mechanical agitation.**

Dispensing Equipment

A complete line of accurate automatic dispensing equipment is available. These dispensers can be located to discharge into the water line, the mixer, or on the sand.

Specifications

Concrete shall be air entrained concrete, containing 4 to 8% entrained air. The air contents in the concrete shall be determined by the pressure method (ASTM Designation C231) or volumetric method (ASTM Designation C173). The air-entraining admixture shall be a completely neutralized rosin solution, such as Daravair 1000, as manufactured by Grace Construction Products, or equal, and comply with *Standard Specification for Air-Entraining Admixtures* (ASTM Designation C260). The air-entraining admixture shall be added at the concrete mixer or batching plant at approximately ½ to 3 fl oz/100 lbs (30 to 200 mL/100 kg) of cement, or in such quantities as to give the specified air contents.

www.graceconstruction.com

North American Customer Service: 1-877-4AD-MIX1 (1-877-423-6491)

Daravair is a registered trademark of W. R. Grace & Co.—Conn.

We hope the information here will be helpful. It is based on data and knowledge considered to be true and accurate and is offered for the users' consideration, investigation and verification, but we do not warrant the results to be obtained. Please read all statements, recommendations or suggestions in conjunction with our technical services, which apply to all goods supplied by us. No statement, recommendation or suggestion is intended for any use which would infringe any patent or copyright. W. R. Grace & Co.—Conn., 62 Whittemore Avenue, Cambridge, MA 02140. In Canada, Grace Canada, Inc., 284 Clements Road, West Ajax, Ontario, Canada L1S 3C6.

This product may be covered by patents or patents pending.
AIR-70 Printed in U.S.A. 506

Copyright 2007, W. R. Grace & Co.—Conn.
FA1011M

GRACE

APPENDIX C: EPOXY ADHESIVE DATA SHEET

Adhesive Anchoring Systems



3.2.7 HIT-RE 500 Epoxy Adhesive Anchoring System

3.2.7.2 Material Specifications

Material Properties for HIT-RE 500 – Cured Adhesive

Bond Strength ASTM C882-91 ¹ 2 day cure 7 day cure	12.4 MPa 12.4 MPa	1800 psi 1800 psi
Compressive Strength ASTM D-695-96 ¹	82.7 MPa	12,000 psi
Compressive Modulus ASTM D-695-96 ¹	1493 MPa	0.22 x 10 ⁶ psi
Tensile Strength 7 day ASTM D-638-97	43.5 MPa	6310 psi
Elongation at break ASTM D-638-97	2.0%	2.0%
Heat Deflection Temperature ASTM D-648-95	63°C	146°F
Absorption ASTM D-570-95	0.06%	0.06%
Linear Coefficient of Shrinkage on Cure ASTM D-2566-86	0.004	0.004
Electrical resistance DIN IEC 93 (12.93)	6.6 x 10 ⁻¹³ Ω/m	1.7 x 10 ⁻¹² Ω/in.

¹ Minimum values obtained as the result of tests at three cure temperatures (23, 40, 60°F).

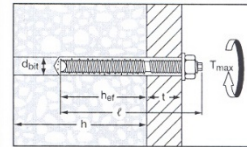
Material Specifications

	Mechanical Properties	
	f_u ksi (MPa)	min. f_u ksi (MPa)
Standard HAS-E rod material meets the requirements of ISO 898 Class 5.8	58 (400)	72.5 (500)
High Strength or 'Super HAS' rod material meets the requirements of ASTM A 193, Grade B7	105 (724)	125 (862)
Stainless HAS rod material meets the requirements of ASTM F 593 (AISI 304/316) Condition CW 3/8" to 5/8"	65 (448)	100 (689)
Stainless HAS rod material meets the requirements of ASTM F 593 (AISI 304/316) Condition CW 3/4" to 1-1/4"	45 (310)	85 (586)
HIS Insert 11MnPb30+C Carbon Steel conforming to DIN 10277-3	54.4 (375)	66.7 (460)
HIS-R Insert X5CrNiMo17122 K700 Stainless Steel conforming to DIN EN 10088-3	50.8 (350)	101.5 (700)
HAS Super & HAS-E Standard Nut Material meets the requirements of SAE J995 Grade 5		
HAS Stainless Steel Nut material meets the requirements of ASTM F 594		
HAS-E Carbon Steel and Stainless Steel Washers meet dimensional requirements of ANSI B18.22.1 Type A Plain		
HAS Super & HAS-E Standard Washers meet the requirements of ASTM F 884, HV		
All HAS-E & HAS Super Rods (except 7/8") & HAS-E Standard, HIS inserts, nuts & washers are zinc plated to ASTM B 633 SC 1		
7/8" Standard HAS-E & HAS Super rods hot-dip galvanized in accordance with ASTM A 153		
Note: Special Order steel rod material may vary from standard materials.		

3.2.7.3 Technical Data

HIT-RE 500 Installation Specification Table for HAS Threaded Rods

Details		HAS Rod Size								
		in. (mm)	3/8 (9.5)	1/2 (12.7)	5/8 (15.9)	3/4 (19.1)	7/8 (22.2)	1 (25.4)	1-1/4 (31.8)	
d_{bit}	bit diameter ¹	in.	7/16	9/16	3/4	7/8	1	1-1/8	1-3/8	
h_{nom}	std. depth of embed.	in. (mm)	3-3/8 (90)	4-1/2 (110)	5-5/8 (143)	6-3/4 (171)	7-7/8 (200)	9 (229)	11-1/4 (286)	
T_{max} max. tightening torque	HAS-E Rods HAS SS HAS-Super	Embed $\geq h_{nom}$	ft lb (Nm)	18 (24)	30 (41)	75 (102)	150 (203)	175 (237)	235 (319)	400 (540)
		Embed $< h_{nom}$	ft lb (Nm)	15 (20)	20 (27)	50 (68)	105 (142)	125 (169)	165 (224)	280 (375)
h	min. base material thickness	-	1.5 hef							
Approximate number of fastenings per cartridge at standard embedment ²										
Small Cartridge			52	28	11	7	5	4	2	
Medium Cartridge			84	45	18	11	8	6	3	
Jumbo Cartridge			255	137	56	37	27	19	12	



¹ Use matched tolerance carbide tipped bits or Hilti matched tolerance DD-B or DD-C diamond core bits.

² Assumes no waste.